The Genomic Loci of Specific Human tRNA Genes Exhibit Ageing-Related DNA Hypermethylation

Richard J. Acton [1,2,3], Wei Yuan [4,5], Fei Gao [6], Yudong Xia [6], Emma Bourne [7], Eva Wozniak [7], Jordana Bell [4], Karen Lillycrop [3], Jun Wang [6], Elaine Dennison [2], Nicholas Harvey [2], Charles A. Mein [7], Tim D. Spector [4], Pirro G. Hysi [4], Cyrus Cooper [2], Christopher G. Bell [1*]

1 William Harvey Research Institute, Barts & The London School of Medicine and Dentistry, Charterhouse Square, Queen Mary University of London, London, U.K.

2 MRC Lifecourse Epidemiology Unit, University of Southampton, Southampton, U.K.

3 Human Development and Health, Institute of Developmental Sciences, University of Southampton, Southampton, U.K.

4 Department of Twin Research & Genetic Epidemiology, St Thomas Hospital, King's College London, London, U.K.

5 Institute of Cancer Research, Sutton, U.K.

6 BGI-Shenzhen, Shenzhen, China

7 Barts & The London Genome Centre, Blizard Institute, Barts & The London School of Medicine and Dentistry, Queen Mary University of London, London, U.K.

* Corresponding author:

Abstract

Understanding how the epigenome deteriorates with age and subsequently impacts on biological function may bring unique insights to ageing-related disease mechanisms. As a central cellular apparatus, tRNAs are fundamental to the information flow from DNA to proteins. Whilst only being transcribed from ˜46kb (<0.002%) of the human genome, their transcripts are the second most abundant in the cell. Furthermore, it is now increasingly recognised that tRNAs and their fragments also have complex regulatory functions. In both their core translational and additional regulatory roles, tRNAs are intimately involved in the control of metabolic processes known to affect ageing. Experimentally DNA methylation can alter tRNA expression, but little is known about the genomic DNA methylation state of tRNAs.

Here, we find that the human genomic tRNA loci (610 tRNA genes termed the tRNAome) are enriched for ageing-related DNA hypermethylation. We initially identified DNA hypermethylation of 44 and 21 specific tRNA genes, at study-wide ($p < 4.34 \times 10^{-9}$) and genome-wide ($p < 4.34 \times 10^{-9}$) significance, respectively, in 4,350 MeDIP-seq peripheral blood DNA methylomes (16 - 82 years). This starkly contrasted with 0 hypomethylated at both these significance levels. Further analysing the 21 genome-wide results, we found 3 of these tRNAs to be independent of major changes in cell-type composition (tRNA-iMet-CAT-1-4, tRNA-Ser-AGA-2-6, tRNA-Ile-AAT-4-1). We also excluded the ageing-related changes being due to the inherent CpG density of the tRNAome by permutation analysis (1,000x, Empirical p-value $< 1 \times 10^{-3}$). We additionally explored 79 tRNA loci in an independent cohort using Fluidigm deep targeted bisulfite-sequencing of pooled DNA (n=190) across a range of 4 timepoints (aged ˜4, ˜28, ˜63, ˜78 years). This revealed these ageing changes to be specific to particular isodecoder copies of these tRNA (tRNAs coding for the same amino acid but with sequence body differences) and included replication of 2 of the 3 genome-wide tRNAs. Additionally, this isodecoder-specificity may indicate the potential for regulatory fragment changes with age.

In this study we provide the first comprehensive evaluation at the genomic DNA methylation state of the human tRNAome, revealing a discreet and strongly directional hypermethylation with advancing age.

Introduction

Ageing is implicated as a risk factor in multiple chronic diseases [1]. Understanding how the ageing process leads to deteriorating biological function is now a major research focus, with hopes to increase the human 'healthspan' and ameliorate the extensive physical, social and economic costs of these ageing-related disorders [2]. Epigenetic processes, which influence or can inform us about cell-type specific gene expression, are altered with age and are, furthermore, one of the fundamental hallmarks of this progression [3,4].

DNA methylation (DNAm) is the most common epigenetic modification of DNA and age-associated changes in this mark in mammalian tissues have been recognised for decades [5]. In fact, these alterations in DNAm with age are extensive with thousands of loci across the genome affected. Many represent 'drift' arising from the imperfect maintenance of the epigenetic state [6]. However, specific genomic regions show distinct directional changes, with loss of DNA methylation in repetitive or transposable elements [7], as well as gains in certain promoters, including the targets of polycomb repressor complex [8] and bivalent domains [9]. These observations with the advent of high-throughput DNAm arrays also permitted the identification of individual CpG sites that exhibit consistent changes with age, enabling the construction of predictors of chronological age known as epigenetic or DNAm 'clocks' [10–13]. Additionally, it was observed that 'acceleration' of this DNAm-derived measure is a biomarker of 'biological' ageing due to associations with morbidity and mortality (Reviewed in [14] & [15]). In a previous investigation of ageing-related DNAm changes within common disease-associated GWAS regions, we identified hypermethylation of the specific transfer RNA gene, tRNA-iMet-CAT-1-4 [16]. The initiator methionine tRNA possesses certain unique properties, including its capacity to be rate limiting for translation [17], association with the translation initiation factor eIF2 [18], and ability to impact the expression of other tRNA genes [19].

tRNAs are evolutionarily ancient [20] and fundamental in the translation process for all domains of life. This translation machinery and the regulation of protein synthesis are controlled by conserved signalling pathways shown to be modifiable in longevity and ageing interventions [21]. Additionally, beyond their core role in the information flow from DNA to protein sequence, tRNAs can fragment into numerous tRNA-derived small RNAs (tsRNAs) [22] with signalling and regulatory functions [23–26]. tsRNA abundance has been linked to locus specific tRNA gene expression, in some cases independent of mature tRNA levels [27].

The 610 annotated tRNA genes of the human tRNAome (gtRNAdb [28]) cover <46 kb (including introns) which represents <0.002% of the human genome [29]. Yet these genes produce the second most abundant RNA species next to ribosomal RNA [30] and are required for the production of all proteins. tRNA genes are transcribed by RNA polymerase III (polIII) [31] and have internal type II polIII promoters [32]. DNAm is able to

repress the expression of tRNA genes experimentally [33] but may also represent co-ordination with the local repressive chromatin state [34]. Transcription is also repressed by the highly conserved polIII specific transcription factor Maf1 [35,36], who's activity is modulated by the Target of Rapamycin Kinase Complex 1 (TORC1) [37]. TORC1 is a highly conserved hub for signals that modulate ageing [38].

tRNAs as well as tsRNAs are integral to the regulation of protein synthesis and stress response, two processes known to be major modulators of ageing. Metabolic processes are also recognised to modulate the age estimates of DNAm clocks [39]. Partial inhibition of translation increases lifespan in multiple model organisms [40] and PolIII inhibition increases longevity acting downstream of TORC1 [41]. Furthermore, certain tsRNAs circulating in serum can be modulated by ageing and caloric restriction [42].

We directly investigated ageing-related changes in the epigenetic DNA methylation state of the entire tRNAome, facilitated by the availability of a large-scale MeDIP-seq dataset. Arrays poorly cover this portion of genome, with even the latest EPIC (850k) arrays only covering <15% of the tRNA genes, with robust probes, and in total only ˜4.7% of all the tRNAome CpGs [43]. tRNA genes sit at the heart not only of the core biological process of translation but at a nexus of signalling networks operating in several different paradigms, from small RNA signalling to large scale chromatin organisation [44]. In summary, tRNA biology, protein synthesis, nutrient sensing, stress response and ageing are all intimately interlinked. In this study, we have identified tRNAome DNA hypermethylation and independently replicated this newly described ageing-related observation.

Results

DNA Methylation of Specific tRNA Gene Loci Changes with Age

Due to tRNAs critical role in translation and evidence of their modulation in ageing and longevity-related pathways, we interrogated these genes for evidence of ageing-related epigenetic changes. Our discovery set was a large-scale peripheral blood-derived DNA methylome dataset comprising of 4350 samples (see Figure 1). This sequencing-based dataset had been generated by Methylated DNA Immunoprecipitation (MeDIP-seq) [45], which relies on the enrichment of methylated fragments of 200-500 bp to give a regional DNAm assessment (500 bp semi-overlapping windows, see Methods). In total the human tRNAome is comprised of 610 tRNAs (gtRNAdb)(see Figure 2), though only 492 are autosomal and do not reside in blacklisted regions of the genome [46]. Due to the small size of these tRNAs (60-86bp, median 73bp, excluding introns which are present in ˜30 tRNAs with sizes from 10-99bp, median 19bp), this fragment-based method enabled a robust examination of the epigenetic state of these highly similar sequences. This was supported by a mappability assessment. The median mappability score density for the tRNAome was 0.90 for 50mers when considering tRNA genes $\pm 500bp$ reflecting the regional nature of the MeDIP-seq assay. In contrast the 50mer mappability density is 0.68 for tRNA genes alone representative of the mappability of reads generated using a technique such as whole-genome bisulfite sequencing (see Figures S1 & S2).

We identified 21 genome-wide significant and 44 study-wide significant results ($p < 4.34 \times 10^{-9}$ and 8.36×10^{-5}, respectively, via linear regression see Methods (batch corrected n=4350). Study-wide significance was calculated conservatively for all 598 autosomal tRNAs. There was a strong directional trend with all results at both significance levels being due to increases in DNA methylation. Age-related changes in cell type proportion are strong in heterogeneous peripheral blood, and include a myeloid skew, loss of naive T cells and increases in senescent cells [47]. A subset of 3 genome-wide and 16 study-wide significant hypermethylation results remained significant even after correcting for potential cell-type changes by including lymphocytes, monocytes, neutrophils and eosinophil cell count data (n=3001, Listed in Table 1, Red in Figure 5). tRNA-iMet-CAT-1-4 is located on chromosome 6. tRNA-Ile-AAT-4-1 and tRNA-Ser-AGA-2-6 are neighbours and are located on chromosome 17 within the 3' UTR of *CTC1* (CST Telomere Replication Complex Component 1). Going forward we refer to these most robustly corrected sets of 3 and 16 tRNA genes as the genome-wide and study-wide significant tRNA genes respectively.

Due to the related nature of these twin samples, we also analysed these data in two subsets of n=1198 & 1206 by selecting one twin from each pair into the seperate sets. This analysis also included correction for Batch and Blood Cell counts. Whilst in these smaller datasets no tRNAs were genome-wide significant, 5 and 7 tRNA genes,

respectively, reached study-wide significance. In these sets 5/5 and 6/7 of these were present in 16 study-wide significant tRNA genes.

Furthermore, we examined a subset of samples with longitudinal data (n=658 methylomes from 329 individuals, median age difference 7.6 yrs). At the nominal significance threshold ($p < 0.05$) this yielded a split of 41 hypermethylating tRNA genes and 22 hypomethylating tRNA genes. Of these hypermethylated tRNAs, 2 are in the previously identified genome-wide significant set of 3 (with tRNA-iMet-CAT-1-4 ranked 3rd by p-value) and 9 are in the study-wide significant set of 16.

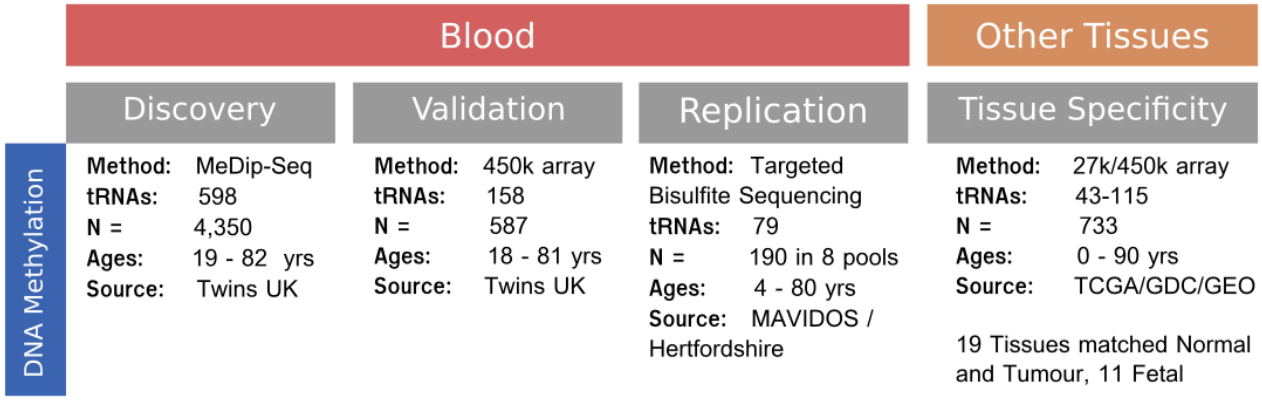

Fig 1. Study Structure. tRNAs differentially methylated with age initially identified in MeDIP-seq, validated (where covered in 450k array) and replicated in targeted bisulfite sequencing of pooled samples. Tissue specificity of these effects was explored in TCGA and foetal tissue data.

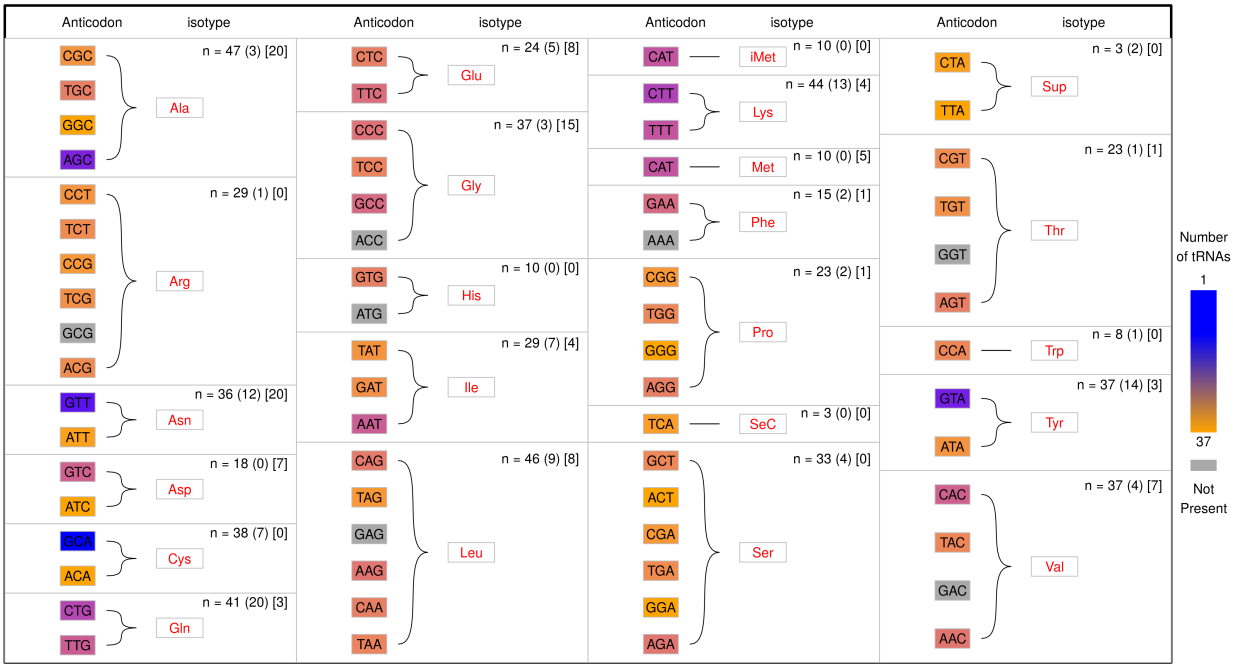

Fig 2. The genetic code as represented in the human tRNAome. The triplet genetic code leads to the incorporation of specific amino acids into an elongating protein via corresponding tRNAs. n is the number of tRNA genes which encode a given amino acid, the number in parentheses is how many of those may be pseudogenes based on their tRNAscan score [48], and the number in square braces is the number in blacklisted regions [46]. There are a total of 610 tRNAs in GtRNAdb [28], 116 of which are potential pseudogenes, and 107 are in blacklisted regions [46]. Notably 7 of the 61 non-STOP codons are missing from the human tRNAome therefore these codons are handled by wobble base matching (*e.g.* GCG Arg, ACC Gly). Also of note are the suppressor and selenocysteine tRNAs. The 20 methionine tRNAs are split equally between initiator methionine and internally incorporating methionine tRNAs, which are structurally distinct. There are also 23 nuclear encoded mitochondrial tRNAs.

tRNA Genes are Enriched for Age Related DNA Hypermethylation

Whilst ageing changes are pervasive throughout the DNA methylome, we identified a strong enrichment for this to occur within the discrete tRNAome (Fisher's Exact Test $p = 1.05 \times 10^{-27}$) (see Figure 3). This is still significant if the 6 of the study-wide significant 16 tRNAs that overlap polycomb or bivalent regions are excluded ($p = 4.66 \times 10^{-15}$)

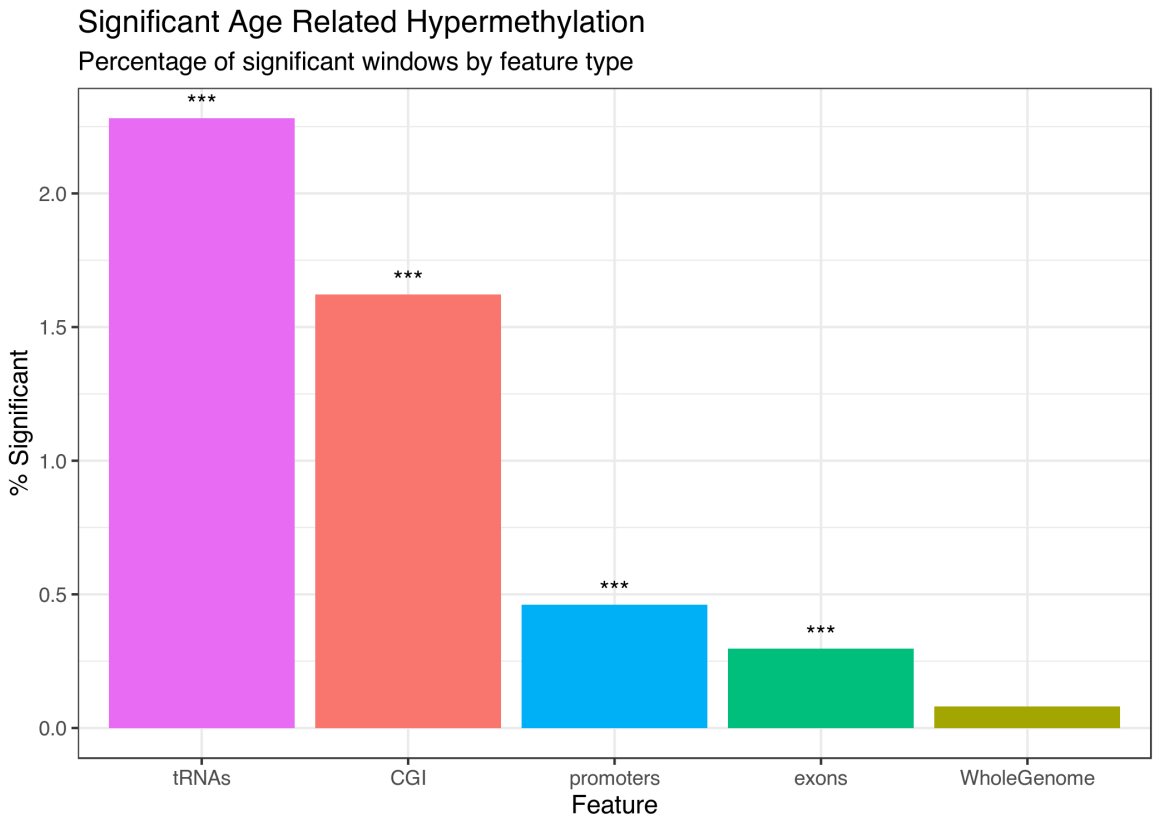

Fig 3. Age-related DNA hypermethylation Genomic Region Enrichment. (n = 3001, tRNAs are enriched compared to the genomic background, Fisher's Exact Test $p < 1.05 \times 10^{-27}$, Blood cell-type and batch corrected).

CpG density itself is known to have a clear impact on the potential for variability of the DNA methylome as well as ageing-related changes [49,50]. To assess whether this hypermethylation finding was being merely driven by the inherent CpG density of the tRNAome, we performed a CpG density matched permutation analysis (1,000X, see Methods). This supported the specific nature of these age-related DNAm changes within the functional tRNAome (Empirical p-value $< 1.0 \times 10^{-3}$, Figure 4). As a point of comparison for this genomic functional unit, we also performed the same permutations for the known age-related changes in the promoters of genes that are polycomb group targets [8] and those with a bivalent chromatin state [9]. We were able to reproduce the enrichment of the polycomb group targets and bivalent regions (Empirical p-value $< 1.0 \times 10^{-3}$) in our dataset.

Table 1. Significantly Hypermethylating tRNAs in blood cell-type and batch corrected model MeDIP-seq. 'Slope' corresponds to the beta value for methylation in the linear model.

tRNA	Location	MeDIP-seq p-value	BiS-seq p-value	BiS-seq slope
tRNA-iMet-CAT-1-4	chr6	2.83e-11	9.35e-04	4.54
tRNA-Ile-AAT-4-1	chr17	3.03e-10	6.88e-04	-0.745
tRNA-Ser-AGA-2-6	chr17	1.16e-10	4.28e-2	0.623

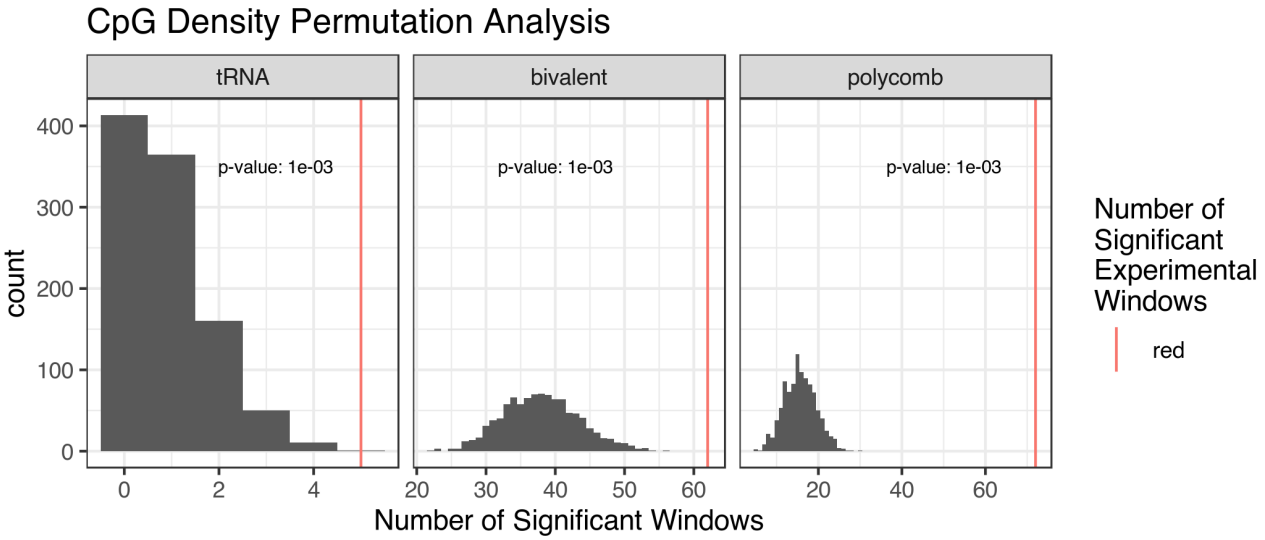

Fig 4. CpG Density Genome-wide Permutation Analysis. Each permutation represented a random set of windows matching the CpG density of the functional unit (bivalent domains, polycomb group target promoters & the tRNAome). These are subsequently assessed for signficant age-related DNAm changes (see Methods). The red line is the observed number of significant loci.

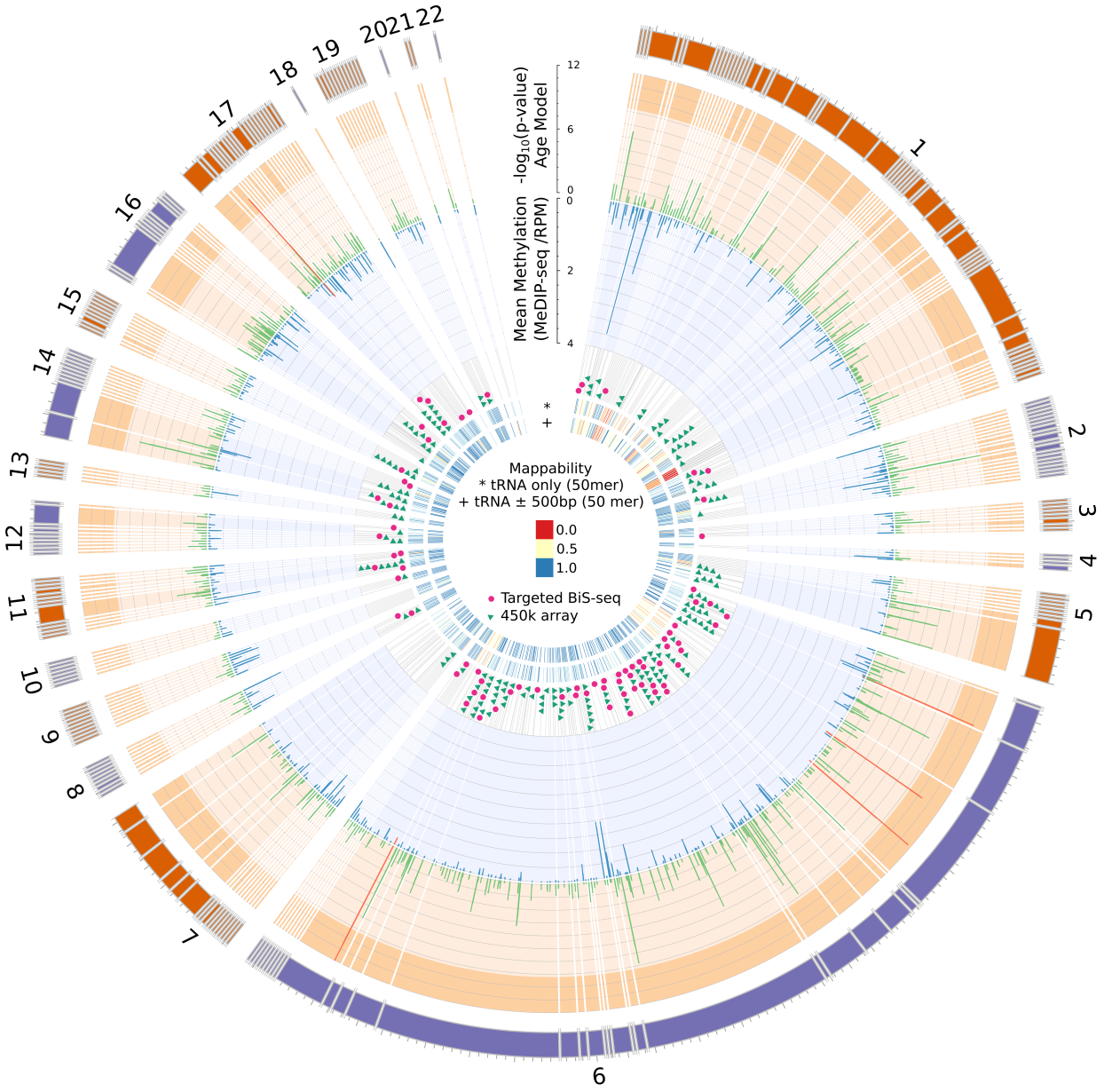

Fig 5. Human tRNAome overview. From the outside in: Chromosome ideograms scaled by the number of tRNA genes (total = 598), as excludes chromosome X (10), Y (0) and contig chr1_gl000192_random (2; see Methods). tRNA genes within 20kbp of one another are grouped with breaks inserted between these clusters. Radial grey lines represent the location of tRNA genes in the genome. $-log_{10}(p-value)$ for the blood cell-type and batch corrected age model are shown for each window overlapping a tRNA gene in green. Mean methylation across all samples (n=3001) in RPM (reads per million base pairs) is shown in blue. Genome-wide significant cell-type & batch corrected ($p < 4.34 \times 10^{-9}$) tRNAs show in red. The 158 Loci covered by 213 probes on the 450k array which directly overlap a tRNA gene are shown with green triangles. The 84 loci targeted for bisulfite sequencing in this study are indicated in magenta. Mappability score density is computed as the area under the encode mappability tracks [51] over the length of the region.

Age-related tRNAome DNA Hypermethylation is even observed in one Newborn versus one Centenarian

We examined an available Whole Genome Bisulphite sequencing (WGBS) dataset from Heyn *et al.* [52] (see Methods) These data consisted of blood-derived DNA WGBS in one newborn child and one 26 year old, and centenarian (103 years). In their analysis, the centenarian was found to have more hypomethylated CpGs than the neonate across all genomic compartments, including promoters, exonic, intronic, and intergenic regions. However, even in this examination of 3 individuals of 3 different age in the 55% of tRNA that possessed coverage, we observed DNA hypermethylation with age among the study-wide significant tRNA hypermethylators. The centenarian was significantly more methylated in this set of tRNAs than the neonate (Wilcoxon rank sum test, 6.14% increase (95% CI -Inf - 4.31), W = 717, p = 6.14×10^{-4}, see Figure 6).

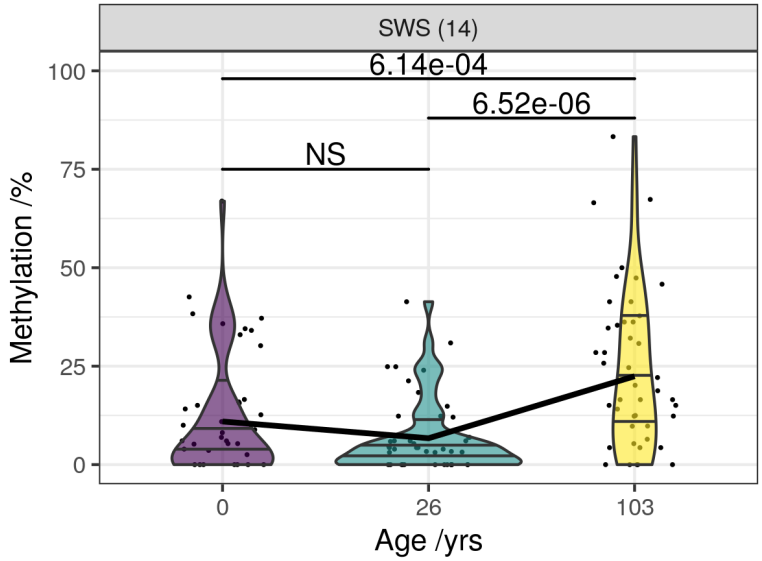

Fig 6. Whole Genome Bisulfite Sequencing Data in a newborn, as adult and a centenarian. Each point represents the methylation level at an individual CpG within a tRNA gene. Numbers in parentheses indicate the number of tRNA genes for which methylation data is shown. SWS: Available study-wide significant tRNA genes.

Age-related Changes Independently Replicated with Targeted Bisulfite Sequencing

In order to further robustly support these-ageing related changes, we attempted to replicate these findings ourselves in an independent ageing dataset. Furthermore, we employed a different technology Targeted bisulfite (BiS) sequencing to also further validate the MeDIP-seq-derived results. These data provide individual CpG resolution to identify what may be driving the regional DNAm changes observed.

We performed this targeted BiS-seq in blood-derived DNA from 8 pools of age-matched individuals at 4 time-points (˜4, ˜28, ˜63, ˜78 years) from a total of 190 individuals, as detailed in Table 2. A total of 79 tRNA

loci generated reliable results post-QC (see Methods). These tRNAs covered a total of 458 CpGs with a median of 6 CpGs per tRNA (range 1-9). Median Coverage per site across pools, technical replicates and batches was 679 reads (mean 5902).

Firstly, we ran the 8 Pooled samples on the Illumina EPIC (850k) array to confirm that our pooling approach was applicable for DNAm ageing-related evaluation. This showed an $R^2 = 0.98$ between pool mean chronological age and Horvath clock DNAm predicted age [11](see Figure 7). Therefore, this confirmed the utility of this novel pooling approach. We also used these array derived data to estimate the major blood cell proportions for each of these pools with the Houseman algorithm [53].

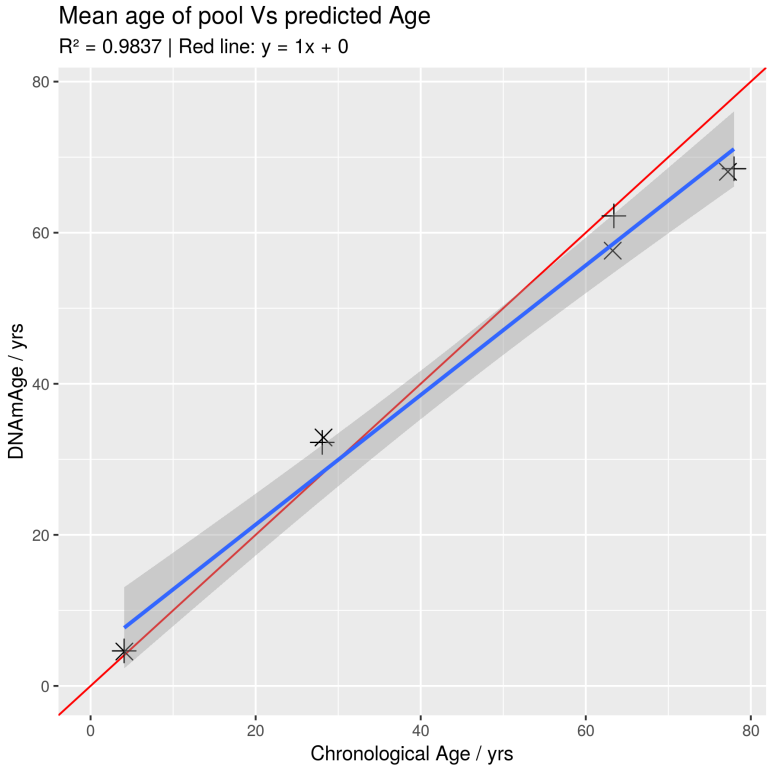

Fig 7. Chronological Age compared with DNAm Age estimated with Horvath's 2013 multi-tissue clock [11] based on EPIC array data for the 8 pooled samples used in the Targeted Bisulfite sequencing (See Table 2 for pool details).

We noted that individual tRNA loci exhibiting age-related changes in DNAm had duplicate or isodecoder (same anticodon but body sequence variation) sequences in the genome, which despite exact or near sequence identity did not show similar changes. tRNA-iMet-CAT-1-4 for instance is 1 of 8 identical copies in the genome and was the only locus that showed significant changes. The results of pairwise differential methylation tests between age groups for the 6 top tRNAs from the MeDIP-seq models are listed in Table 3.

Of the 3 top hits in MeDIP-seq, tRNA-iMet-CAT-1-4 (Figure 9c) and tRNA-Ser-AGA-2-6 (Figure 9i)

exceeded nominal significance (p-values = 9.35×10^{-4} & 4.28×10^{-2} , respectively). However, tRNA-Ile-AAT-4-1 (Figure 9n) showed a nominal decrease in DNAm with age. tRNA tRNA-Leu-TAG-2-1 from the study-wide significant set also showed nominally significant hypermethylation with age (Figure 9u). Also, four of the individual CpGs in tRNA-iMet-CAT-1-4 exhibited nominally significant increases in DNAm with Age (Figure 8).

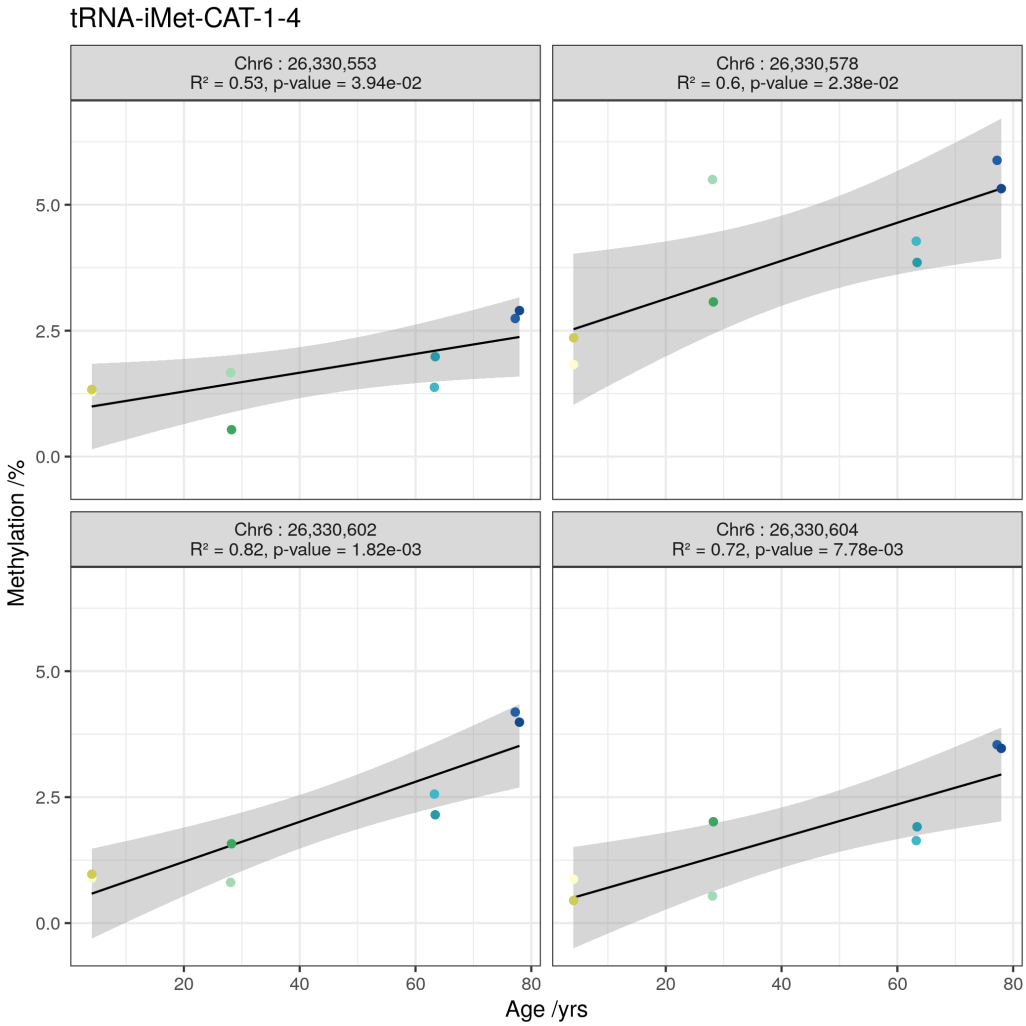

Fig 8. Individual CpG methylation increases (nominally significant $p < 0.05$) in tRNA-iMet-CAT-1-4.

Table 2. Summary information on participants in each pool.

Pool	Mean Age	Sex	Min Age	Max Age	n
Pool 1	4.07	Male	3.99	4.38	20
Pool 2	4.09	Female	3.99	4.36	20
Pool 3	28.07	Female	25.87	29.80	25
Pool 4	28.23	Female	26.05	30.01	25
Pool 5	63.40	Female	62.80	63.80	25
Pool 6	63.26	Female	62.70	63.70	25
Pool 7	77.96	Female	75.50	80.50	25
Pool 8	77.22	Female	74.40	80.10	25

Table 3. Pairwise Differences in Methylation between Age groups by tRNA. p-values are for pairwise methylation differences (see Methods)[54].

tRNA	num. CpGs	comparison	p-value	delta
tRNA-Ile-AAT-4-1	8	4 vs. 28	1.518e-01	-0.2
		4 vs. 63	1.774e-01	-0.234
		4 vs. 78	3.060e-01	0.0113
		28 vs. 63	7.152e-01	-0.0334
		28 vs. 78	1.553e-01	0.212
		63 vs. 78	2.057e-01	0.245
tRNA-iMet-CAT-1-4	5	4 vs. 28	8.403e-02	0.0116
		4 vs. 63	1.716e-01	0.0125
		4 vs. 78	1.997e-04*	0.0368
		28 vs. 63	3.943e-01	0.000869
		28 vs. 78	1.724e-02*	0.0252
		63 vs. 78	6.224e-02	0.0243
tRNA-Ser-AGA-2-6	9	4 vs. 28	4.222e-01	0.0573
		4 vs. 63	3.968e-01	0.0274
		4 vs. 78	4.651e-01	0.0423
		28 vs. 63	1.095e-01	-0.0299
		28 vs. 78	2.126e-01	-0.015
		63 vs. 78	2.201e-01	0.0149

Select Duplicates & Isodecoders of Hypermethylating tRNA loci remain unchanged We targeted a selection of these duplicate and isodecoder loci for bisulfite sequencing in order to confirm that the identified DNAm changes are specific to a given locus and not general to related tRNAs. Examining the tRNA-iMet-CAT-1 family, only the previously identified 1-4 version confirmed significant hypermethylation (not 1-2, 1-3 or 1-5)(Figure 9a-e). Likewise the tRNA-Ser-AGA-2-6 version was supported compared to 2-1,2-4 and 2-5(Figure 9f-j)).

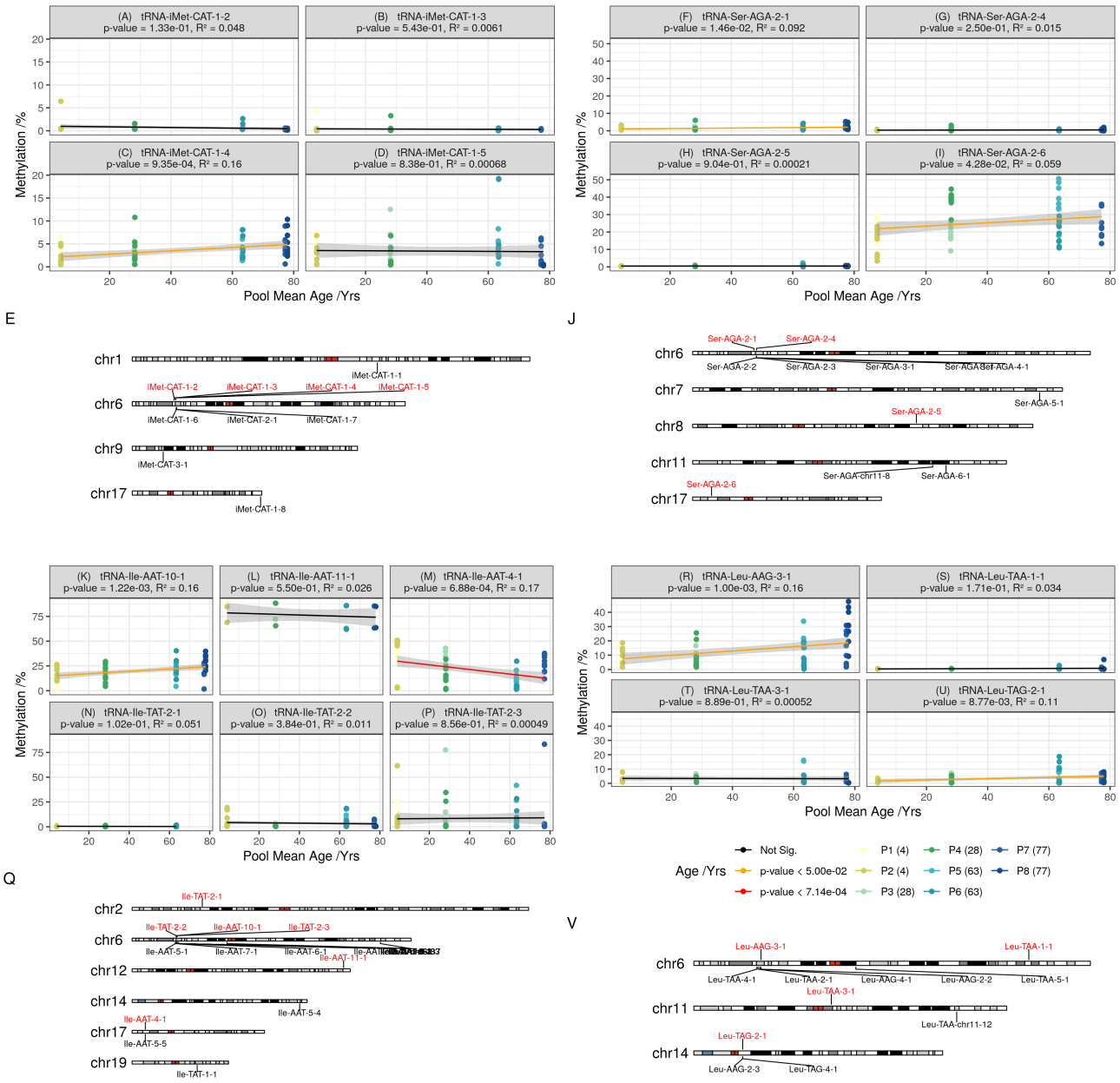

Fig 9. (A-Q) Mean methylation across replicates at each CpG in each pool for select tRNAs. Ideograms show the locations of all tRNAs with the same anticodon, with those featured in the scatter plots highlighted in red and placed above the ideogram. (R-V) Except for leucine isoacceptors tRNAs are not all of the same codon and only tRNAs on the same chromosome as those plotted are labelled on the ideograms. (experiment-wide Bonferroni $p = 6.41 \times 10^{-4}$).

DNA methylation 450k Array Data Validates the MeDIP-seq Results

Although DNA methylation array poorly cover the tRNAome, we wished to attempt to see if this BiS-based but differing and well-established technology was supportive at all of our DNA hypermethylation findings. TwinsUK

had available 450k array on 587 individuals, and this platform includes 143 probes, covering 103 tRNAs. All the 3 top tRNAs in the MeDIP-seq results were covered by this data set, and 7 of the 16 study-wide significant set. 9 tRNAs show significant ($p < 4.58 \times 10^{-4}$) increases in DNA methylation with age in models corrected for blood cell counts including all 3 of the 3 tRNAs identified in the MeDIP-seq as genome-wide significant and 5 of the 7 study-wide significant set present on the array (Figure 10). Although it should be noted that 56 of these 143 probes are within the non-robust set of Zhou et al. [43], including 1 of the genome-wide, and 1 of the study-wide results (covering tRNA-Ile-AAT-4-1 & tRNA-Val-AAC-4-1), respectively.

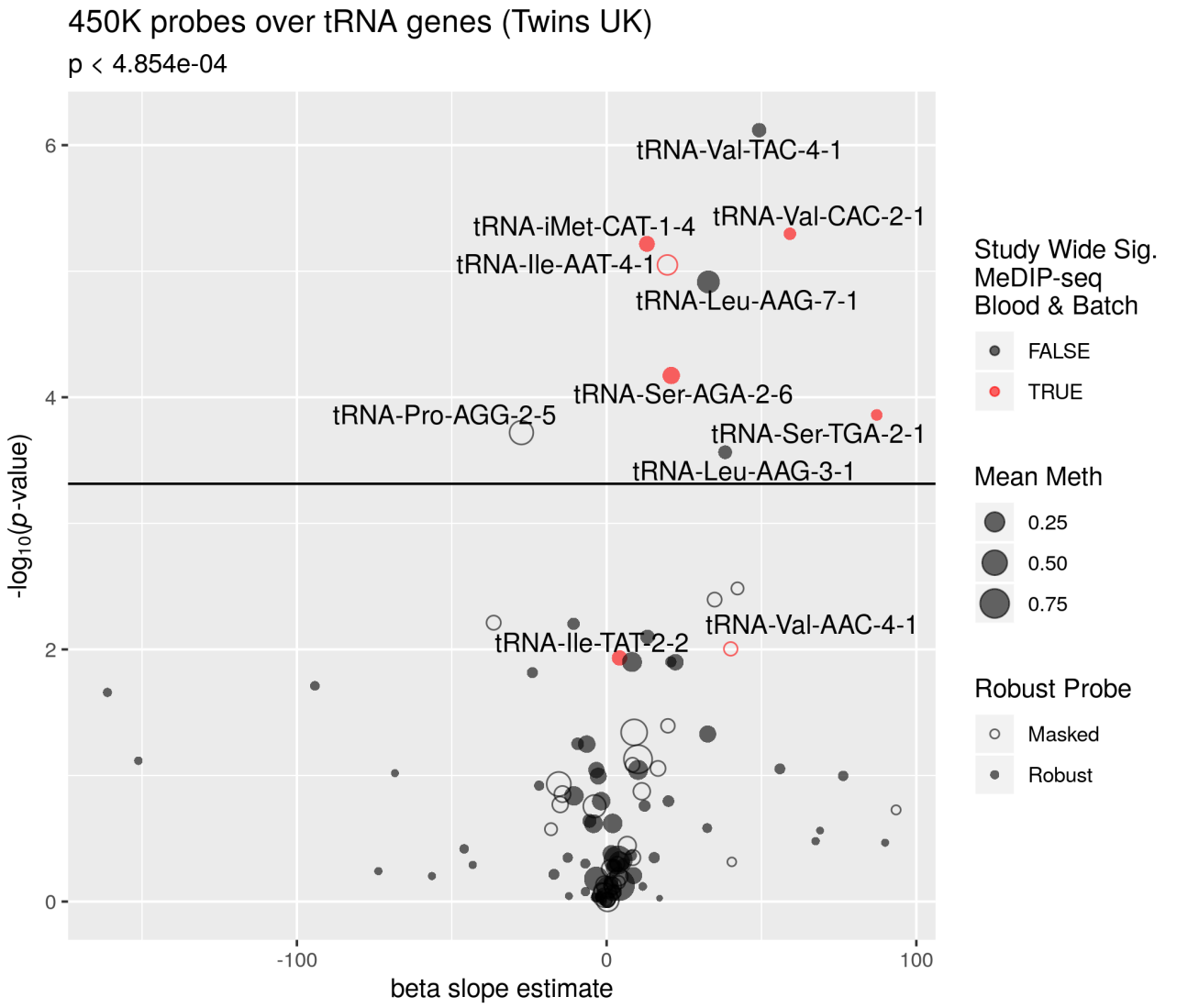

Fig 10. Volcano-like plot. tRNAs are labelled if they are significant here or were in the MeDIP-seq data (Red). Model slope: the model coefficient for the methylation values. Unfilled circles indicate those probes in the general mask generated by Zhou et al. [43]. Significance threshold: $0.05/103 \approx 4.58 \times 10^{-4}$ (the number of tRNA genes examined).

Ageing-Related tRNA Loci show increased Enhancer-Related Chromatin Signatures

We further explored the activity of the tRNAome in public Chromatin segmentation data in blood (Epilogos Blood & T-cells set) [55]. This shows proportionally more Enhancer-related (Enh, EnhBiv & EnhG) chromatin states at tRNA genes hypermethylating with age than the stronger Promoter-related (TSS) in other tRNAs. (Figure 11). Whereas these characteristics are less frequently predominant in the rest of the tRNAs (Figure 11). Age-hypermethylating tRNA are enriched for enhancer chromatin states compared to the rest of the tRNAome (Fisher's Exact test p = 0.01).

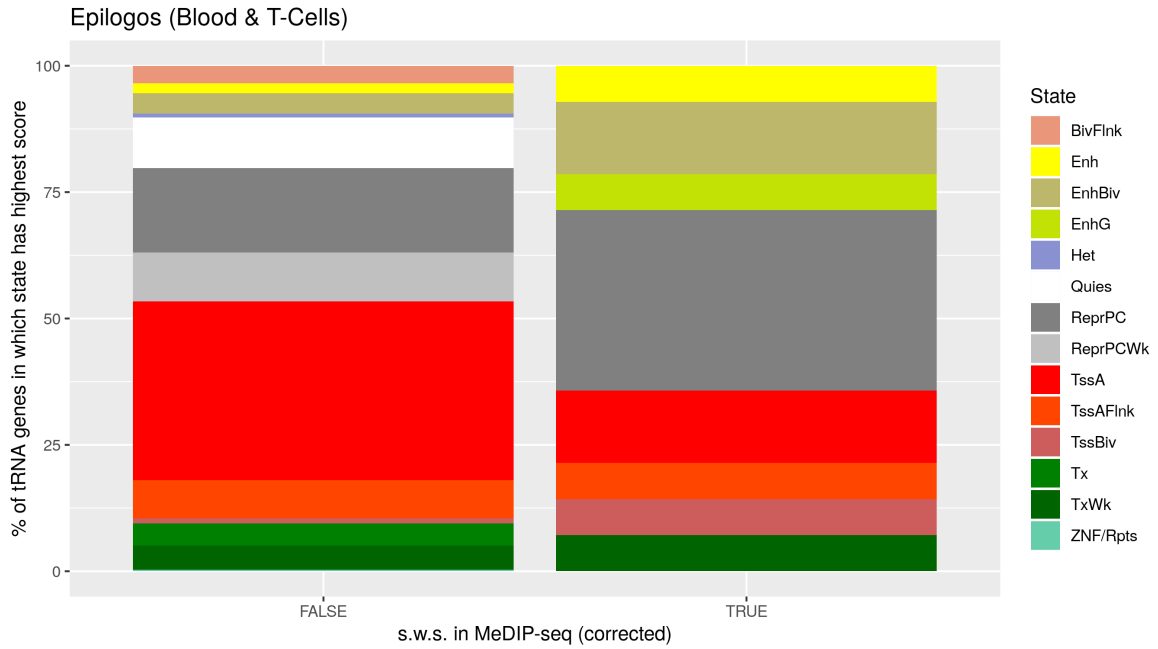

Fig 11. Chromatin segmentation data from the Epilogos [55] 'Blood & T-cell' 15 State model (tRNA genes +/- 200bp). Frequency with which a model state was the predominant state at a given tRNA. Proportions of predominant tRNA state for the 14 study-wide significant age-hypermethylating tRNAs covered compared to other 371 available tRNAs.

Age Hypermethylating tRNAs are more methylated in Lymphoid than Myeloid cells

Three tRNA genes remained genome-wide significant and 16 study-wide significant following correction for major cell-type fraction. This is suggestive of either cell-type independent change or, presumably less likely, a very large effect in a minor cell-type fraction. tRNAs have exhibited tissue-specific expression [56–58] and blood cell-type populations change with age. Specifically, there is shift to favour the production of cells in the myeloid lineage [47]. These points lead us to examine tRNA gene DNAm in sorted cell populations. We used a publically available 450k array dataset [59]) that has been used in the construction of cell-type specific DNAm references for cell-type fraction prediction using the Houseman algorithm [53] (see Methods). This consists of data from 6

individuals (aged 38 ± 13.6/yrs) from seven isolated cell populations (CD4+ T cells, CD8+ T cells, CD56+ NK cells, CD19+ B cells, CD14+ monocytes, neutrophils, and eosinophils). We found that tRNA gene DNAm could separate myeloid from lymphoid lineages (Figures 12 & S4).

Of the eight study-wide significant tRNAs with array coverage, we identified that collectively these eight are significantly more methylated in the lymphoid than the myeloid lineage (1.1% difference, Wilcoxon rank sum test $p = 1.50 \times 10^{-6}$ 95% CI 0.7%-∞). Thus, any age related increases in myeloid cell proportion would be expected to dampen rather than exaggerate the age-related hypermethylation signal that we observed. In addition tRNA-Ile-AAT-4-1 and tRNA-Ser-AGA-2-6 have the highest variance in their DNAm of all 129 tRNAs covered in this dataset. This could represent ageing-related changes as these samples range across almost 3 decades. Another possibly may be that these loci as well as hypermethylating are also increasing their variability with age in a similar fashion to those identified by Slieker *et al.* [60]. In that study they identified that those loci accruing methylomic variability were associated with fundamental ageing mechanisms.

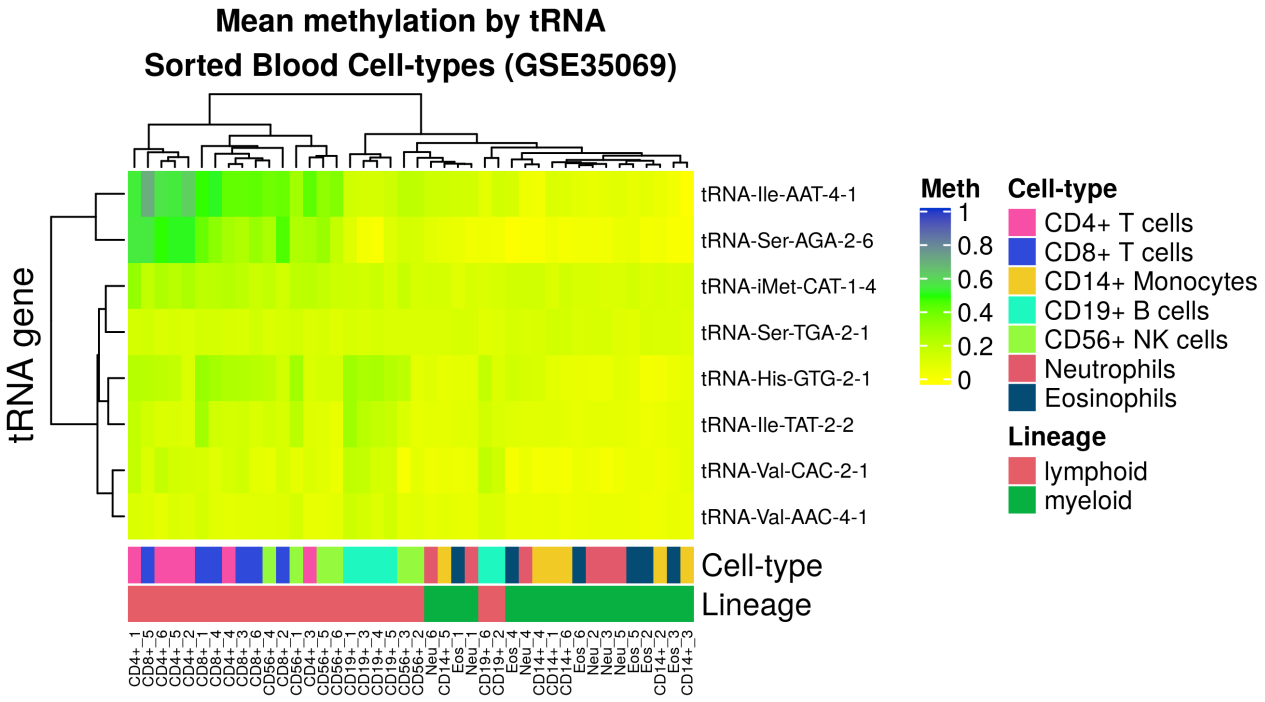

Fig 12. Heatmap [61] of mean methylation of probes covering each tRNA in 7 cell-type fractions from 6 Male individuals. Data from GSE35069 [59]. Of the 16 study-wide significant hypermethylating tRNAs, 8 are covered by this dataset.

tRNA Gene DNA Methylation in Other Tissues

Some tRNA gene expression has been shown to be highly tissue specific [56–58]. It follows that our observations of changes in DNAm with age in blood might be specific to that tissue. We used a mix of 450k and 27k array data from 'solid tissue normal' samples made available by TCGA (The Cancer Genome Atlas) and data from foetal tissue [62,63] downloaded from GEO (see Methods). The samples from TCGA range in age from 15-90 (n = 733). Only 43 tRNA genes had adequate data to compare across tissues in this dataset and 115 in the foetal tissue data.

tRNA Genes also Hypermethylate with Age in Solid Tissue

Only 2 of the 3 tRNA genes we identified as genome-wide significant and a further 1 of the study-wide significant tRNA genes are present in the set of 45 tRNA genes in the TCGA data, thus limiting our ability to draw conclusions about the tissue specificity of our results. Solid tissue samples have a strong preponderance for low levels of methylation consistent with the active transcription of many tRNA genes and show slight increasing methylation with age but age accounts for very little of the variance (linear regression slope estimate = 1.52; $R^2 = 0.0002$; p-value 1.34×10^{-3} (Figure S5d). In a pan-tissue analysis we found that 10 tRNA genes showed changes in DNAm with age, 9 of which were hypermethylation (p-value $< 1.1 \times 10^{-3}$). One of these tRNA genes, tRNA-Ser-TGA-2-1 was also present in study-wide significant set of tRNA genes. Figures S6 & S7 illustrate minimal tissue specific differences. Interestingly, however, tRNA-iMet-CAT-1-4 and tRNA-Ser-AGA-2-6 appeared more variable in methylation state than many other tRNAs in the TCGA normal tissue samples (Figure S6) and indeed have the highest variance in DNA methylation across tissues (Figure S5c).

Expression of tRNAs in Blood with Age

Having observed specific tRNA gene isodecoders hypermethylating with age we explored the expression of tsRNA in blood cell-types. We devised a bioinformatic approach to attempt to assay tRNA transcription in order to use standard publicly available small RNA-seq datasets. We created customised MINTmap [64] reference designed to include only fragments which unambiguously map to a single tRNA gene locus and which overlap the 5' or 3' end of the genomic tRNA sequence by at least one base with no mismatches. This reference is intended to capture pre-tRNAs prior to processing and CCA addition operating under the assumption that the levels of pre-tRNAs will be informative about the amount of transcription taking place at the tRNA loci (see Methods). Our custom MINTmap reference build yielded 383 fragments mapping to 92 distinct tRNA loci in this data. The lack of coverage of age hypermethylating tRNAs by uniquely attributable RNA-seq reads prevented us from drawing any

strong conclusions about the relationship between DNAm changes and changes in tRNA transcription.

Using the original MINTmap reference optimised to detect tRNA fragments derived from mature tRNAs there were 5384 unique fragments derived from as many as 417 tRNA loci. However, the mapping between fragments and loci in this reference is many to many, with each tRNA gene able to give rise to many fragments and each fragment attributable to at least 1 and usually many tRNA genes. We limited our examination of these fragments to those with a length of greater than or equal to 40nt to capture reads more likely to be derived from mature tRNAs rather than tRFs or tRNA halves (Figure S8). We identified 48 tsRNAs with nominally significant expression changes ($p < 0.05$), 8 increased and 40 decreased in abundance with age. For example 5 of 6 fragments showing significant age-related expression changes derived from the Gln-CTG family of tRNAs are decreasing with age (Figure 13). This is suggestive that expression of some tRNA genes may decline with age but this possibility is in need of additional tRNA expression data before it can be asserted with confidence.

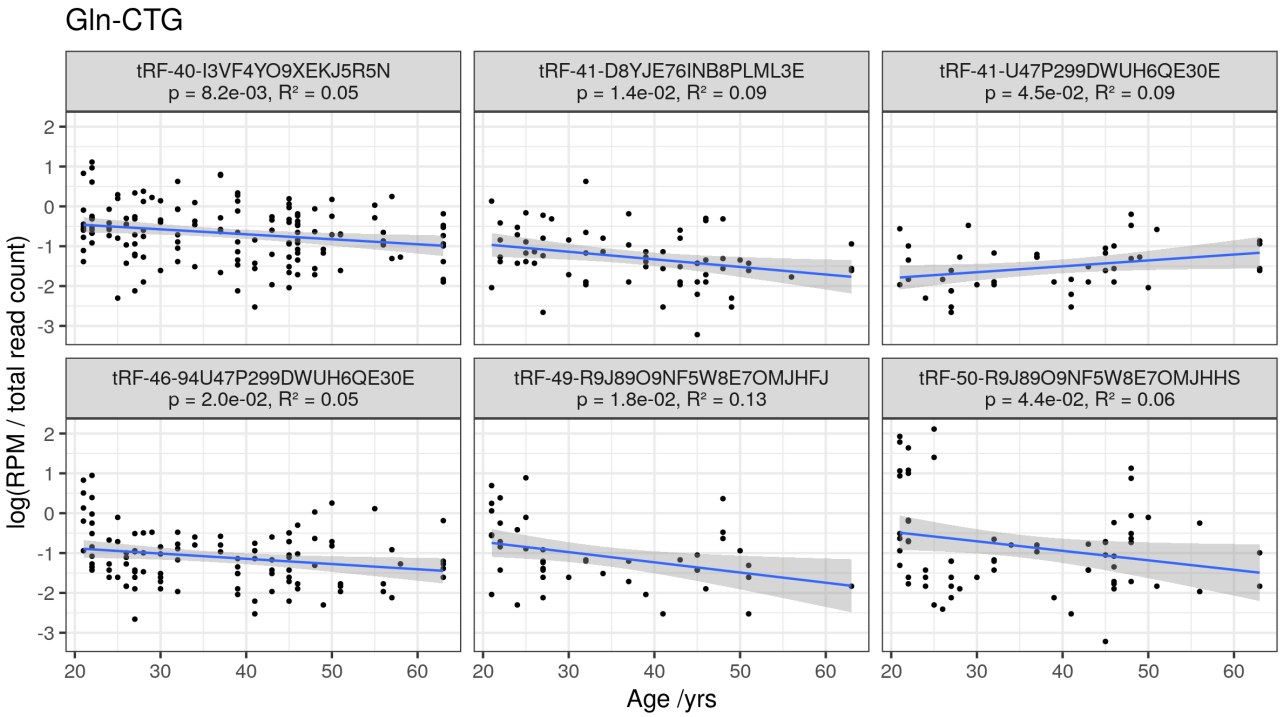

Fig 13. tRNA fragments derived from the Gln-CTG family of tRNAs, selected as tRNA-Gln-CTG-7-1 is one of the 16 study-wide significant age-hypermethylating tRNA genes. Pane titles contain the MINTbase Plates, unique identifiers of the tRNA fragments [22].

Mice also show age-related tRNA gene DNA hypermethylation

We examined the DNA methylation of the mouse tRNAome in using data from a reduced representation bisulfite sequencing (RRBS) experiment performed by Petkovich et al. [65]. These data from 152 mice covered 51 tRNA

genes and 385 CpGs after QC (see Methods), representing ˜11% of the mouse tRNAome. The mice ranged in age from 0.67-35 months.

Three of the 51 tRNAs showed Bonferroni significant DNA methylation changes with age (p-value $< 1.08 \times 10^{-4}$) and all were in the hypermethylation direction. These three are tRNA-Asp-GTC-1-12, tRNA-Ile-AAT-1-4, tRNA-Glu-TTC-1-3 (Figure 14).

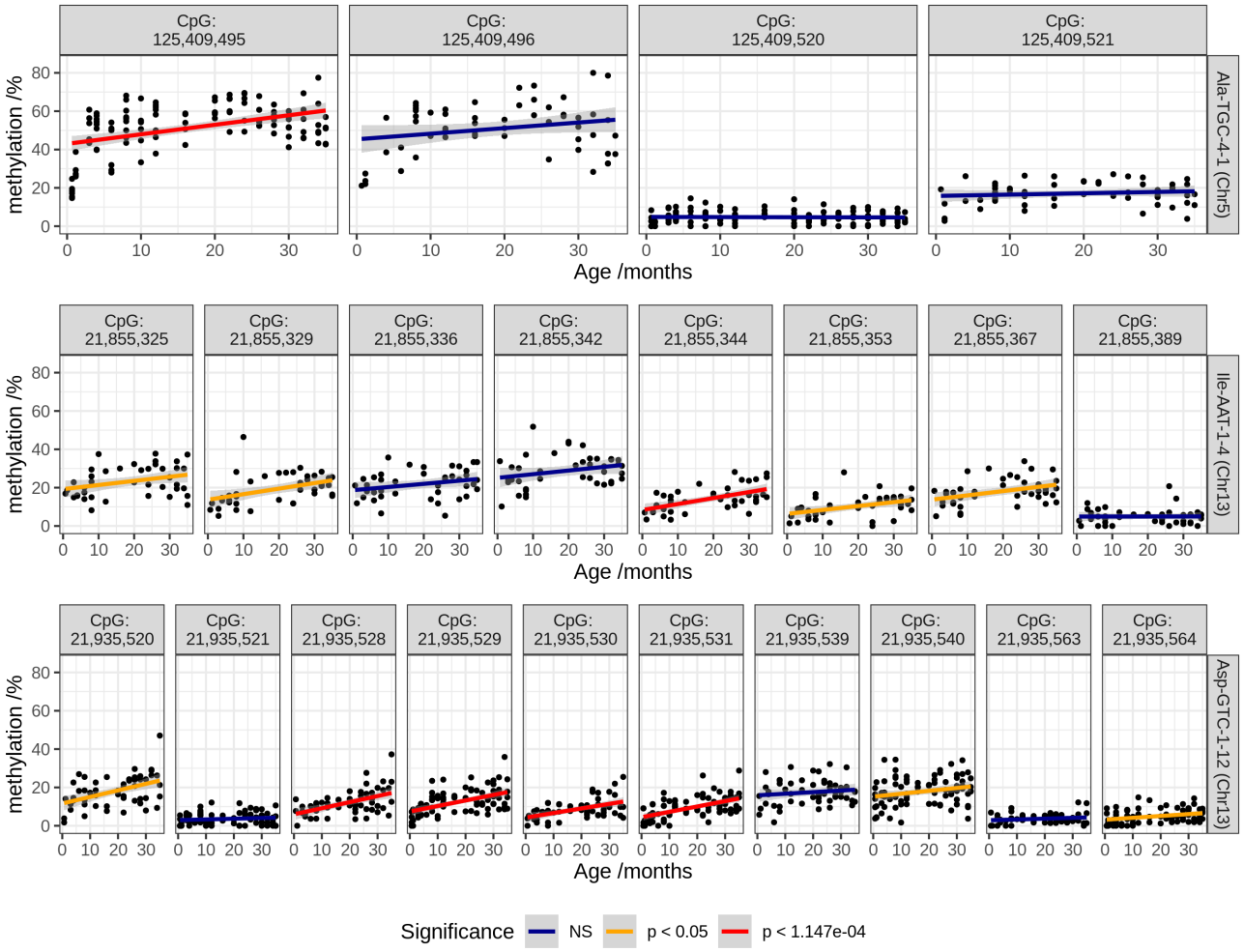

Fig 14. DNA methylation of CpGs in 3 tRNA which significantly hypermethylate with age in mice. 6 CpGs reach bonferroni significance and 7 show nominally significant increases.

Discussion

Our work has identified a previously unknown enrichment for age-related epigenetic changes within the tRNA genes of the human genome. This observation was strongly directional with increasing DNA methylation with age [66].

The MeDIP-seq dataset employed brought advantages in exploring this undefined terrain of the tRNAome. Firstly, being genome-wide it provides much increased access, as these regions are poorly covered by current arrays. Secondly, being a fragment-based regional assessment of DNA methylation, the individual but highly similar small tRNA genes can be surrounded by unique sequence.

We determined by genome-wide permutation that this strong hypermethylation signal was specific to the tRNAome, and not merely driven by the underlying CpG density of these loci. A targeted BiS-seq experiment validated the defined nature of the tRNA change in an independent dataset, with a successful pooling approach, which may also be useful for other ageing-related targeted DNA methylome evaluations. Additionally, we gained support for our results from limited DNA methylation array data.

We subsequently explored further what was driving this age-related phenomenon and its possible biological implications. As this result was observed in peripheral blood, we were well aware that we were examining DNA derived from a heterogeneous cell type population [67]. Moreover, that there are well known age-related proportional changes in peripheral blood cell composition [47]. The TwinsUK MeDIP-seq and 450k array DNA methylation data included measured haematological values. Therefore, we adjusted for major cell type effects, such as a myeloid skew, and distinct tRNAs were still significant. Although, a caveat to our study is that this can not exclude changes in minor specific sub-cell fractions types. However, that these age-related effects were strong enough to be observed in both a regional MEDIP-seq assessment and a pooled sequencing approach, implies that they not extremely subtle. We examined age-related tRNA gene DNA methylation changes in the limited subset of mouse tRNA genes covered in publicly available RRBS data (˜13%) and were able to identify tRNAs exhibiting DNA hypermethylation with age in this set. This suggests that age-related tRNA gene hypermethylation may not be unique to humans, but at least observed across mammals.

Due to the high number of hypermethylating tRNA prior to cell-type correction, we were also curious whether the epigenetic state of this small tRNAome fraction of genome could capture and in fact be a defined fingerprint of cell type. We found that tRNA gene DNA methylation could separate myeloid from lymphoid lineages. There also was some suggestion of more fine-grained blood cell-type signatures in tRNA DNAm, such as the separation of CD19+ B cells from CD4/8+ T cells. Ageing is also known to lead to an increase in senescent cells (*e.g.* CD8+ CD28- cells). Whether these epigenetic changes in the tRNAome uniquely represent these cell-types will require

technical advances to enable future single cell DNA methylome analysis to accurately assess these regions. If further supported, the epigenetic state of these loci may aid the taxonomy of cell-type definition.

This signal within the tRNA families was observed to occur at specific Isodecoders. After correcting for major cell types, we identified 2 tRNA genes tRNA-iMet-CAT-1-4 and tRNA-Ser-AGA-2-6 which had the most consistent hypermethylation across 3 different assays. Isodecoders expand in number with organismal complexity and the high prevalence in mammals has been suggested due to their additional regulatory functionality [68,69]. They also have distinct translational efficiency [70], which can also have consequences in human disease [71]. Furthermore, there is great complexity to the fragmentation of tRNA [23], with physiological processes such as stress shown to induce fragment production [72]. These resultant tsRNAs can feedback on protein synthesis by regulating ribosome biogenesis [73] and others have diverse regulatory functions such as targeting transposable element transcripts [74]. They are also observed to circulate in the blood in a cell-free fashion, and fragment levels can be modulated by ageing and calorie restriction [42]. The isodecoder specific nature of our findings frame a possible hypothesis for regulatory change with age and future work will be required to unravel this potential.

Whilst, the expression of the tRNA genes has long been simplified as 'constitutive', some observations have indicated that many tRNA genes are expressed in a tissue-specific fashion in diverse organisms [57,58]. Although others have found the majority of isodecoders are transcribed in different cell types [29]. Several transcription factors acting via TFIIIB [75] have a negative (the tumour suppressors p53 [76] and Rb [77]) or positive (the proto-oncogene c-Myc) influence [75]. Regulatory sequence in the flanking or the internal regions of tRNA genes do not explain tRNA expression variation [78]. Whilst DNAm is able to repress the expression of tRNA genes [33], the broader chromatin environment also affects tRNA transcription. Due to the co-ordinated nature of epigenomic modifications, it may also be revealing to evaluate ageing-related histone modification in these tRNA loci.

Changes in the epigenetic state of specific tRNA could be modulating transcription efficiency or even codon availability in the ageing cell. tRNA gene dosage is quite closely matched to amino acid usage frequency in the human exome. However, the transcriptome codon usage frequency and tRNA gene expression have been claimed to vary with the replicative state of cells, separating differentiated from replicating cells [79]. Others have argued that these differences are substantially explained by variation in GC content [80] and that codon usage frequencies are observed to be mostly invariant in the transcriptomes of a wide range of tissues, as well as across developmental time [78]. Although, experimental stress-related states have revealed changes with an over-representation of codons that are translated by rare tRNAs [81].

tRNA sequences themselves are under strong structural (both secondary and tertiary) [68] as well as functional constraint, which leads to an order of magnitude reduction in variation compared the background

genomic mutation rate [29]. However, polymorphic tRNA could be another potential caveat to our work. Although, there is no significant population variation in, for example, tRNA iMet sequences in 1,000 Genomes data. Indeed, there are only 11 new isodecoder sequences with high confidence (tRNAscan scores ≥ 50) at >1% population frequency [29]. There is also some evidence for tRNA copy number variation at specific loci, although this remains under-characterised [82,83]. Another potential cause we considered was whether age-related somatic copy number increases could be occurring in these loci. Population or somatic copy number expansions could lead to increased methylated reads in MeDIP-seq without any epigenetic state change. However, this would not be consistent with the targeted and array BiS conversion methodologies, where the proportion of methylated to unmethylated reads would still be constant.

It is worth noting the parallels with known cancer and ageing epigenetic changes, and that tRNAs are also dysregulated in cancer [84], with proposed utility as prognostic markers [85]. Furthermore, the early replicating state of tRNA loci, potentially associated with high expression [86], may make them prone to hypermethylate, as is observed in early replicating loci in both cancer [87] and senescent cells [88]. Interestingly, tRNA gene loci may also play a role in local as well as large scale genome organisation [44]. tRNA gene clusters act as insulators [89] and have extensive long-range chromatin interactions with other tRNA gene loci [44]. The coordinated transcription of tRNAs at subnuclear foci and the B-box sequence elements bound by TFIIIC and not PolIII may represent an organising principle for 3D-chromatin by providing spatial constraints [90]. Therefore, these tRNA epigenetic changes could contribute to the structural changes that are also observed in ageing [91].

In conclusion, due to the unique challenges that make the tRNAome difficult to examine it has remained epigenetically under-characterised despite its critical importance for cell function. We directly interrogated the epigenetic DNA methylation state of the functionally important tRNAome, across the age spectrum in a range of datasets as well as methodologies and identified an enrichment for age-related DNA hypermethylation in the human tRNA genes.

Methods

Participants

Participants in the 'EpiTwins' study are adult volunteers from the TwinsUK Register. The participants were aged between 16 and 82 years, with a median of ˜55 years (cohort profile [92]). Ethics for the collection of these data were approved by Guy's & St Thomas' NHS Foundation Trust Ethics Committee (EC04/015—15-Mar-04) and written informed consent was obtained from all participants.

Participants for our targeted bisulfite sequencing of select tRNA loci were drawn from two studies. Samples from participants aged 4 and 28 years are from the MAVIDOS [93] study and participants aged 63 and 78 years are from the Hertfordshire cohort study [94]. Due to a limited number of available samples, the two 4 year old pools contained DNA from 20 individuals each, with all other pools having 25 contributing individuals. Pool 1, the first 4 year old pool used DNA from all male samples, with all other pools using all female samples. Thus, the total number of participants was 190 (see Table 2). Samples from the 28 year old time point are all from pregnant women at ˜11 weeks gestation.

tRNA annotation information

Genomic coordinates of the tRNA genes were downloaded from GtRNAdb [28]. The 2 tRNAs located in chr1_gl000192_random are tRNA-Gly-CCC-8-1 & tRNA-Asn-ATT-1-2 (Supplementary File S1). Stem/loop structure annotations were inferred from output of `tRNAscan` [48] with a custom `perl6` script. The 213 probes overlapping tRNA genes were derived from intersecting the tRNA gene annotation data from gtRNAdb with the Illumina 450k array manifest annotation for the hg19 genome build using bedtools v2.17.0 [95]. We excluded 107 tRNAs from blacklisted regions of hg19 [46].

DNA methylome data

TwinsUK MeDIP-seq methylomes

The Methylated DNA Immunoprecipitation sequencing (MeDIP-seq) data was processed as previously described [16,96]. These processed data are available from the European Genome-phenome Archive (EGA) (https://www.ebi.ac.uk/ega) under study number EGAS00001001910 and dataset EGAD00010000983. The dataset used in this work consists of 4350 whole blood methylomes with age data. 4054 are female and 270 male. 3001 have full blood counts. There are 3652 individuals in this data set. These individuals originate from 1933 unique families. There are 1234 monozygotic (MZ) twin pairs (2468 individuals), and 458 dizygotic (DZ) twin

pairs (916 individuals).

MeDIP-seq used a monoclonal anti-5mC antibody to bind denatured fragmented genomic DNA at methylated CpG sites. This antibody-bound fraction of DNA was isolated and sequenced [45]. MeDIP-seq 50-bp single-end sequencing reads were aligned to the hg19/GRCh37 assembly of the human genome and duplicates were removed. `MEDIPS` (v1.0) was used for the MeDIP-seq specific analysis [97]. This produced reads per million base pairs (RPM) values binned into 500bp windows with a 250bp slide in the BED format, resulting in ˜12.8 million windows on the genome. MeDIP-seq data from regions of interest was extracted using Bedtools v2.17.0 [95].

Analysis of DNA methylome data for Significant Ageing-related changes

All analysis was performed in R/3.5.2. Linear models were fitted to age using the MeDIP-seq DNA methylome data, as quantile normalised RPM scores at each 500bp window. Models were fitted with: 1. No covariates; 2. Batch information as a fixed effect; 3. Blood cell-type counts for neutrophils, monocytes, eosinophils, and lymphocytes as fixed effects; and 4. Batch and Blood Cell counts as fixed effects. Model 1 & 2 were fitted on the full set of 4350 as batch information was available for all samples but blood cell count data was only available for a subset of 3001 methylomes. Models 1 & 2 fitted in the n=3001 subset were similar to those fitted in the complete set of 4350. Models 3 & 4 were fitted in the n=3001 subset with full covariate information and sets of significant tRNAs identified at study-wide and genone wide levels in model 4 were used in subsequent analyses. Models were also fitted for two unrelated subsets created by selecting one twin from each pair (Monozygotic or Dizygotic), yeilding sets with n = 1198 & 1206 DNA methylomes. One additional model was fitted for longitudinal analysis, samples were selected by identifying individuals with a DNA methylome at more than one time point and filtering for only those with a minimum of 5 years between samples. This yielded 658 methylomes from 329 individuals with age differences of 5-16.1 yrs, median 7.6 yrs. Models for this set included participant identifier as a fixed effect in addition to blood cell counts and batch information.

Permutation Analysis for Enrichment with Age-related Changes

We performed a permutation analysis to determine whether the CpG distribution of sets of the tRNAome was the principle driver of the ageing-related changes observed. Windows overlapping tRNAs have a higher proportion of windows with a greater CpG density than their surrounding sequences (see supplementary Figure S3). CpGs residing within moderate CpG density loci are the most dynamic in the genome [49] and CpG dense CpG island regions include specific ageing-related changes [8,9,16]. For comparison we also performed the permuation in the CGI regions from the Polycomb group protein target promoters in Teschendorff *et al.* [8] and bivalent loci from ENCODE ChromHmm 'Poised Promoter' classification in the GM12878 cell-line [98]. A

random set of 500bp windows representing an equivalent CpG density distribution of the feature set in question were selected from the genome-wide data. Above a certain CpG density there are insufficient windows to sample without replacement within a permutation. Furthermore, above ˜≥ 18% CpG density CpG Islands become consistently hypomethylated [99]. Therefore, all windows with a CpG density of ≥ 18% (45 CpGs per 500bp) were grouped and sampled from the same pool. i.e. a window overlapping a tRNA gene which had a 20% density could be represented in permutation by one with any density ≥ 18%. This permutation was performed 1,000 times to determine an Empirical p value by calculating the number of times the permutation result exceeded the observed number of significant windows in the feature set. $Empirical\ p-value = \frac{r+1}{N+1}$, where r is the sum of significant windows in all permutations and N is number of permutations [100].

Neonate and Centenarian Whole Genome Bisulfite Sequencing

DNA methylation calls were downloaded from GEO:GSE31263 and intersected with tRNA genes using bedtools v2.17.0 [95].

Sample pooling and EPIC array

We performed an Illumina Infinium DNA methylation EPIC array ((C) Illumina) and targeted bisulfite sequencing of select tRNA gene loci. Here we used DNA extracted from whole blood and pooled into 8 samples from unrelated individuals at 4 time-points with 2 pools at each time-point. The timepoints were 4, 28, 63, and 78 years. Using the EPIC array we were able to infer the DNAm age using the Horvath DNAm clock [11] and blood cell-type composition of our samples using the Houseman algorithm [53].

Targeted Bisulfite Sequencing

We selected tRNA loci for targeted sequencing in which have had observed changes and DNAm with age and closely related tRNAs in which changes were not observed. Primer design was performed using 'methPrimer' [101] (Supplementary File S2). A total of 84 tRNA loci were targeted and 79 subsequently generated reliable results post-QC. The targeted tRNAs covered a total of 723 CpGs with a median of 8 CpGs per tRNA (range 1-13), data passing QC was generated for 458 CpGs, median 6 (range 1-9) per tRNA.

Quality was assessed before and after read trimming using `fastqc` [102] and `multiqc` [103] to visualise the results. Targeting primers were trimmed with `cutadapt` [104] and a custom `perl5` script. Quality trimming was performed with `trim_galore` [105]. Alignment and methylation calling was performed with `Bismark` (v0.20.0) [106] making use of `bowtie2` [107]. The alignment was performed against both the whole hg19 genome and just the tRNAome +/- 100bp to assess the possible impact of off-target mapping. Mapping to the whole genome did

produce purported methylation calls at a larger number of loci than mapping just to the tRNAome (683,783 vs 45,861 respectively). Introducing a minimum coverage threshold of 25 reads dramatically reduced this and brought the number of sites into line with that in the tRNAome set (36,065 vs 33,664 respectively) suggesting a small number of ambiguously mapping reads. All subsequent analysis was performed using the alignment to just the tRNAome with a minimum coverage of 25 reads.

We performed pairwise differential methylation analysis of the tRNA genes at the different time points using `RnBeads` [54] with `limma` [108] and a minimum coverage of 25 reads. We also performed linear regression predicting age from DNA methylation at the targeted tRNA sites, permitting us to compare rates of increase with age. For the linear regression, we used only CpG sites with more than 25 reads mapped to the regions of the genome targeted for amplification.

TwinsUK Illumina 450k array methylomes

Illumina Infinium DNA methylation 450k arrays ((C) Illumina) were also performed on TwinsUK participants, in 770 Blood-derived DNA samples which had matched MeDIP-seq data. These data were preprocessed in the form of methylation 'beta' values pre-processed as previously described [16,96]. Cell-type correction was performed using cell-count data and the following model: `lm(age ~ beta + eosinophils + lymphocytes + monocytes + neutrophils)`.

Chromatin Segmentation Data

Epilogos chromatin segmentation data [55] was downloaded for the tRNA gene regions +/- 200bp from https://explore.altius.org/tabix/epilogos/hg19.15.Blood_T-cell.KL.gz using the `tabix` utility. The data used was the 'Blood & T-cell' 15 State model based on segmentation of 14 cell-types. This data was manipulated and visualised with `R` and `ggplot2`.

Isolated Blood Cell Type Specific Data

Data from 7 cell-type fractions from 6 Male individuals was downloaded from GSE35069 [59] using `GEOquery` [109]. Five of the 6 top age hypermethylating tRNAs are covered by this array dataset.

Cancer and Tissue Specific Methylation Data

Data was downloaded from the TCGA (The Cancer Genome Atlas) via the GDC (genomic data commons) data portal [110] using the `GenomicDataCommons` `R` package. Data from foetal tissue [62,63] was downloaded from

GEO (GSE72867, GSE30654). From the TCGA, we selected samples for which DNAm data was available from both the primary site and normal solid tissue, and for which we could infer an approximate age (within one year). We selected those probes overlapping tRNA genes yielding 73,403 data points across 19 tissues with an age range of 15-90yrs (median 63.4) (Supplementary File S3)

Assaying tRNA expression in blood with MINTmap

We used small RNA-seq data from sorted blood cell fractions [111] (GSE100467) and the MINTmap [64] tRNA fragment alignment tool. This dataset covered 42 individuals aged 21-63. We also created a customised MINTmap reference designed to include only fragments which unambiguously map to a single tRNA gene locus and which overlap the 5' or 3' end of the genomic tRNA sequence by at least one base with no mismatches. This reference is intended to capture pre-tRNAs prior to processing and CCA addition operating under the assumption that the levels of pre-tRNAs will be informative about the amount of transcription taking place at the tRNA loci. This approach provides at most a many to one mapping of tRNA fragment to a tRNA gene.

Assaying the expression of tRNA genes presents numerous difficulties [27], and usually requires variants on standard RNA-seq protocols. Our custom MINTmap reference build yielded 383 fragments mapping to 92 distinct tRNA loci in this data. To control quality only fragments with more than 20 total instances in the dataset and present in more than 20 individuals were considered.

The maximum length of a fragment was limited to 50nt, due to the read length of the small RNA-seq data.

Mouse RRBS Analysis

We downloaded methylation calls and coverage information resulting from RRBS performed by Petkovich *et al.* [65] from GEO using `GEOquery` [109] GSE80672. These data from 152 mice covered 68 tRNA and 436 CpGs after QC requiring >50 reads per CpG and >10 data points per tRNA. We excluded 5 tRNAs from blacklisted regions of mm10 [46]. After QC there were 58 tRNA genes and 385 CpGs. We performed simple linear modeling to predict age from methylation level at each tRNA and each CpG.

Data availability

The MeDIP-seq data supporting the results of this article are available in the EMBL-EBI European Genome-phenome Archive (EGA) under Data set Accession number EGAD00010000983 (https://www.ebi.ac.uk/ega/datasets/ EGAD00010000983). The targeted BiS-sequencing data will be available on publication.

Code availablity

Available at `https://github.com/richardjacton`

Acknowledgements

We gratefully acknowlege the individuals from TwinsUK, Mavidos and the Hertfordshrie cohort. TwinsUK received funding from the Wellcome Trust (Ref: 081878/Z/06/Z), European Community's Seventh Framework Programme (FP7/2007-2013), the National Institute for Health Research (NIHR)-funded BioResource, Clinical Research Facility and Biomedical Research Centre based at Guy's and St Thomas' NHS Foundation Trust in partnership with King's College London. Further funding support for the EpiTwin project was obtained from the European Research Council (project number 250157) and BGI. SNP Genotyping was performed by The Wellcome Trust Sanger Institute and National Eye Institute via NIH/CIDR. The authors would like to thank Nikki Graham for her assistance with the identification and pooling of the MAVIDOS and Hertfordshire DNA samples. The authors also acknowledge the use of the IRIDIS High Performance Computing Facility, and associated support services at the University of Southampton, in the completion of this work. The MRC-LEU is supported by the Medical Research Council (MRC). CGB recieved support from Diabetes UK (16/0005454). RJA was in receipt of a MRC Doctoral fund (1820097).

Author Contributions

RJA designed experiments and analysed all the processed and experimental data. CGB conceived and designed the experiments. TDS, KW and JW conceived and provided TwinsUK MeDIP-seq data. YX, FG and JW produced raw MeDIP-seq data with WY and JB processing and quality controlling these data. WY contributed an analysis concept. CC, NH, ED, and KL provided MAVIDOS and Hertfordshire sample data. EB, EW, and CAM performed the targeted BiS sequencing experiment. PGH contributed additional data and discussion of results. RJA and CGB wrote the paper. All authors reviewed and approved the final manuscript.

References

1. Partridge L, Deelen J, Slagboom PE. Facing up to the global challenges of ageing. Nature. Springer US; 2018;561: 45–56. doi:10.1038/s41586-018-0457-8

2. Campisi J, Kapahi P, Lithgow GJ, Melov S, Newman JC, Verdin E. From discoveries in ageing research to therapeutics for healthy ageing. Nature. Springer US; 2019;571: 183–192. doi:10.1038/s41586-019-1365-2

3. López-Otín C, Blasco MA, Partridge L, Serrano M, Kroemer G. The hallmarks of aging. Cell. 2013;153: 1194–217. doi:10.1016/j.cell.2013.05.039

4. Booth LN, Brunet A. The Aging Epigenome. Molecular Cell. Elsevier Inc. 2016;62: 728–744. doi:10.1016/j.molcel.2016.05.013

5. Wilson VL, Jones PA. DNA methylation decreases in aging but not in immortal cells. Science (New York, NY). 1983;220: 1055–7. Available: `http://www.ncbi.nlm.nih.gov/pubmed/6844925`

6. Fraga MF, Ballestar E, Paz MF, Ropero S, Setien F, Ballestar ML, et al. From The Cover: Epigenetic differences arise during the lifetime of monozygotic twins. Proceedings of the National Academy of Sciences. 2005;102: 10604–10609. doi:10.1073/pnas.0500398102

7. Chuong EB, Elde NC, Feschotte C. Regulatory activities of transposable elements: from conflicts to benefits. Nature Reviews Genetics. Nature Publishing Group; 2017;18: 71–86. doi:10.1038/nrg.2016.139

8. Teschendorff AE, Menon U, Gentry-Maharaj A, Ramus SJ, Weisenberger DJ, Shen H, et al. Age-dependent DNA methylation of genes that are suppressed in stem cells is a hallmark of cancer. Genome research. 2010;20: 440–6. doi:10.1101/gr.103606.109

9. Rakyan VK, Down TA, Maslau S, Andrew T, Yang TP, Beyan H, et al. Human aging-associated DNA hypermethylation occurs preferentially at bivalent chromatin domains. Genome Research. 2010;20: 434–439. doi:10.1101/gr.103101.109

10. Hannum G, Guinney J, Zhao L, Zhang L, Hughes G, Sadda S, et al. Genome-wide methylation profiles reveal quantitative views of human aging rates. Molecular cell. Elsevier Inc. 2013;49: 359–367. doi:10.1016/j.molcel.2012.10.016

11. Horvath S. DNA methylation age of human tissues and cell types. Genome biology. 2013;14: R115. doi:10.1186/gb-2013-14-10-r115

12. Weidner CI, Lin Q, Koch CM, Eisele L, Beier F, Ziegler P, et al. Aging of blood can be tracked by DNA methylation changes at just three CpG sites. Genome biology. 2014;15: R24. doi:10.1186/gb-2014-15-2-r24

13. Bell CG, Lowe R, Adams PD, Baccarelli AA, Beck S, Bell JT, et al. DNA methylation aging clocks: challenges and recommendations. Genome biology. 2019;20: 249. doi:10.1186/s13059-019-1824-y

14. Horvath S, Raj K. DNA methylation-based biomarkers and the epigenetic clock theory of ageing. Nature Reviews Genetics. Springer US; 2018;19: 371–384. doi:10.1038/s41576-018-0004-3

15. Field AE, Robertson NA, Wang T, Havas A, Ideker T, Adams PD. DNA Methylation Clocks in Aging: Categories, Causes, and Consequences. Molecular Cell. Elsevier Inc. 2018;71: 882–895. doi:10.1016/j.molcel.2018.08.008

16. Bell CG, Xia Y, Yuan W, Gao F, Ward K, Roos L, et al. Novel regional age-associated DNA methylation changes within human common disease-associated loci. Genome Biology. 2016;17: 193. doi:10.1186/s13059-016-1051-8

17. Rideout EJ, Marshall L, Grewal SS. Drosophila RNA polymerase III repressor Maf1 controls body size and developmental timing by modulating tRNAiMet synthesis and systemic insulin signaling. Proceedings of the National Academy of Sciences. 2012;109: 1139–1144. doi:10.1073/pnas.1113311109

18. Kolitz SE, Lorsch JR. Eukaryotic initiator tRNA: Finely tuned and ready for action. FEBS Letters. 2010;584: 396–404. doi:10.1016/j.febslet.2009.11.047

19. Pavon-Eternod M, Gomes S, Rosner MR, Pan T. Overexpression of initiator methionine tRNA leads to global reprogramming of tRNA expression and increased proliferation in human epithelial cells. RNA. 2013;19: 461–466. doi:10.1261/rna.037507.112

20. Eigen M, Lindemann B, Tietze M, Winkler-Oswatitsch R, Dress A, Haeseler A von. How old is the genetic code? Statistical geometry of tRNA provides an answer. Science. 1989;244: 673–679. doi:10.1126/science.2497522

21. Tavernarakis N. Ageing and the regulation of protein synthesis: a balancing act? Trends in Cell Biology. 2008;18: 228–235. doi:10.1016/j.tcb.2008.02.004

22. Pliatsika V, Loher P, Magee R, Telonis AG, Londin E, Shigematsu M, et al. MINTbase v2.0: a comprehensive database for tRNA-derived fragments that includes nuclear and mitochondrial fragments from all The Cancer Genome Atlas projects. Nucleic Acids Research. Oxford University Press; 2018;46: D152–D159. doi:10.1093/nar/gkx1075

23. Schimmel P. The emerging complexity of the tRNA world: mammalian tRNAs beyond protein synthesis. Nature reviews Molecular cell biology. Nature Publishing Group; 2018;19: 45–58. doi:10.1038/nrm.2017.77

24. Lee YS, Shibata Y, Malhotra A, Dutta A. A novel class of small RNAs: tRNA-derived RNA fragments (tRFs). Genes & development. 2009;23: 2639–49. doi:10.1101/gad.1837609

25. Li S, Xu Z, Sheng J. tRNA-Derived Small RNA: A Novel Regulatory Small Non-Coding RNA. Genes. 2018;9: 246. doi:10.3390/genes9050246

26. Xu W-L, Yang Y, Wang Y-D, Qu L-H, Zheng L-L. Computational Approaches to tRNA-Derived Small RNAs. Non-Coding RNA. 2017;3: 2. doi:10.3390/ncrna3010002

27. Torres AG, Reina O, Stephan-Otto Attolini C, Ribas de Pouplana L. Differential expression of human tRNA genes drives the abundance of tRNA-derived fragments. Proceedings of the National Academy of Sciences. 2019;116: 201821120. doi:10.1073/pnas.1821120116

28. Chan PP, Lowe TM. GtRNAdb: a database of transfer RNA genes detected in genomic sequence. Nucleic acids research. 2009;37: D93–7. doi:10.1093/nar/gkn787

29. Parisien M, Wang X, Pan T. Diversity of human tRNA genes from the 1000-genomes project. RNA Biology. 2013;10: 1853–1867. doi:10.4161/rna.27361

30. Lodish H, Berk A, Zipursky SL, Matsudaira P, Baltimore D, Darnell J. Molecular Cell Biology, 4th edition [Internet]. 4th ed. New York: W. H. Freeman; 2000. Available: https://www.ncbi.nlm.nih.gov/books/NBK21475/

31. Schramm L. Recruitment of RNA polymerase III to its target promoters. Genes & Development. 2002;16: 2593–2620. doi:10.1101/gad.1018902

32. Canella D, Praz V, Reina JH, Cousin P, Hernandez N. Defining the RNA polymerase III transcriptome: Genome-wide localization of the RNA polymerase III transcription machinery in human cells. Genome research. 2010;20: 710–21. doi:10.1101/gr.101337.109

33. Besser D, Götz F, Schulze-Forster K, Wagner H, Kröger H, Simon D. DNA methylation inhibits transcription by RNA polymerase III of a tRNA gene, but not of a 5S rRNA gene. FEBS letters. 1990;269: 358–62. doi:10.1016/0014-5793(90)81193-R

34. Varshney D, Vavrova-Anderson J, Oler AJ, Cowling VH, Cairns BR, White RJ. SINE transcription by RNA polymerase III is suppressed by histone methylation but not by DNA methylation. Nature communications. Nature Publishing Group; 2015;6: 6569. doi:10.1038/ncomms7569

35. Murawski M, Szczesniak B, Zoladek T, Hopper AK, Martin NC, Boguta M. maf1 mutation alters the subcellular localization of the Mod5 protein in yeast. Acta biochimica Polonica. 1994;41: 441–8. Available: http://www.ncbi.nlm.nih.gov/pubmed/7732762

36. Pluta K, Lefebvre O, Martin NC, Smagowicz WJ, Stanford DR, Ellis SR, et al. Maf1p, a Negative Effector of RNA Polymerase III in Saccharomyces cerevisiae. Molecular and Cellular Biology. 2001;21: 5031–5040. doi:10.1128/MCB.21.15.5031-5040.2001

37. Mange F, Praz V, Migliavacca E, Willis IM, Schütz F, Hernandez N. Diurnal regulation of RNA polymerase III transcription is under the control of both the feeding–fasting response and the circadian clock. Genome Research. 2017;27: 973–984. doi:10.1101/gr.217521.116

38. Kennedy BK, Lamming DW. The Mechanistic Target of Rapamycin: The Grand ConducTOR of Metabolism and Aging. Cell Metabolism. Elsevier Inc. 2016;23: 990–1003. doi:10.1016/j.cmet.2016.05.009

39. Nwanaji-Enwerem JC, Weisskopf MG, Baccarelli AA. Multi-tissue DNA methylation age: Molecular relationships and perspectives for advancing biomarker utility. Ageing Research Reviews. Elsevier; 2018;45: 15–23. doi:10.1016/j.arr.2018.04.005

40. Hansen M, Taubert S, Crawford D, Libina N, Lee S-J, Kenyon C. Lifespan extension by conditions that inhibit translation in Caenorhabditis elegans. Aging Cell. 2007;6: 95–110. doi:10.1111/j.1474-9726.2006.00267.x

41. Filer D, Thompson MA, Takhaveev V, Dobson AJ, Kotronaki I, Green JWM, et al. RNA polymerase III limits longevity downstream of TORC1. Nature. Nature Publishing Group; 2017;552: 263–267. doi:10.1038/nature25007

42. Dhahbi JM, Spindler SR, Atamna H, Yamakawa A, Boffelli D, Mote P, et al. 5' tRNA halves are present as abundant complexes in serum, concentrated in blood cells, and modulated by aging and calorie restriction. BMC Genomics. 2013;14: 298. doi:10.1186/1471-2164-14-298

43. Zhou W, Laird PW, Shen H. Comprehensive characterization, annotation and innovative use of Infinium DNA methylation BeadChip probes. Nucleic Acids Research. 2016;45: gkw967. doi:10.1093/nar/gkw967

44. Van Bortle K, Phanstiel DH, Snyder MP. Topological organization and dynamic regulation of human tRNA genes during macrophage differentiation. Genome Biology. Genome Biology; 2017;18: 180. doi:10.1186/s13059-017-1310-3

45. Down TA, Rakyan VK, Turner DJ, Flicek P, Li H, Kulesha E, et al. A Bayesian deconvolution strategy for immunoprecipitation-based DNA methylome analysis. Nature Biotechnology. 2008;26: 779–785. doi:10.1038/nbt1414

46. Amemiya HM, Kundaje A, Boyle AP. The ENCODE Blacklist: Identification of Problematic Regions of the Genome. Scientific Reports. 2019;9: 9354. doi:10.1038/s41598-019-45839-z

47. Geiger H, Haan G de, Florian MC. The ageing haematopoietic stem cell compartment. Nature Reviews Immunology. Nature Publishing Group; 2013;13: 376–389. doi:10.1038/nri3433

48. Lowe TM, Chan PP. tRNAscan-SE On-line: integrating search and context for analysis of transfer RNA genes. Nucleic Acids Research. 2016;44: W54–W57. doi:10.1093/nar/gkw413

49. Ziller MJ, Gu H, Müller F, Donaghey J, Tsai LT-Y, Kohlbacher O, et al. Charting a dynamic DNA methylation landscape of the human genome. Nature. 2013;500: 477–81. doi:10.1038/nature12433

50. Christensen BC, Houseman EA, Marsit CJ, Zheng S, Wrensch MR, Wiemels JL, et al. Aging and Environmental Exposures Alter Tissue-Specific DNA Methylation Dependent upon CpG Island Context. Schübeler D, editor. PLoS Genetics. 2009;5: e1000602. doi:10.1371/journal.pgen.1000602

51. Derrien T, Estellé J, Marco Sola S, Knowles DG, Raineri E, Guigó R, et al. Fast Computation and Applications of Genome Mappability. Ouzounis CA, editor. PLoS ONE. 2012;7: e30377.

doi:10.1371/journal.pone.0030377

52. Heyn H, Li N, Ferreira HJ, Moran S, Pisano DG, Gomez A, et al. Distinct DNA methylomes of newborns and centenarians. Proceedings of the National Academy of Sciences. 2012;109: 10522–10527. doi:10.1073/pnas.1120658109

53. Houseman EA, Accomando WP, Koestler DC, Christensen BC, Marsit CJ, Nelson HH, et al. DNA methylation arrays as surrogate measures of cell mixture distribution. BMC Bioinformatics. 2012;13: 86. doi:10.1186/1471-2105-13-86

54. Müller F, Scherer M, Assenov Y, Lutsik P, Walter J, Lengauer T, et al. RnBeads 2.0: comprehensive analysis of DNA methylation data. Genome Biology. Genome Biology; 2019;20: 55. doi:10.1186/s13059-019-1664-9

55. Meuleman W. Epilogos [Internet]. 2019. Available: `https://epilogos.altius.org/%20https://github.com/Altius/epilogos`

56. Schmitt BM, Rudolph KLM, Karagianni P, Fonseca NA, White RJ, Talianidis I, et al. High-resolution mapping of transcriptional dynamics across tissue development reveals a stable mRNA–tRNA interface. Genome Research. 2014;24: 1797–1807. doi:10.1101/gr.176784.114

57. Dittmar KA, Goodenbour JM, Pan T. Tissue-specific differences in human transfer RNA expression. PLoS genetics. 2006;2: e221. doi:10.1371/journal.pgen.0020221

58. Sagi D, Rak R, Gingold H, Adir I, Maayan G, Dahan O, et al. Tissue- and Time-Specific Expression of Otherwise Identical tRNA Genes. Chisholm AD, editor. PLOS Genetics. 2016;12: e1006264. doi:10.1371/journal.pgen.1006264

59. Reinius LE, Acevedo N, Joerink M, Pershagen G, Dahlén S-E, Greco D, et al. Differential DNA Methylation in Purified Human Blood Cells: Implications for Cell Lineage and Studies on Disease Susceptibility. Ting AH, editor. PLoS ONE. 2012;7: e41361. doi:10.1371/journal.pone.0041361

60. Slieker RC, Iterson M van, Luijk R, Beekman M, Zhernakova DV, Moed MH, et al. Age-related accrual of methylomic variability is linked to fundamental ageing mechanisms. Genome biology. Genome Biology; 2016;17: 191. doi:10.1186/s13059-016-1053-6

61. Gu Z, Eils R, Schlesner M. Complex heatmaps reveal patterns and correlations in multidimensional genomic data. Bioinformatics. 2016;32: 2847–2849. doi:10.1093/bioinformatics/btw313

62. Yang Z, Wong A, Kuh D, Paul DS, Rakyan VK, Leslie RD, et al. Correlation of an epigenetic mitotic clock with cancer risk. Genome Biology. Genome Biology; 2016;17: 205. doi:10.1186/s13059-016-1064-3

63. Nazor KL, Altun G, Lynch C, Tran H, Harness JV, Slavin I, et al. Recurrent Variations in DNA Methylation in Human Pluripotent Stem Cells and Their Differentiated Derivatives. Cell Stem Cell. 2012;10:

620–634. doi:10.1016/j.stem.2012.02.013

64. Loher P, Telonis AG, Rigoutsos I. MINTmap: fast and exhaustive profiling of nuclear and mitochondrial tRNA fragments from short RNA-seq data. Scientific reports. Nature Publishing Group; 2017;7: 41184. doi:10.1038/srep41184

65. Petkovich DA, Podolskiy DI, Lobanov AV, Lee S-G, Miller RA, Gladyshev VN. Using DNA Methylation Profiling to Evaluate Biological Age and Longevity Interventions. Cell Metabolism. 2017;25: 954–960.e6. doi:10.1016/j.cmet.2017.03.016

66. Ehrlich M. DNA hypermethylation in disease: mechanisms and clinical relevance. Epigenetics. Taylor & Francis; 2019;14: 1141–1163. doi:10.1080/15592294.2019.1638701

67. Lappalainen T, Greally JM. Associating cellular epigenetic models with human phenotypes. Nature Reviews Genetics. Nature Publishing Group; 2017;18: 441–451. doi:10.1038/nrg.2017.32

68. Goodenbour JM, Pan T. Diversity of tRNA genes in eukaryotes. Nucleic acids research. 2006;34: 6137–46. doi:10.1093/nar/gkl725

69. Keam SP, Young PE, McCorkindale AL, Dang THY, Clancy JL, Humphreys DT, et al. The human Piwi protein Hiwi2 associates with tRNA-derived piRNAs in somatic cells. Nucleic Acids Research. 2014;42: 8984–8995. doi:10.1093/nar/gku620

70. Geslain R, Pan T. Functional Analysis of Human tRNA Isodecoders. Journal of Molecular Biology. 2010;396: 821–831. doi:10.1016/j.jmb.2009.12.018

71. Kirchner S, Cai Z, Rauscher R, Kastelic N, Anding M, Czech A, et al. Alteration of protein function by a silent polymorphism linked to tRNA abundance. Hurst L, editor. PLOS Biology. 2017;15: e2000779. doi:10.1371/journal.pbio.2000779

72. Li S, Shi X, Chen M, Xu N, Sun D, Bai R, et al. Angiogenin promotes colorectal cancer metastasis via tiRNA production. International Journal of Cancer. 2019; ijc.32245. doi:10.1002/ijc.32245

73. Kim HK, Fuchs G, Wang S, Wei W, Zhang Y, Park H, et al. A transfer-RNA-derived small RNA regulates ribosome biogenesis. Nature. Nature Publishing Group; 2017;552: 57–62. doi:10.1038/nature25005

74. Martinez G, Choudury SG, Slotkin RK. tRNA-derived small RNAs target transposable element transcripts. Nucleic Acids Research. 2017;45: 5142–5152. doi:10.1093/nar/gkx103

75. Gomez-Roman N, Grandori C, Eisenman RN, White RJ. Direct activation of RNA polymerase III transcription by c-Myc. Nature. 2003;421: 290–294. doi:10.1038/nature01327

76. Crighton D. p53 represses RNA polymerase III transcription by targeting TBP and inhibiting promoter occupancy by TFIIIB. The EMBO Journal. 2003;22: 2810–2820. doi:10.1093/emboj/cdg265

77. Sutcliffe JE, Brown TRP, Allison SJ, Scott PH, White RJ. Retinoblastoma Protein Disrupts Interactions

Required for RNA Polymerase III Transcription. Molecular and Cellular Biology. 2000;20: 9192–9202. doi:10.1128/MCB.20.24.9192-9202.2000

78. Schmitt BM, Rudolph KLM, Karagianni P, Fonseca NA, White RJ, Talianidis I, et al. High-resolution mapping of transcriptional dynamics across tissue development reveals a stable mRNA-tRNA interface. Genome research. 2014;24: 1797–807. doi:10.1101/gr.176784.114

79. Gingold H, Tehler D, Christoffersen NR, Nielsen MM, Asmar F, Kooistra SM, et al. A Dual Program for Translation Regulation in Cellular Proliferation and Differentiation. Cell. Elsevier Inc. 2014;158: 1281–1292. doi:10.1016/j.cell.2014.08.011

80. Rudolph KLM, Schmitt BM, Villar D, White RJ, Marioni JC, Kutter C, et al. Codon-Driven Translational Efficiency Is Stable across Diverse Mammalian Cell States. Galtier N, editor. PLoS genetics. 2016;12: e1006024. doi:10.1371/journal.pgen.1006024

81. Gingold H, Dahan O, Pilpel Y. Dynamic changes in translational efficiency are deduced from codon usage of the transcriptome. Nucleic acids research. 2012;40: 10053–63. doi:10.1093/nar/gks772

82. Iben JR, Maraia RJ. tRNA gene copy number variation in humans. Gene. 2014;536: 376–384. doi:10.1016/j.gene.2013.11.049

83. Darrow EM, Chadwick BP. A novel tRNA variable number tandem repeat at human chromosome 1q23.3 is implicated as a boundary element based on conservation of a CTCF motif in mouse. Nucleic Acids Research. 2014;42: 6421–6435. doi:10.1093/nar/gku280

84. Huang S-q, Sun B, Xiong Z-p, Shu Y, Zhou H-h, Zhang W, et al. The dysregulation of tRNAs and tRNA derivatives in cancer. Journal of Experimental & Clinical Cancer Research. Journal of Experimental & Clinical Cancer Research; 2018;37: 101. doi:10.1186/s13046-018-0745-z

85. Krishnan P, Ghosh S, Wang B, Heyns M, Li D, Mackey JR, et al. Genome-wide profiling of transfer RNAs and their role as novel prognostic markers for breast cancer. Scientific Reports. Nature Publishing Group; 2016;6: 32843. doi:10.1038/srep32843

86. Müller CA, Nieduszynski CA. DNA replication timing influences gene expression level. The Journal of Cell Biology. 2017;216: 1907–1914. doi:10.1083/jcb.201701061

87. Du Q, Bert SA, Armstrong NJ, Caldon CE, Song JZ, Nair SS, et al. Replication timing and epigenome remodelling are associated with the nature of chromosomal rearrangements in cancer. Nature Communications. Springer US; 2019;10: 416. doi:10.1038/s41467-019-08302-1

88. Cruickshanks HA, McBryan T, Nelson DM, VanderKraats ND, Shah PP, Tuyn J van, et al. Senescent cells harbour features of the cancer epigenome. Nature Cell Biology. 2013;15: 1495–1506. doi:10.1038/ncb2879

89. Raab JR, Chiu J, Zhu J, Katzman S, Kurukuti S, Wade PA, et al. Human tRNA genes function as

chromatin insulators. The EMBO journal. Nature Publishing Group; 2012;31: 330–50. doi:10.1038/emboj.2011.406

90. Noma K-i, Cam HP, Maraia RJ, Grewal SIS. A role for TFIIIC transcription factor complex in genome organization. Cell. 2006;125: 859–72. doi:10.1016/j.cell.2006.04.028

91. Sun L, Yu R, Dang W. Chromatin Architectural Changes during Cellular Senescence and Aging. Genes. 2018;9: 211. doi:10.3390/genes9040211

92. Moayyeri A, Hammond CJ, Valdes AM, Spector TD. Cohort Profile: TwinsUK and Healthy Ageing Twin Study. International Journal of Epidemiology. 2013;42: 76–85. doi:10.1093/ije/dyr207

93. Harvey NC, Javaid K, Bishop N, Kennedy S, Papageorghiou AT, Fraser R, et al. MAVIDOS Maternal Vitamin D Osteoporosis Study: study protocol for a randomized controlled trial. The MAVIDOS Study Group. Trials. 2012;13: 13. doi:10.1186/1745-6215-13-13

94. Syddall H, Aihie Sayer A, Dennison E, Martin H, Barker D, Cooper C. Cohort Profile: The Hertfordshire Cohort Study. International Journal of Epidemiology. 2005;34: 1234–1242. doi:10.1093/ije/dyi127

95. Quinlan AR, Hall IM. BEDTools: a flexible suite of utilities for comparing genomic features. Bioinformatics. University of Utah; 2010;26: 841–842. doi:10.1093/bioinformatics/btq033

96. Bell CG, Gao F, Yuan W, Roos L, Acton RJ, Xia Y, et al. Obligatory and facilitative allelic variation in the DNA methylome within common disease-associated loci. Nature Communications. 2018;9: 8. doi:10.1038/s41467-017-01586-1

97. Lienhard M, Grimm C, Morkel M, Herwig R, Chavez L. MEDIPS: genome-wide differential coverage analysis of sequencing data derived from DNA enrichment experiments. Bioinformatics. 2014;30: 284–286. doi:10.1093/bioinformatics/btt650

98. Ernst J, Kheradpour P, Mikkelsen TS, Shoresh N, Ward LD, Epstein CB, et al. Mapping and analysis of chromatin state dynamics in nine human cell types. Nature. 2011;473: 43–49. doi:10.1038/nature09906

99. Bell CG, Wilson GA, Butcher LM, Roos C, Walter L, Beck S. Human-specific CpG "beacons" identify loci associated with human-specific traits and disease. Epigenetics. 2012;7: 1188–99. doi:10.4161/epi.22127

100. North BV, Curtis D, Sham PC. A Note on the Calculation of Empirical P Values from Monte Carlo Procedures. The American Journal of Human Genetics. 2003;72: 498–499. doi:10.1086/346173

101. Li L-C, Dahiya R. MethPrimer: designing primers for methylation PCRs. Bioinformatics (Oxford, England). 2002;18: 1427–31. Available: `http://www.ncbi.nlm.nih.gov/pubmed/12424112`

102. Andrews S. FastQC [Internet]. Cambridge: Babraham Bioinformatics; 2010. Available: `http://www.bioinformatics.babraham.ac.uk/projects/fastqc`

103. Ewels P, Magnusson M, Lundin S, Käller M. MultiQC: summarize analysis results for multiple tools and

samples in a single report. Bioinformatics (Oxford, England). 2016;32: 3047–8. doi:10.1093/bioinformatics/btw354

104. Martin M. Cutadapt removes adapter sequences from high-throughput sequencing reads. EMBnetjournal. 2011;17: 10. doi:10.14806/ej.17.1.200

105. Krueger F. Trim Galore [Internet]. 2015. Available: `https://www.bioinformatics.babraham.ac.uk/projects/trim%7B/_%7Dgalore/`

106. Krueger F, Andrews SR. Bismark: a flexible aligner and methylation caller for Bisulfite-Seq applications. Bioinformatics. 2011;27: 1571–1572. doi:10.1093/bioinformatics/btr167

107. Langmead B, Salzberg SL. Fast gapped-read alignment with Bowtie 2. Nature methods. 2012;9: 357–9. doi:10.1038/nmeth.1923

108. Ritchie ME, Phipson B, Wu D, Hu Y, Law CW, Shi W, et al. limma powers differential expression analyses for RNA-sequencing and microarray studies. Nucleic Acids Research. 2015;43: e47–e47. doi:10.1093/nar/gkv007

109. Sean D, Meltzer PS. GEOquery: A bridge between the Gene Expression Omnibus (GEO) and BioConductor. Bioinformatics. 2007;23: 1846–1847. doi:10.1093/bioinformatics/btm254

110. Grossman RL, Heath AP, Ferretti V, Varmus HE, Lowy DR, Kibbe WA, et al. Toward a Shared Vision for Cancer Genomic Data. New England Journal of Medicine. 2016;375: 1109–1112. doi:10.1056/NEJMp1607591

111. Juzenas S, Venkatesh G, Hübenthal M, Hoeppner MP, Du ZG, Paulsen M, et al. A comprehensive, cell specific microRNA catalogue of human peripheral blood. Nucleic Acids Research. 2017;45: 9290–9301. doi:10.1093/nar/gkx706

Supplementary materials

Supplementary Figures

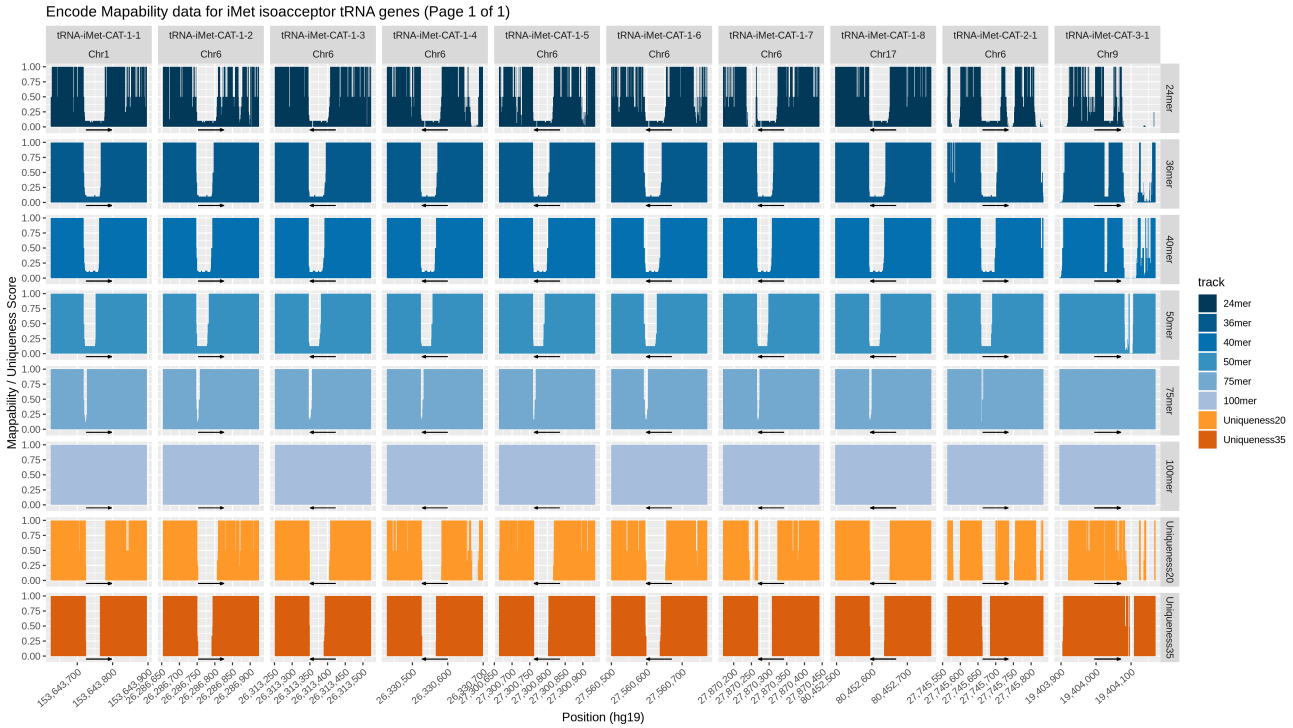

Fig S1. Example of mappability data from the encode mappability tracks [51] for the initiator methionine tRNA genes.

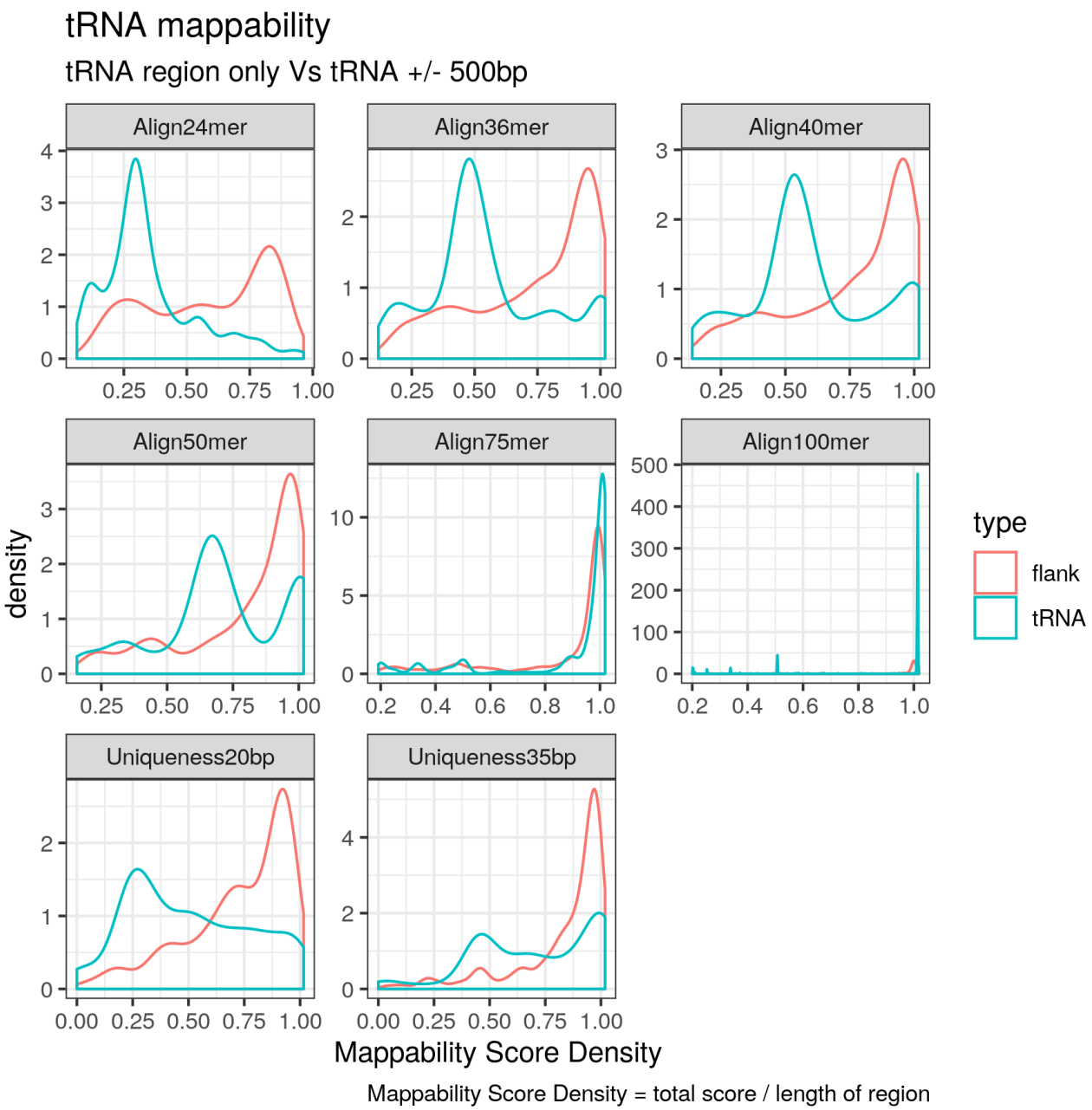

Fig S2. Mappability score density of the tRNAome increases with read length and is greater when flanking regions ($\pm 500bp$) are included. Mappability score density is computed as the area under the encode mappability tracks [51] over the length of the region.

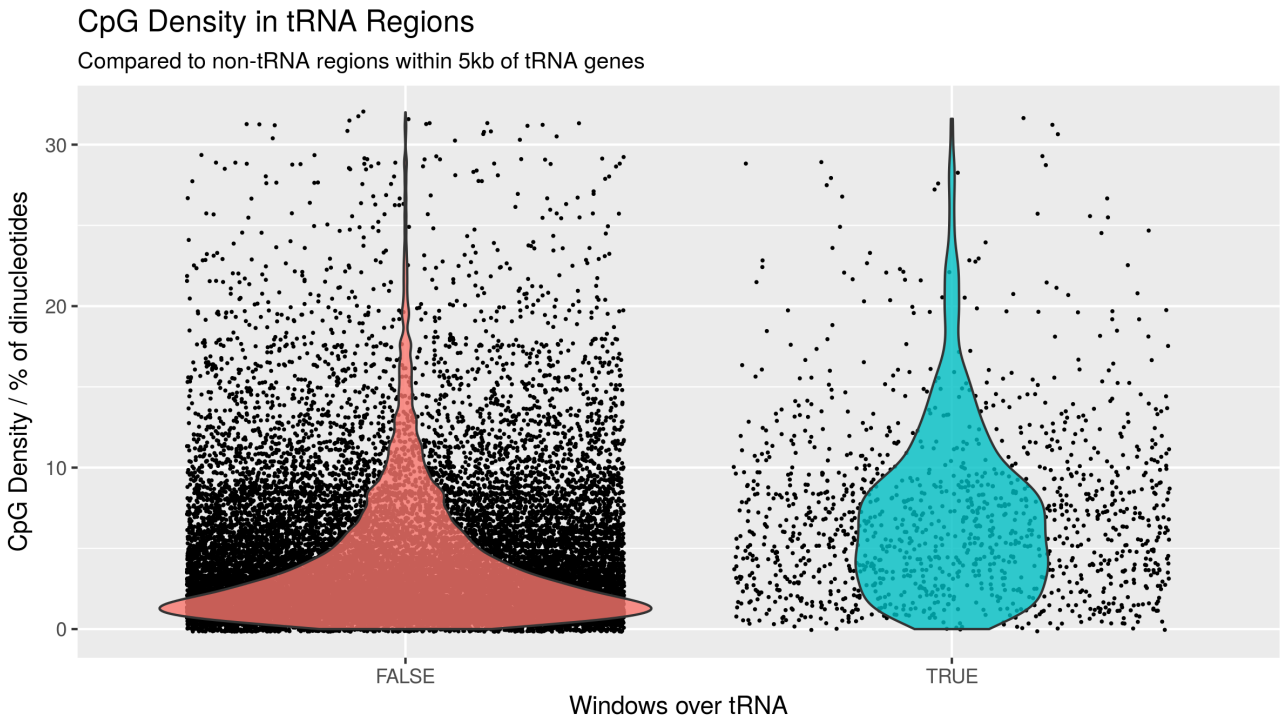

Fig S3. CpG Density in windows overlapping tRNA genes compared to that of non-tRNA overlapping windows in flanking sequences (+/-5kb)

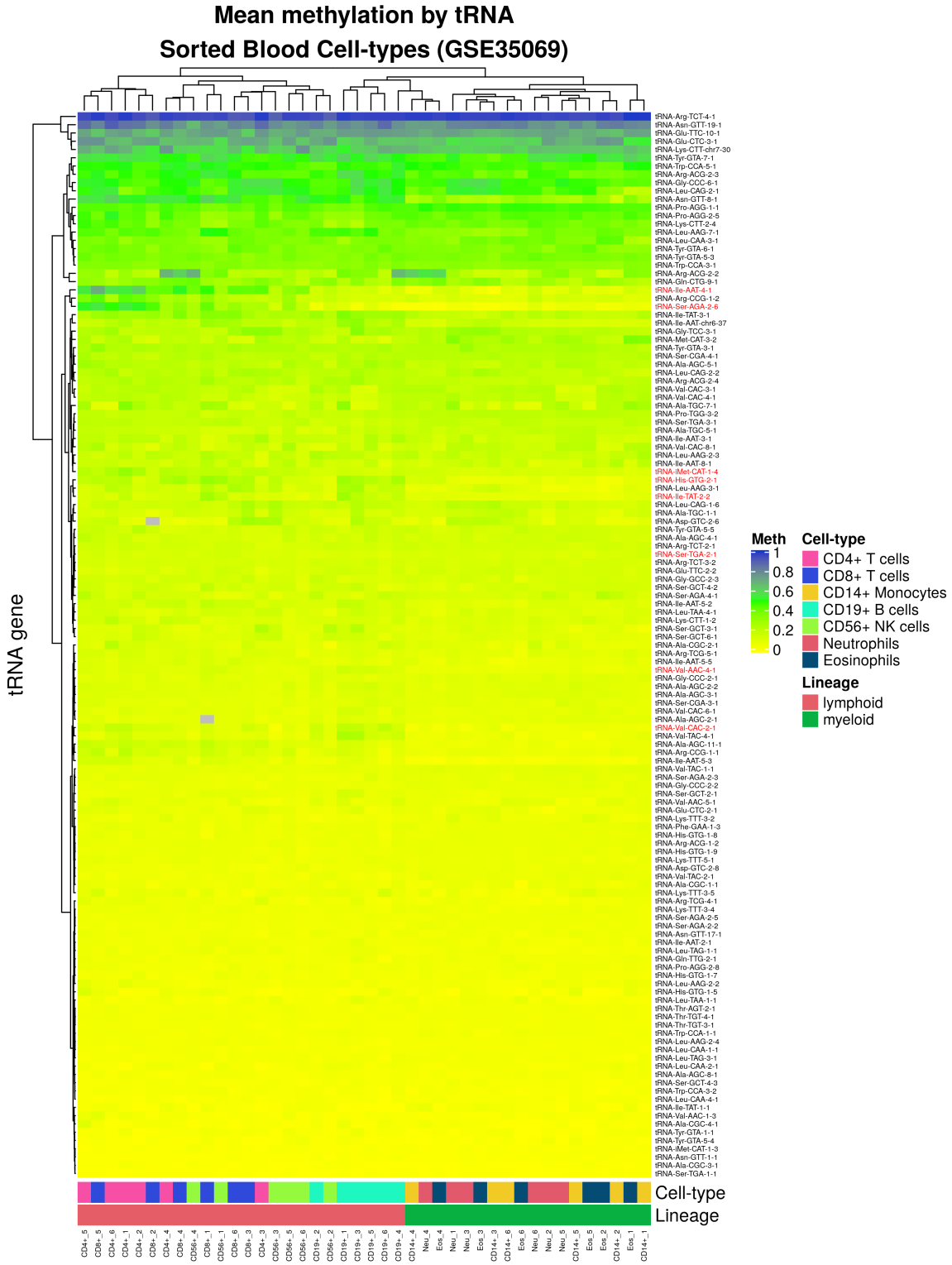

Fig S4. Heatmap Mean Methylation of probes covering each tRNA in 7 cell-type fractions from 6 Male individuals. Showing all 150 tRNAs covered by 213 probes on the Illumina 450k array. Data from GSE35069 [59] downloaded using `GEOquery` [109]. Generated with the `ComplexHeatmap` `R` package [61].

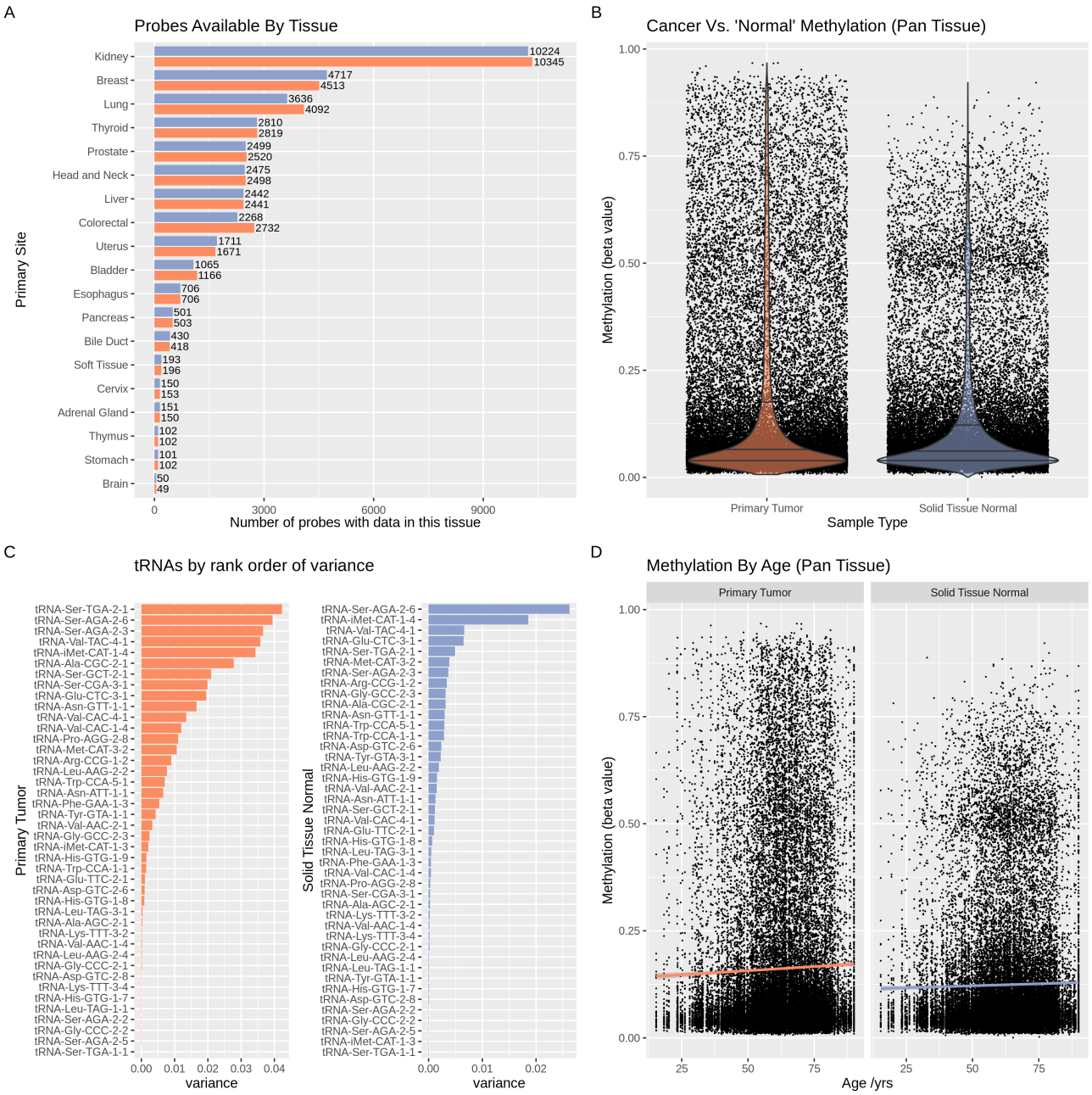

Fig S5. Global properties of tRNA methylation data for 45 tRNA genes across 19 tissues with matched normal and tumour samples from 733 cases in TCGA [62,63].

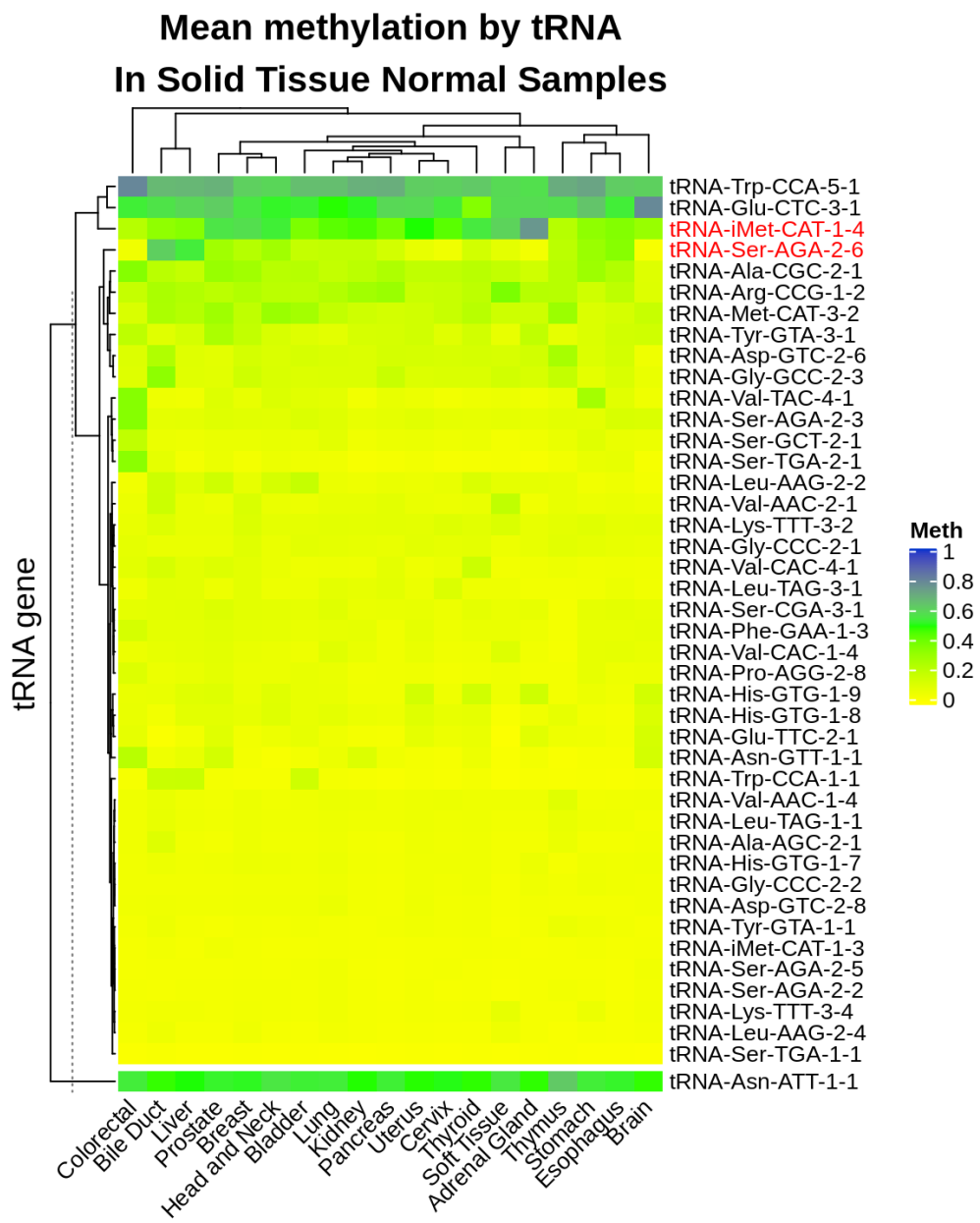

Fig S6. Mean Methylation of 43 tRNAs in 19 tissues. Possible pseudogene (tRNA-Asn-ATT-1-1) is shown in a separate cluster beneath the main heatmap [61].

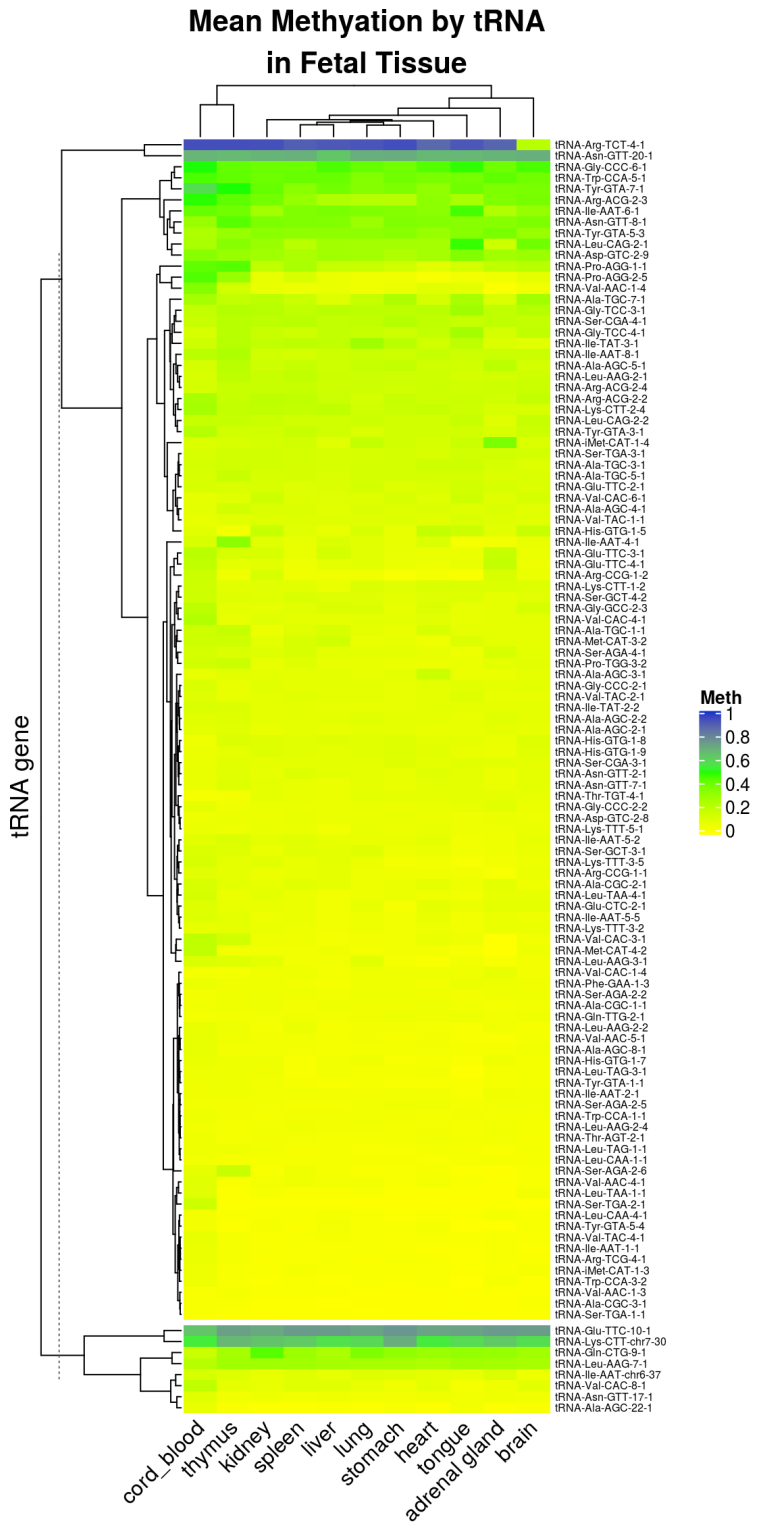

Fig S7. Mean Methylation of 115 tRNAs in 11 tissues. Possible pseudogenes are shown in a separate cluster beneath the main heatmap [61].

MINTmap reference Fragment distribution

In the original MINTmap reference (Figure S8b) there are peaks at around 18nt, 22nt and 32nt. This is consistent with the expected tRNA fragment size distributions with 'tRNA halves' at 30-33nt and other tRFs at 18nt and 22nt. In our custom reference (Figure S8a) whilst there is still a peak at ˜18nt, with suggestions of peaks near 22nt and 32nt the tRNA fragment length distribution is somewhat different from that of the standard MINTmap reference. There are larger peaks at ˜28 and ˜40nt consistent with the longer fragments expected given that this reference aimed to target fragments derived from pre-tRNAs not tRFs derived from mature tRNAs.

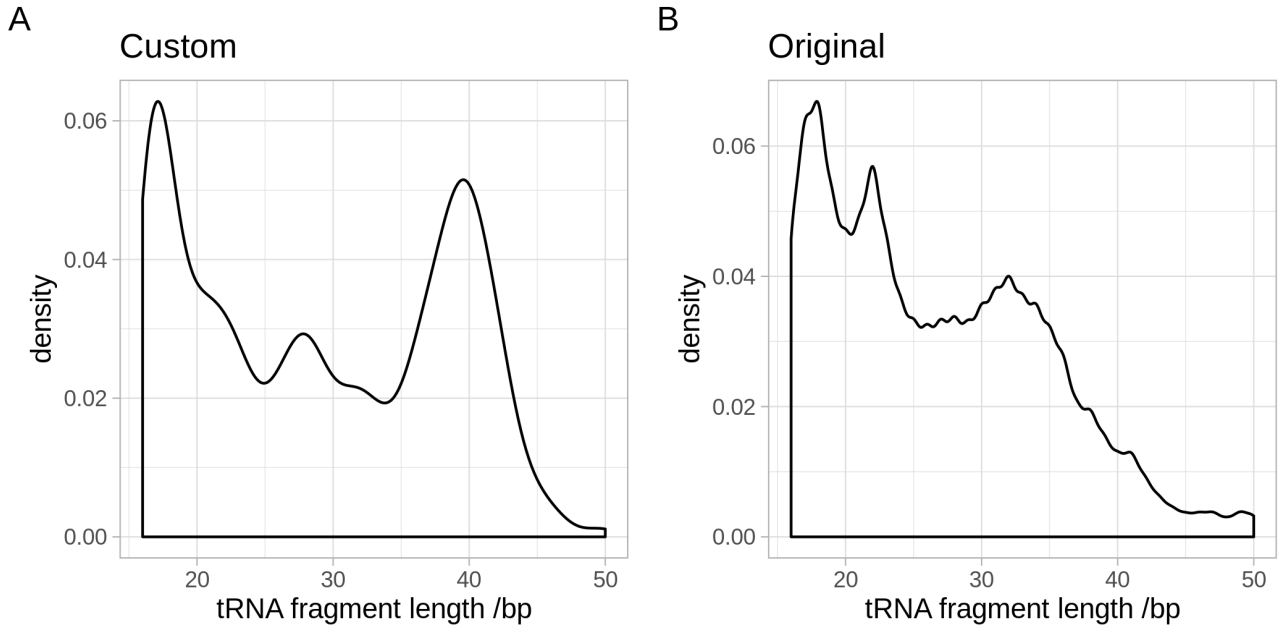

Fig S8. Comparison of the fragment size distributions between our custom reference (A) and the original the MINTmap reference (B).

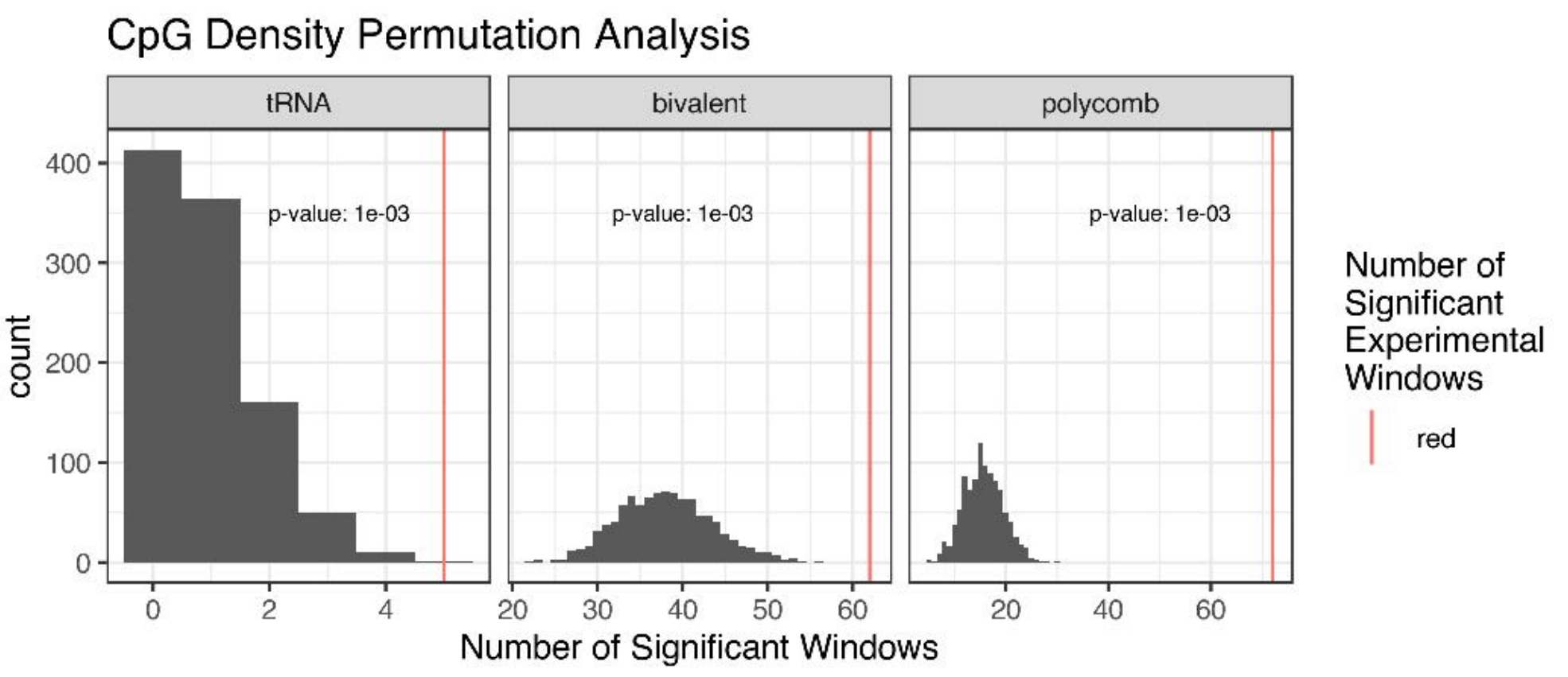
CpG Density Permutation Analysis
tRNA
bivalent
polycomb
p-value: 1e-03
p-value: 1e-03
p-value: 1e-03
count
400
300
200
100
0
0
2
4
20
30
40
50
60
20
40
60
Number of Significant Windows
Number of Significant Experimental Windows
red

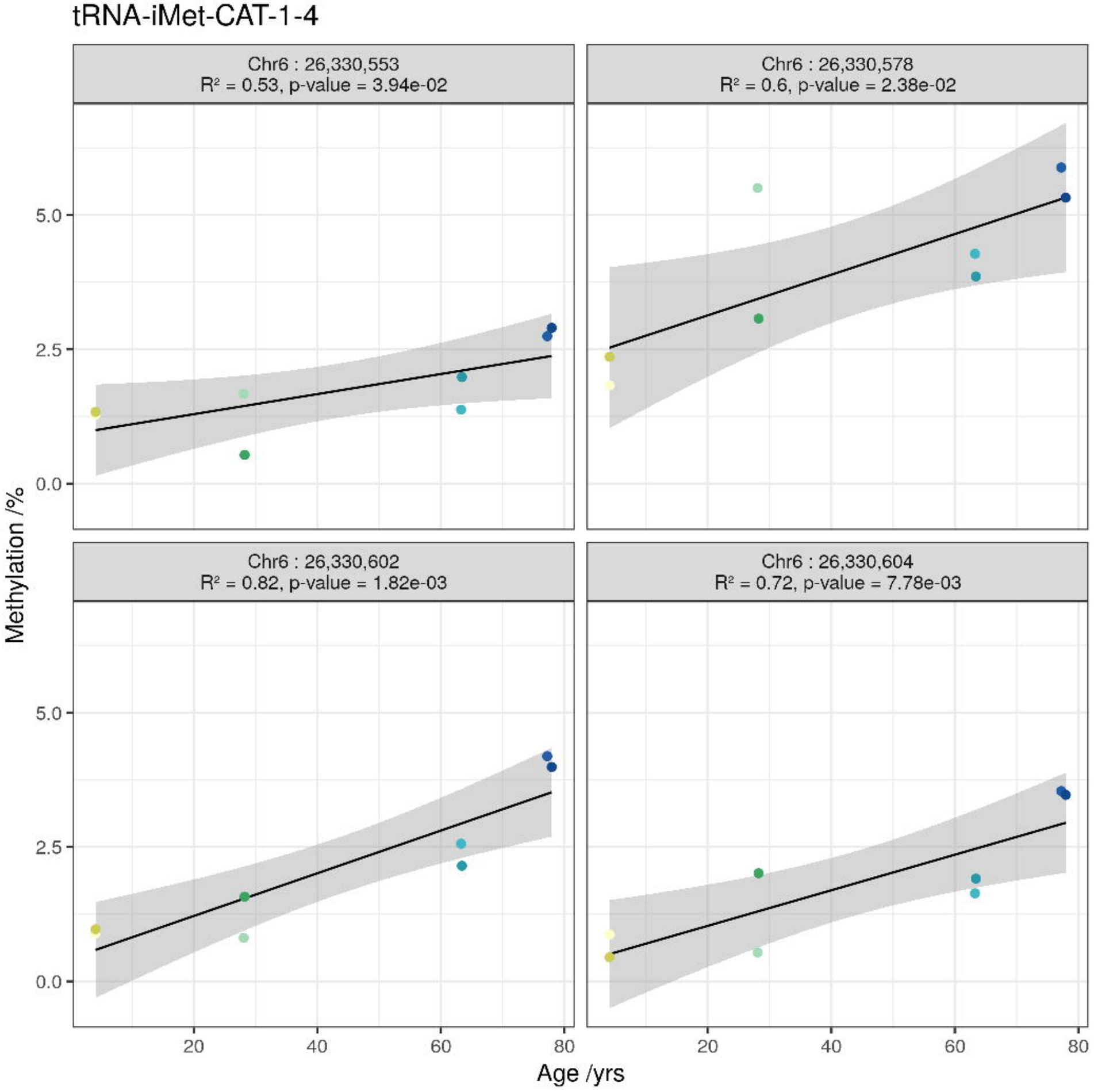
tRNA-iMet-CAT-1-4
Chr6 : 26,330,553
R² = 0.53, p-value = 3.94e-02
Chr6 : 26,330,578
R² = 0.6, p-value = 2.38e-02
Chr6 : 26,330,602
R² = 0.82, p-value = 1.82e-03
Chr6 : 26,330,604
R² = 0.72, p-value = 7.78e-03
Methylation /%
0.0
2.5
5.0
20
40
60
80
Age /yrs

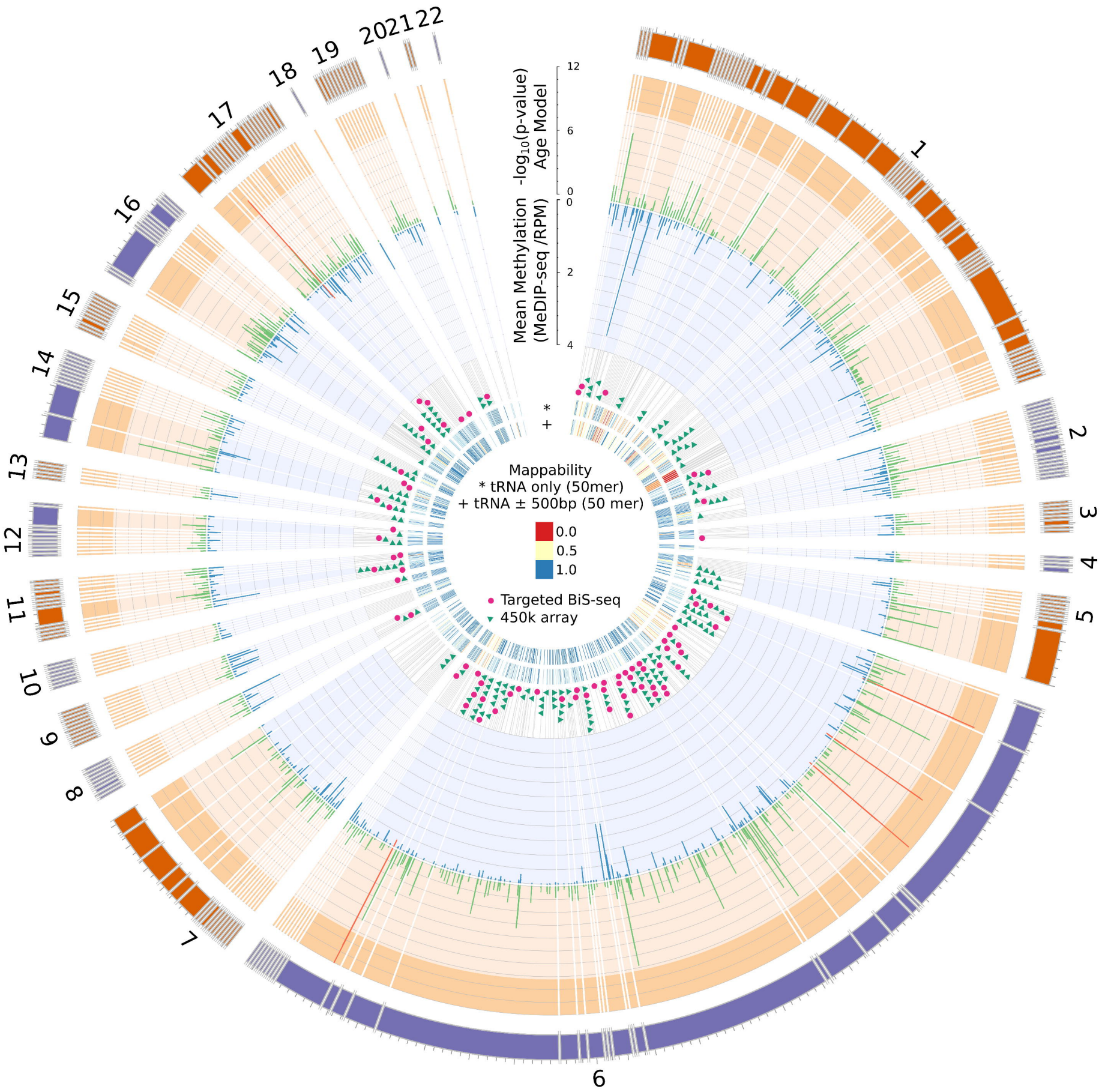
1
2
3
4
5
6
7
8
9
10
11
12
13
14
15
16
17
18
19
20
21
22
-log10(p-value) Age Model
12
6
0
Mean Methylation (MeDIP-seq /RPM)
0
2
4
+ *
Mappability
* tRNA only (50mer)
+ tRNA ± 500bp (50 mer)
0.0
0.5
1.0
Targeted BiS-seq
450k array

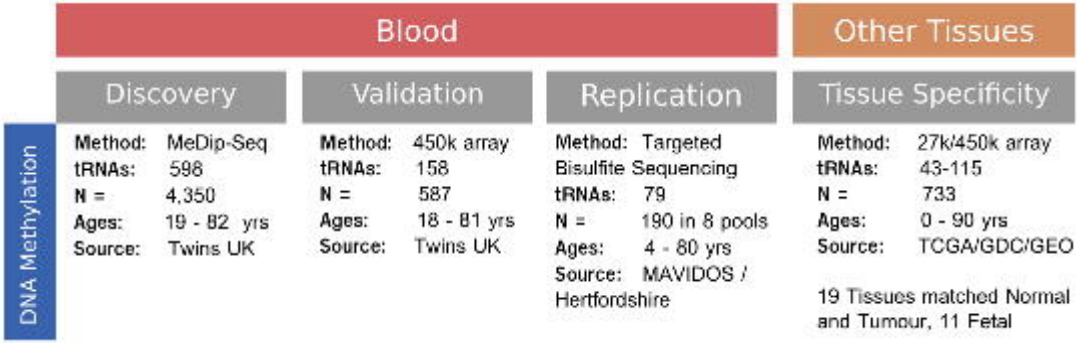
Blood
Other Tissues
Discovery
Validation
Replication
Tissue Specificity
DNA Methylation
Method: MeDip-Seq
tRNAs: 598
N = 4,350
Ages: 19 - 82 yrs
Source: Twins UK
Method: 450k array
tRNAs: 158
N = 587
Ages: 18 - 81 yrs
Source: Twins UK
Method: Targeted Bisulfite Sequencing
tRNAs: 79
N = 190 in 8 pools
Ages: 4 - 80 yrs
Source: MAVIDOS / Hertfordshire
Method: 27k/450k array
tRNAs: 43-115
N = 733
Ages: 0 - 90 yrs
Source: TCGA/GDC/GEO
19 Tissues matched Normal and Tumour, 11 Fetal

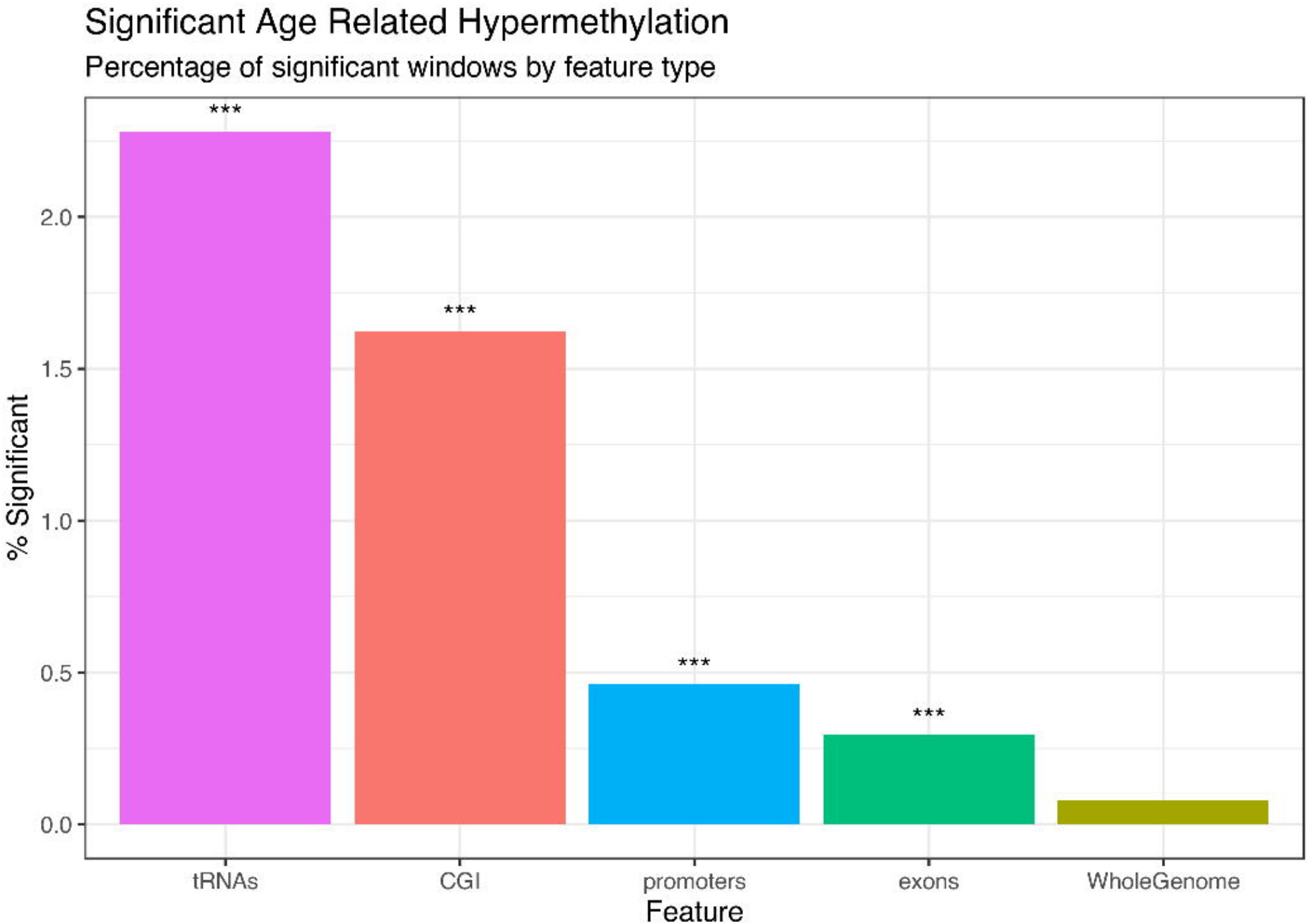
Significant Age Related Hypermethylation
Percentage of significant windows by feature type
% Significant
2.0
1.5
1.0
0.5
0.0
***
***
***
***
tRNAs
CGI
promoters
exons
WholeGenome
Feature

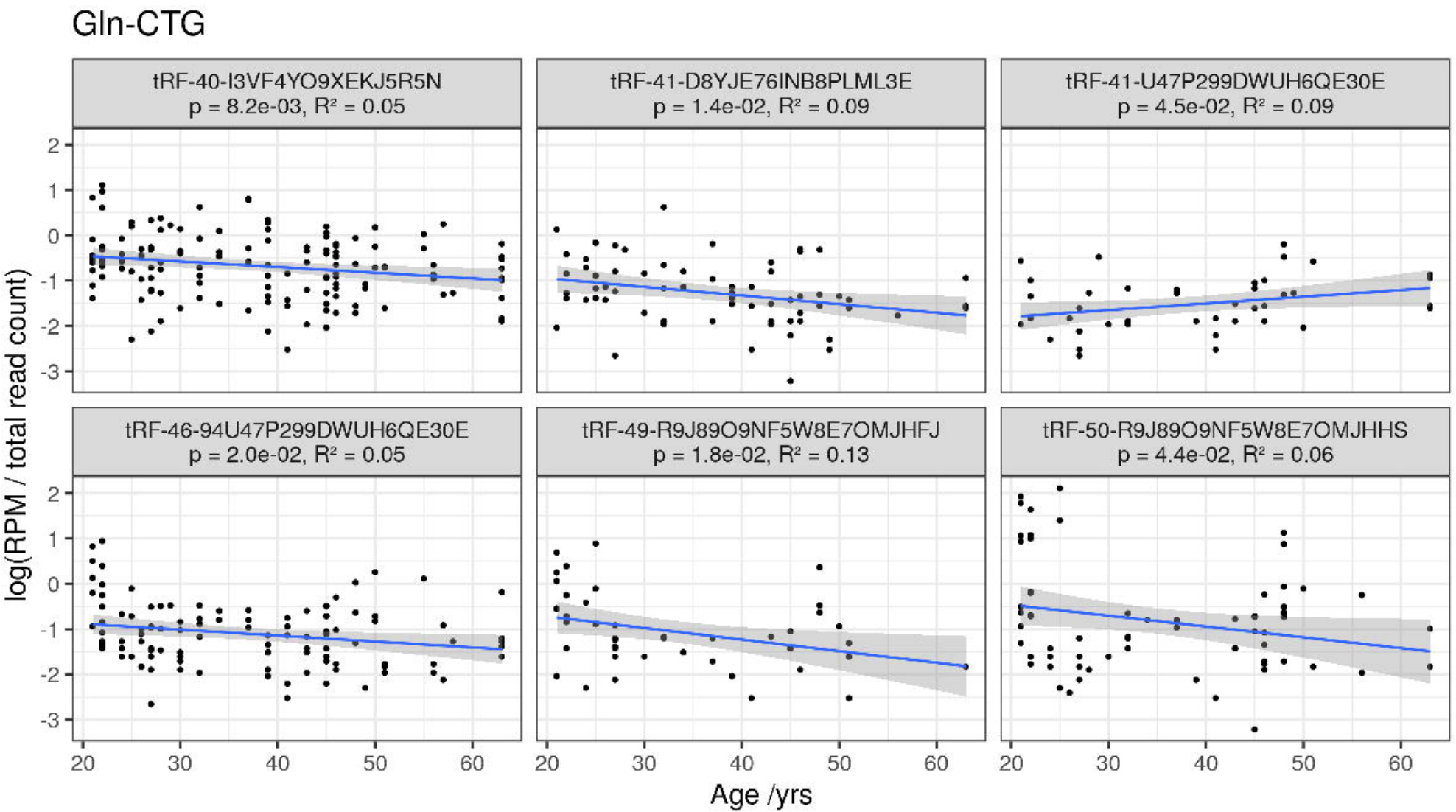
Gln-CTG
tRF-40-I3VF4YO9XEKJ5R5N
p = 8.2e-03, R² = 0.05
tRF-41-D8YJE76INB8PLML3E
p = 1.4e-02, R² = 0.09
tRF-41-U47P299DWUH6QE30E
p = 4.5e-02, R² = 0.09
tRF-46-94U47P299DWUH6QE30E
p = 2.0e-02, R² = 0.05
tRF-49-R9J89O9NF5W8E7OMJHFJ
p = 1.8e-02, R² = 0.13
tRF-50-R9J89O9NF5W8E7OMJHHS
p = 4.4e-02, R² = 0.06
log(RPM / total read count)
Age /yrs

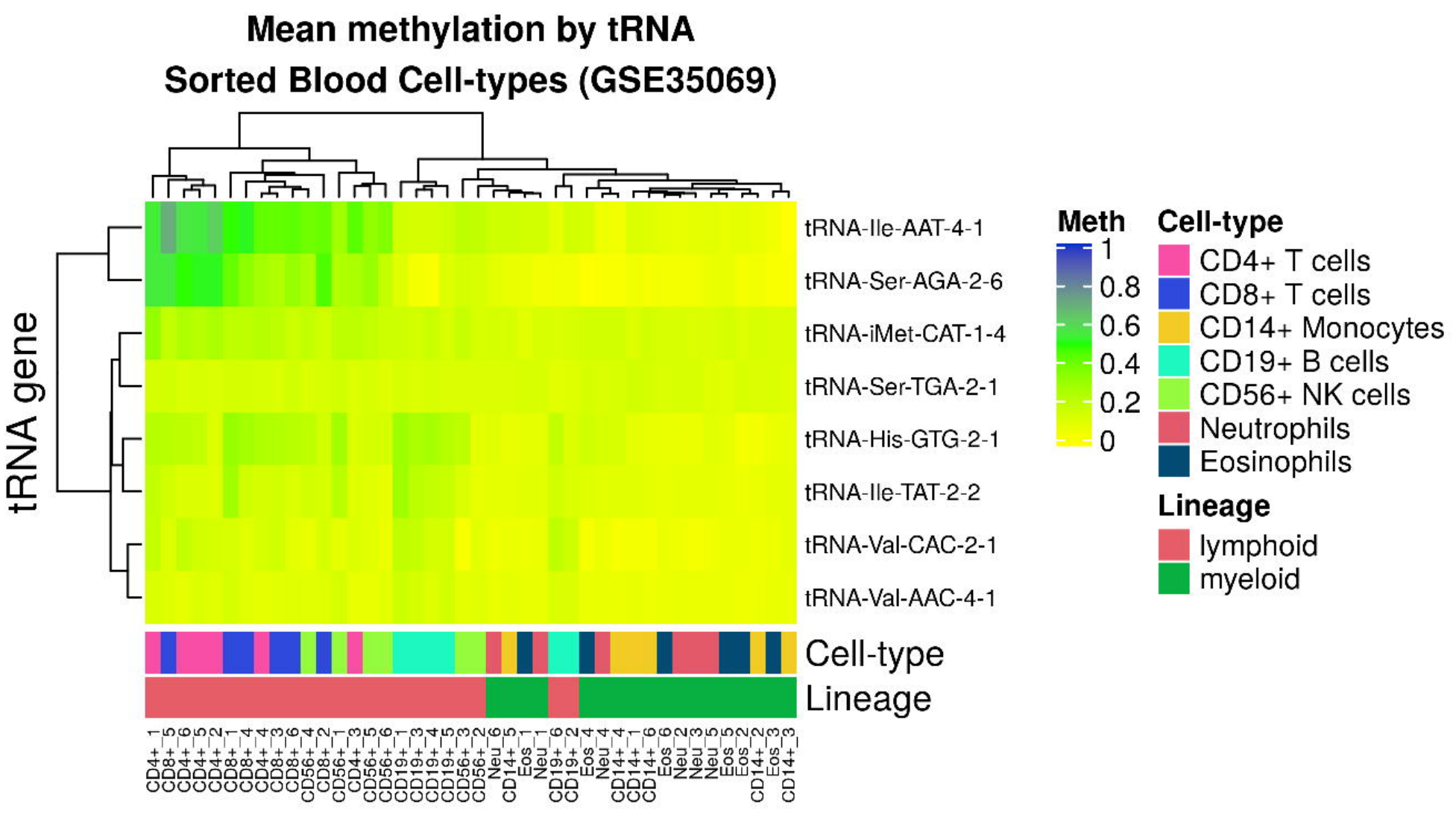
Mean methylation by tRNA
Sorted Blood Cell-types (GSE35069)
tRNA gene
tRNA-Ile-AAT-4-1
tRNA-Ser-AGA-2-6
tRNA-iMet-CAT-1-4
tRNA-Ser-TGA-2-1
tRNA-His-GTG-2-1
tRNA-Ile-TAT-2-2
tRNA-Val-CAC-2-1
tRNA-Val-AAC-4-1
Cell-type
Lineage
CD4+_1
CD8+_5
CD4+_6
CD4+_5
CD4+_2
CD8+_1
CD8+_4
CD4+_4
CD8+_3
CD8+_6
CD56+_4
CD8+_2
CD56+_1
CD4+_3
CD56+_5
CD56+_6
CD19+_1
CD19+_3
CD19+_4
CD19+_5
CD56+_3
CD56+_2
Neu_6
CD14+_5
Eos_1
Neu_1
CD19+_6
CD19+_2
Eos_4
Neu_4
CD14+_4
CD14+_1
CD14+_6
Eos_6
Neu_2
Neu_3
Neu_5
Eos_5
Eos_2
CD14+_2
Eos_3
CD14+_3
Meth
1
0.8
0.6
0.4
0.2
0
Cell-type
CD4+ T cells
CD8+ T cells
CD14+ Monocytes
CD19+ B cells
CD56+ NK cells
Neutrophils
Eosinophils
Lineage
lymphoid
myeloid

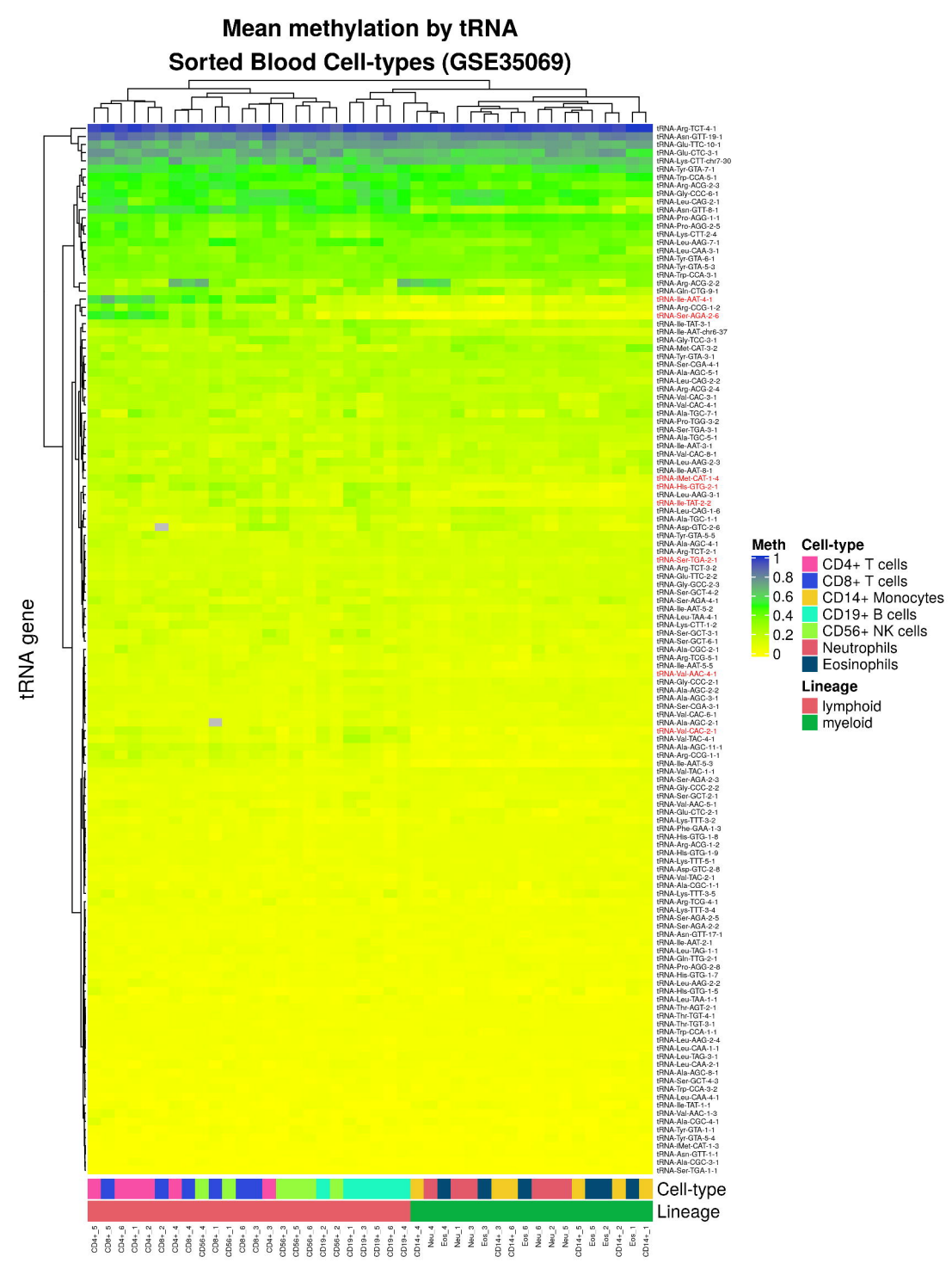
Mean methylation by tRNA
Sorted Blood Cell-types (GSE35069)
tRNA gene
Meth
1
0.8
0.6
0.4
0.2
0
Cell-type
CD4+ T cells
CD8+ T cells
CD14+ Monocytes
CD19+ B cells
CD56+ NK cells
Neutrophils
Eosinophils
Lineage
lymphoid
myeloid
Cell-type
Lineage

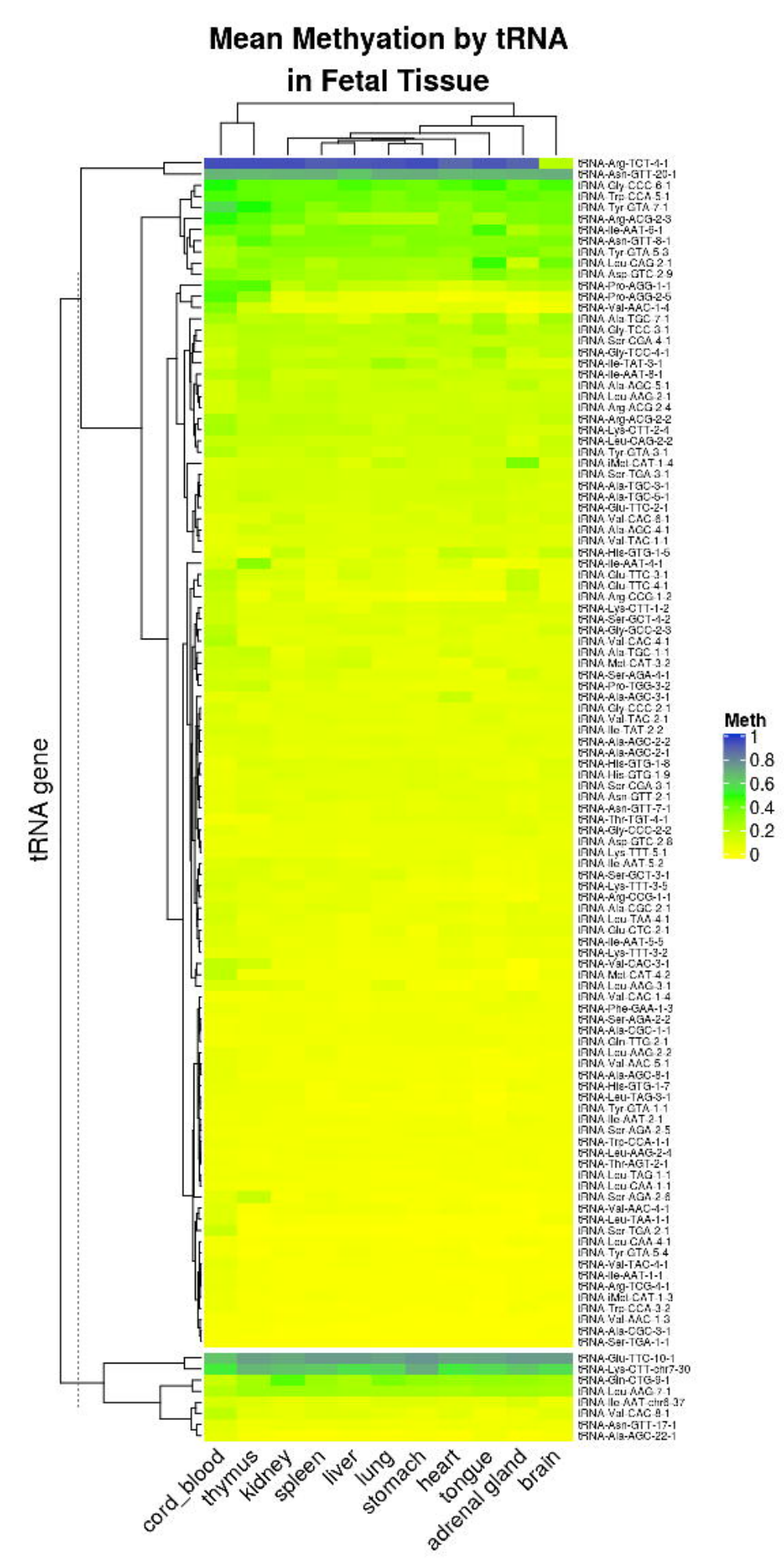
Mean Methyation by tRNA
in Fetal Tissue
tRNA gene
Meth
1
0.8
0.6
0.4
0.2
0
cord_blood
thymus
kidney
spleen
liver
lung
stomach
heart
tongue
adrenal gland
brain

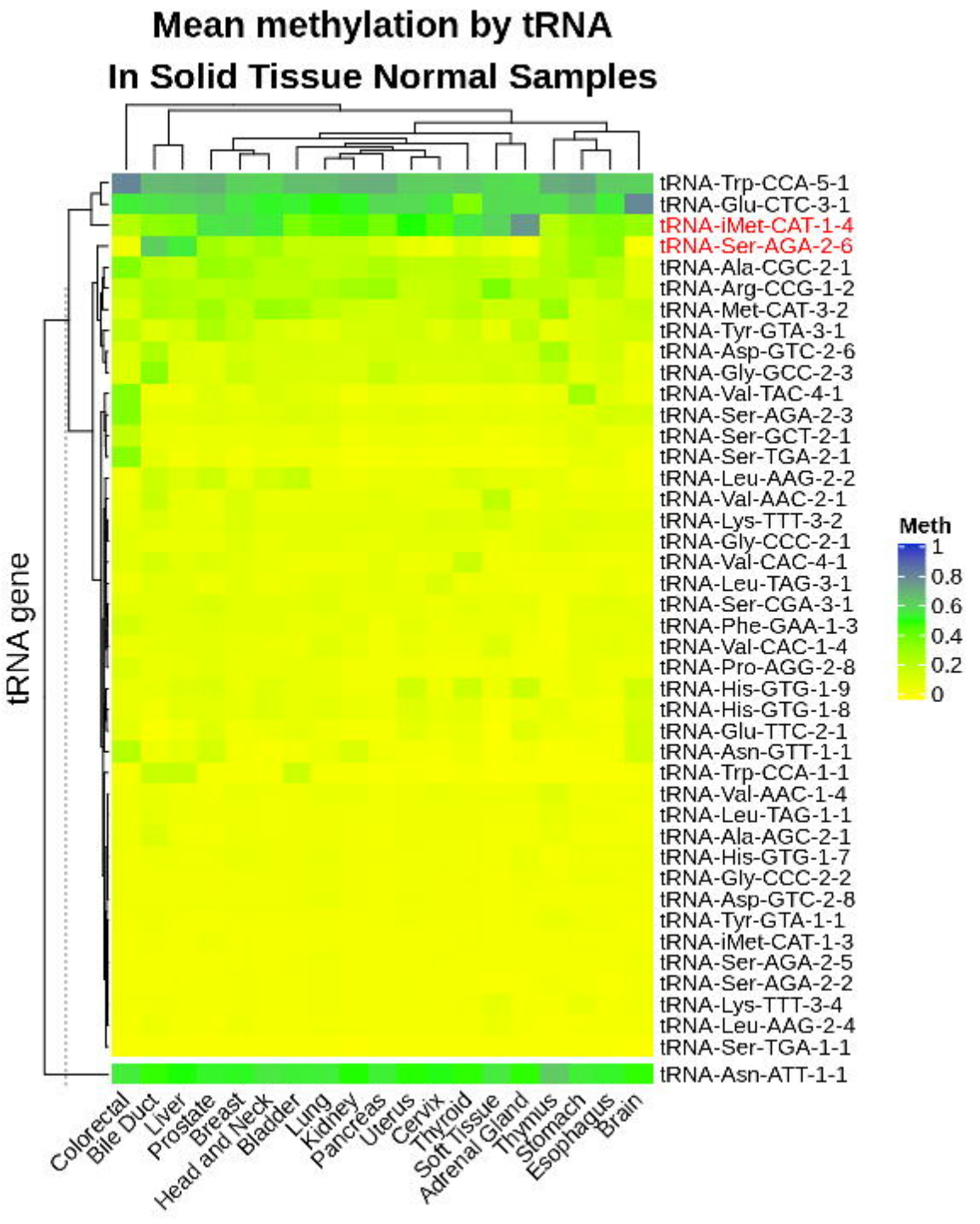
Mean methylation by tRNA
In Solid Tissue Normal Samples
tRNA gene
tRNA-Trp-CCA-5-1
tRNA-Glu-CTC-3-1
tRNA-iMet-CAT-1-4
tRNA-Ser-AGA-2-6
tRNA-Ala-CGC-2-1
tRNA-Arg-CCG-1-2
tRNA-Met-CAT-3-2
tRNA-Tyr-GTA-3-1
tRNA-Asp-GTC-2-6
tRNA-Gly-GCC-2-3
tRNA-Val-TAC-4-1
tRNA-Ser-AGA-2-3
tRNA-Ser-GCT-2-1
tRNA-Ser-TGA-2-1
tRNA-Leu-AAG-2-2
tRNA-Val-AAC-2-1
tRNA-Lys-TTT-3-2
tRNA-Gly-CCC-2-1
tRNA-Val-CAC-4-1
tRNA-Leu-TAG-3-1
tRNA-Ser-CGA-3-1
tRNA-Phe-GAA-1-3
tRNA-Val-CAC-1-4
tRNA-Pro-AGG-2-8
tRNA-His-GTG-1-9
tRNA-His-GTG-1-8
tRNA-Glu-TTC-2-1
tRNA-Asn-GTT-1-1
tRNA-Trp-CCA-1-1
tRNA-Val-AAC-1-4
tRNA-Leu-TAG-1-1
tRNA-Ala-AGC-2-1
tRNA-His-GTG-1-7
tRNA-Gly-CCC-2-2
tRNA-Asp-GTC-2-8
tRNA-Tyr-GTA-1-1
tRNA-iMet-CAT-1-3
tRNA-Ser-AGA-2-5
tRNA-Ser-AGA-2-2
tRNA-Lys-TTT-3-4
tRNA-Leu-AAG-2-4
tRNA-Ser-TGA-1-1
tRNA-Asn-ATT-1-1
Meth
1
0.8
0.6
0.4
0.2
0
Colorectal
Bile Duct
Liver
Prostate
Breast
Head and Neck
Bladder
Lung
Kidney
Pancreas
Uterus
Cervix
Thyroid
Soft Tissue
Adrenal Gland
Thymus
Stomach
Esophagus
Brain

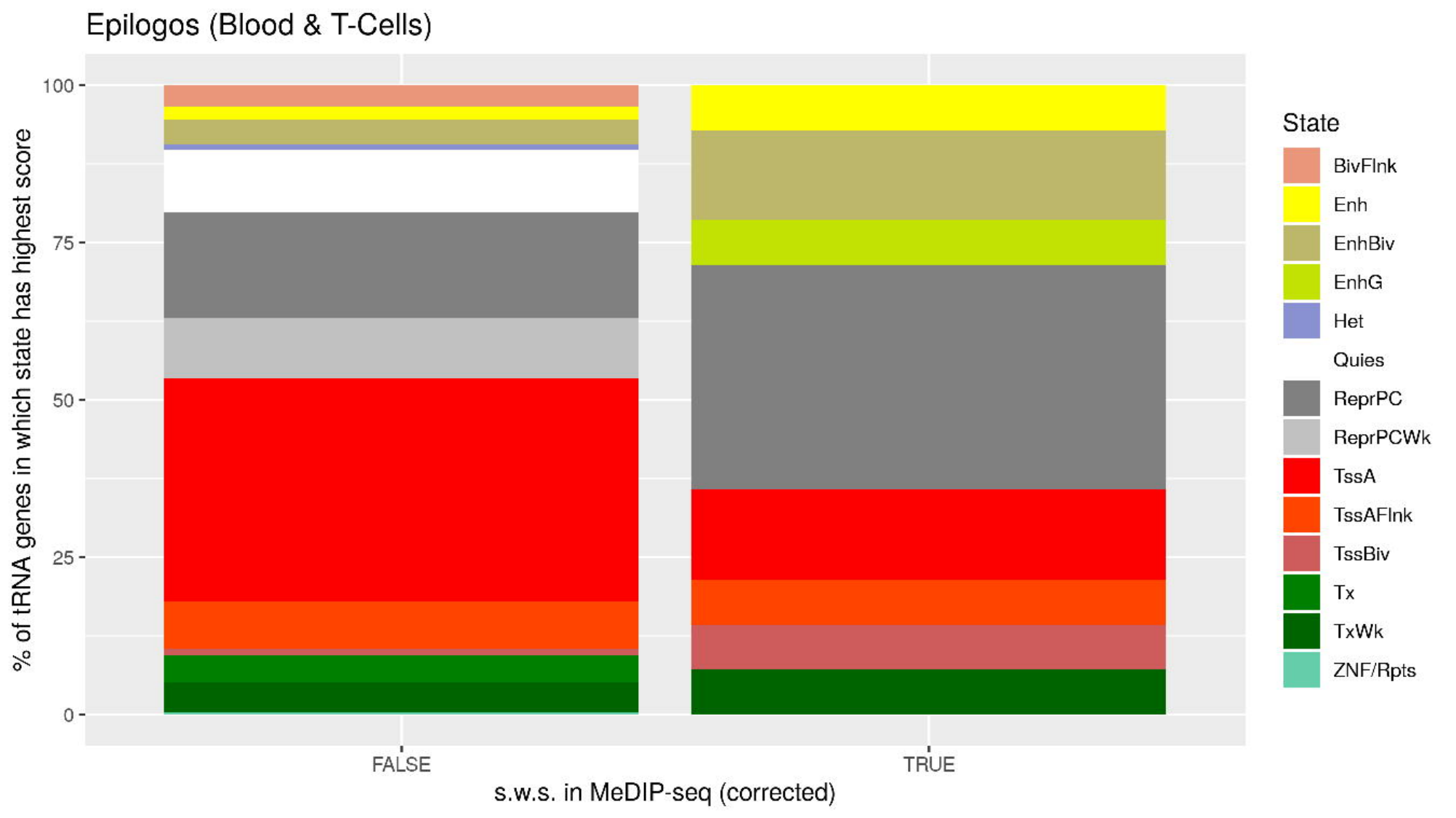
Epilogos (Blood & T-Cells)
% of tRNA genes in which state has highest score
100
75
50
25
0
FALSE
TRUE
s.w.s. in MeDIP-seq (corrected)
State
BivFlnk
Enh
EnhBiv
EnhG
Het
Quies
ReprPC
ReprPCWk
TssA
TssAFlnk
TssBiv
Tx
TxWk
ZNF/Rpts

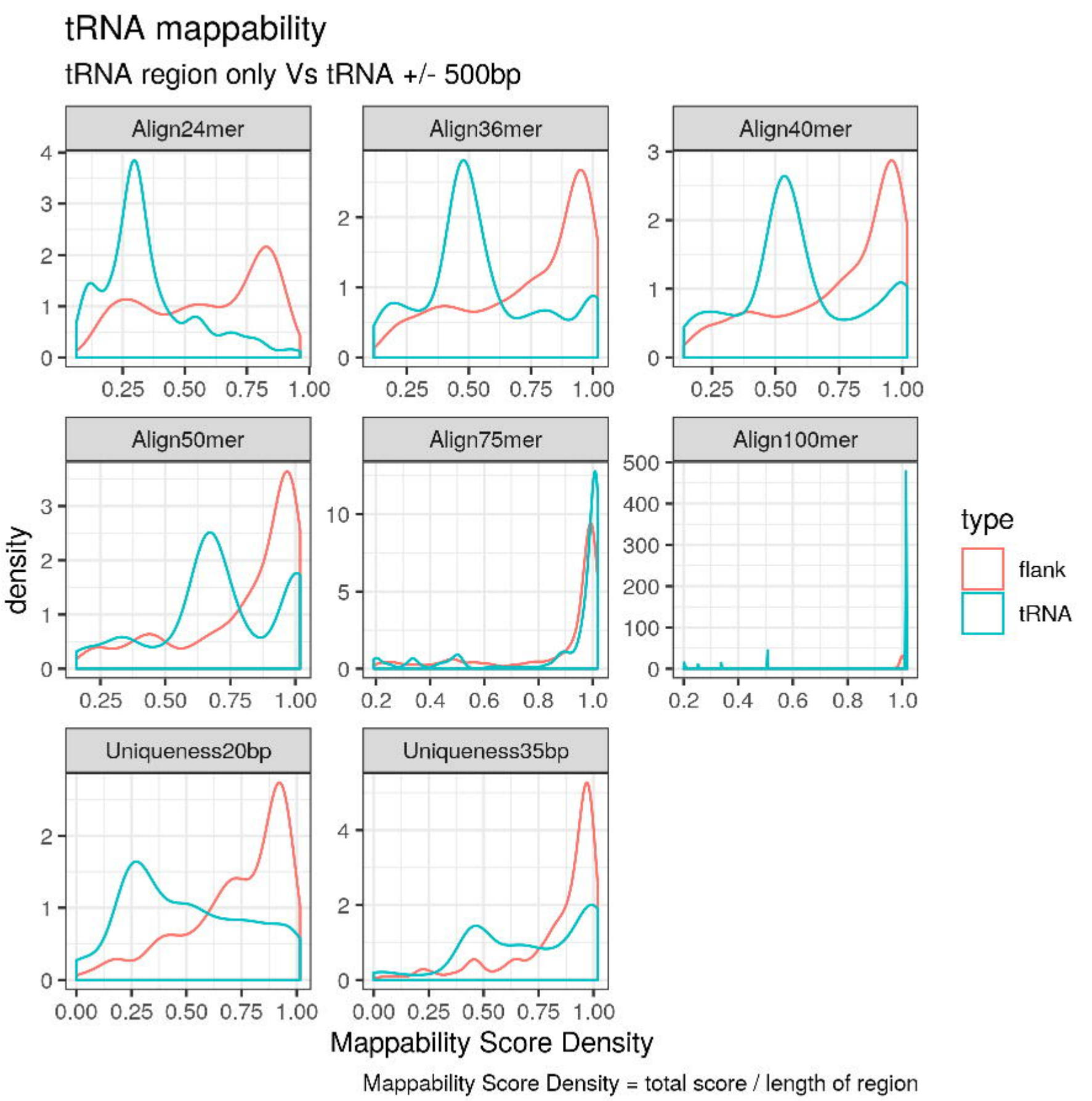
tRNA mappability
tRNA region only Vs tRNA +/- 500bp
Align24mer
Align36mer
Align40mer
Align50mer
Align75mer
Align100mer
Uniqueness20bp
Uniqueness35bp
density
Mappability Score Density
type
flank
tRNA
Mappability Score Density = total score / length of region

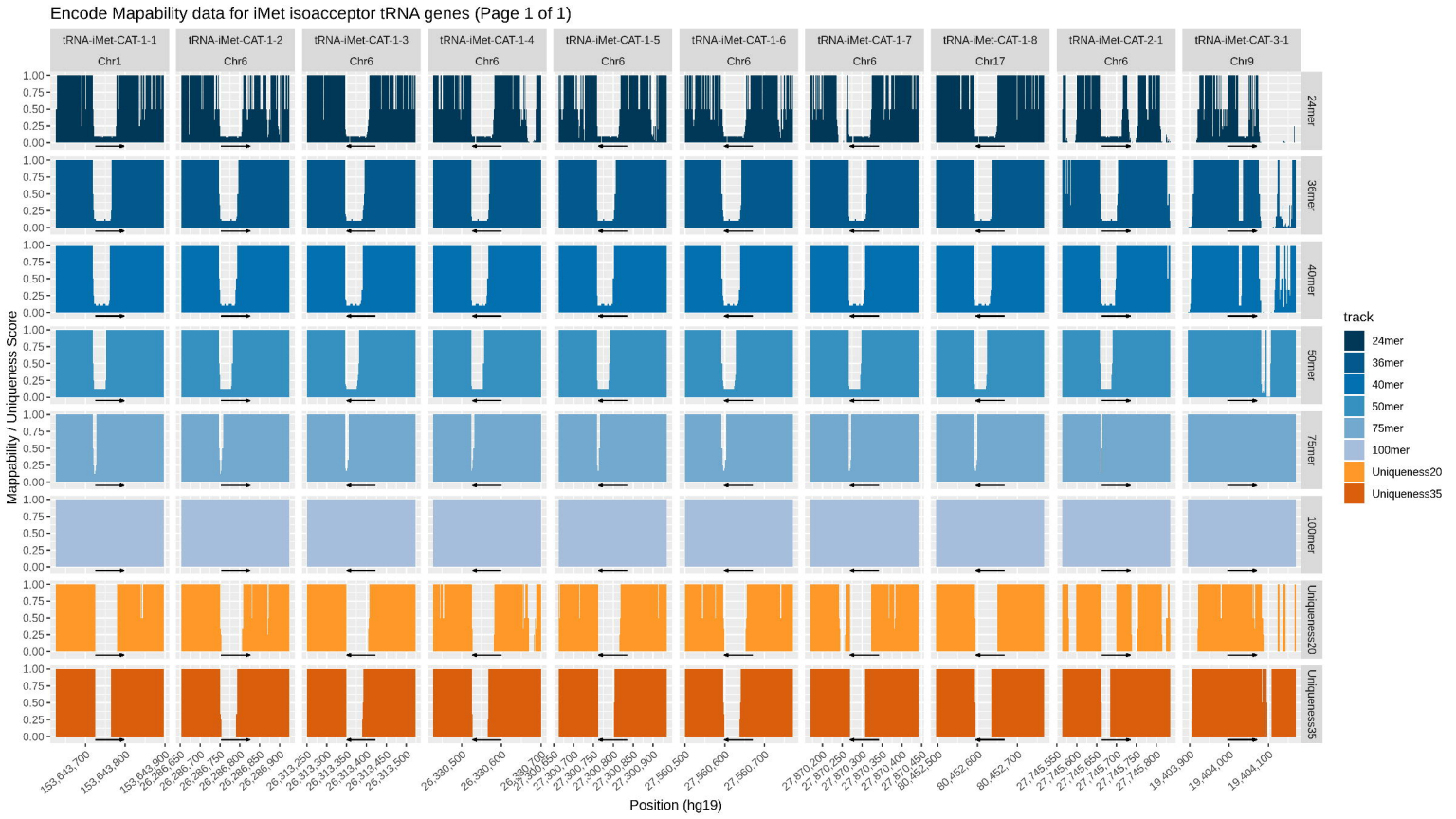
Encode Mapability data for iMet isoacceptor tRNA genes (Page 1 of 1)
tRNA-iMet-CAT-1-1
Chr1
tRNA-iMet-CAT-1-2
Chr6
tRNA-iMet-CAT-1-3
Chr6
tRNA-iMet-CAT-1-4
Chr6
tRNA-iMet-CAT-1-5
Chr6
tRNA-iMet-CAT-1-6
Chr6
tRNA-iMet-CAT-1-7
Chr6
tRNA-iMet-CAT-1-8
Chr17
tRNA-iMet-CAT-2-1
Chr6
tRNA-iMet-CAT-3-1
Chr9
24mer
36mer
40mer
50mer
75mer
100mer
Uniqueness20
Uniqueness35
Mappability / Uniqueness Score
1.00
0.75
0.50
0.25
0.00
track
24mer
36mer
40mer
50mer
75mer
100mer
Uniqueness20
Uniqueness35
153,643,700
153,643,800
153,643,900
26,286,650
26,286,700
26,286,750
26,286,800
26,286,850
26,286,900
26,313,250
26,313,300
26,313,350
26,313,400
26,313,450
26,313,500
26,330,500
26,330,600
26,330,700
27,300,650
27,300,700
27,300,750
27,300,800
27,300,850
27,300,900
27,560,500
27,560,600
27,560,700
27,870,200
27,870,250
27,870,300
27,870,350
27,870,400
27,870,450
80,452,500
80,452,600
80,452,700
27,745,550
27,745,600
27,745,650
27,745,700
27,745,750
27,745,800
19,403,900
19,404,000
19,404,100
Position (hg19)

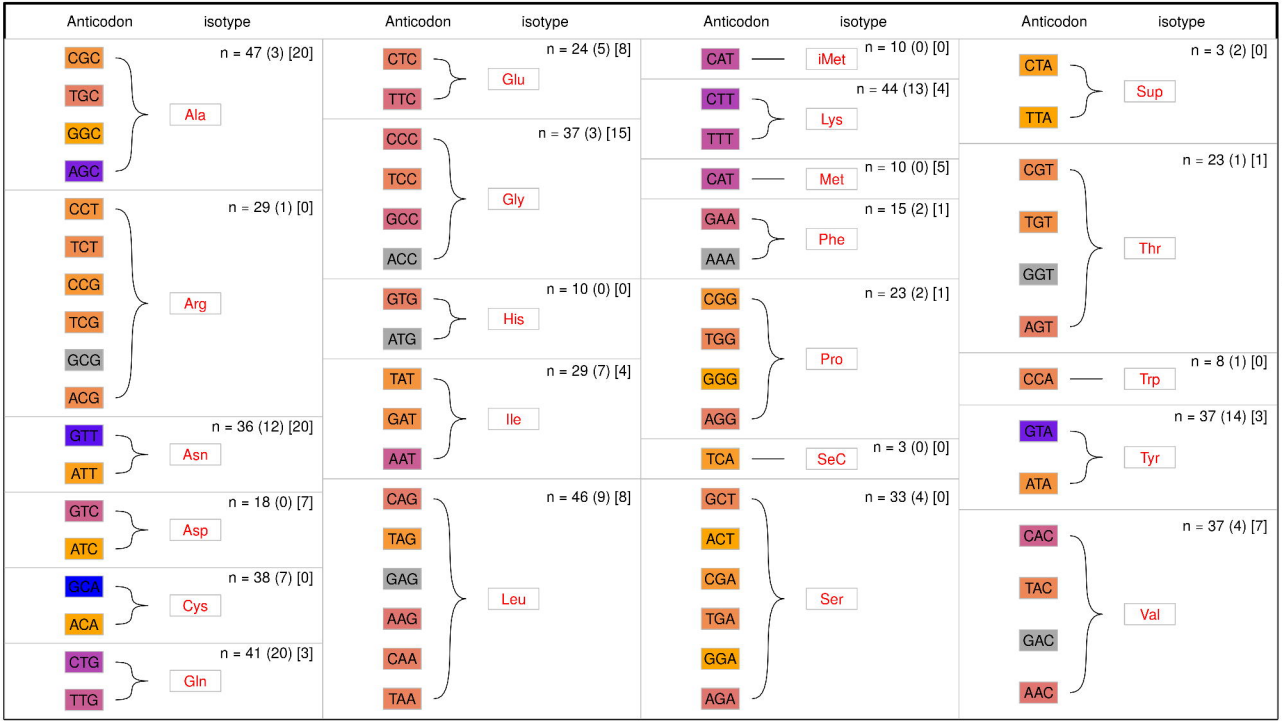
Anticodon
isotype
CGC
TGC
GGC
AGC
Ala
n = 47 (3) [20]
CCT
TCT
CCG
TCG
GCG
ACG
Arg
n = 29 (1) [0]
GTT
ATT
Asn
n = 36 (12) [20]
GTC
ATC
Asp
n = 18 (0) [7]
GCA
ACA
Cys
n = 38 (7) [0]
CTG
TTG
Gln
n = 41 (20) [3]
CTC
TTC
Glu
n = 24 (5) [8]
CCC
TCC
GCC
ACC
Gly
n = 37 (3) [15]
GTG
ATG
His
n = 10 (0) [0]
TAT
GAT
AAT
Ile
n = 29 (7) [4]
CAG
TAG
GAG
AAG
CAA
TAA
Leu
n = 46 (9) [8]
CAT
iMet
n = 10 (0) [0]
CTT
TTT
Lys
n = 44 (13) [4]
CAT
Met
n = 10 (0) [5]
GAA
AAA
Phe
n = 15 (2) [1]
CGG
TGG
GGG
AGG
Pro
n = 23 (2) [1]
TCA
SeC
n = 3 (0) [0]
GCT
ACT
CGA
TGA
GGA
AGA
Ser
n = 33 (4) [0]
CTA
TTA
Sup
n = 3 (2) [0]
CGT
TGT
GGT
AGT
Thr
n = 23 (1) [1]
CCA
Trp
n = 8 (1) [0]
GTA
ATA
Tyr
n = 37 (14) [3]
CAC
TAC
GAC
AAC
Val
n = 37 (4) [7]
Number of tRNAs
1
37
Not Present

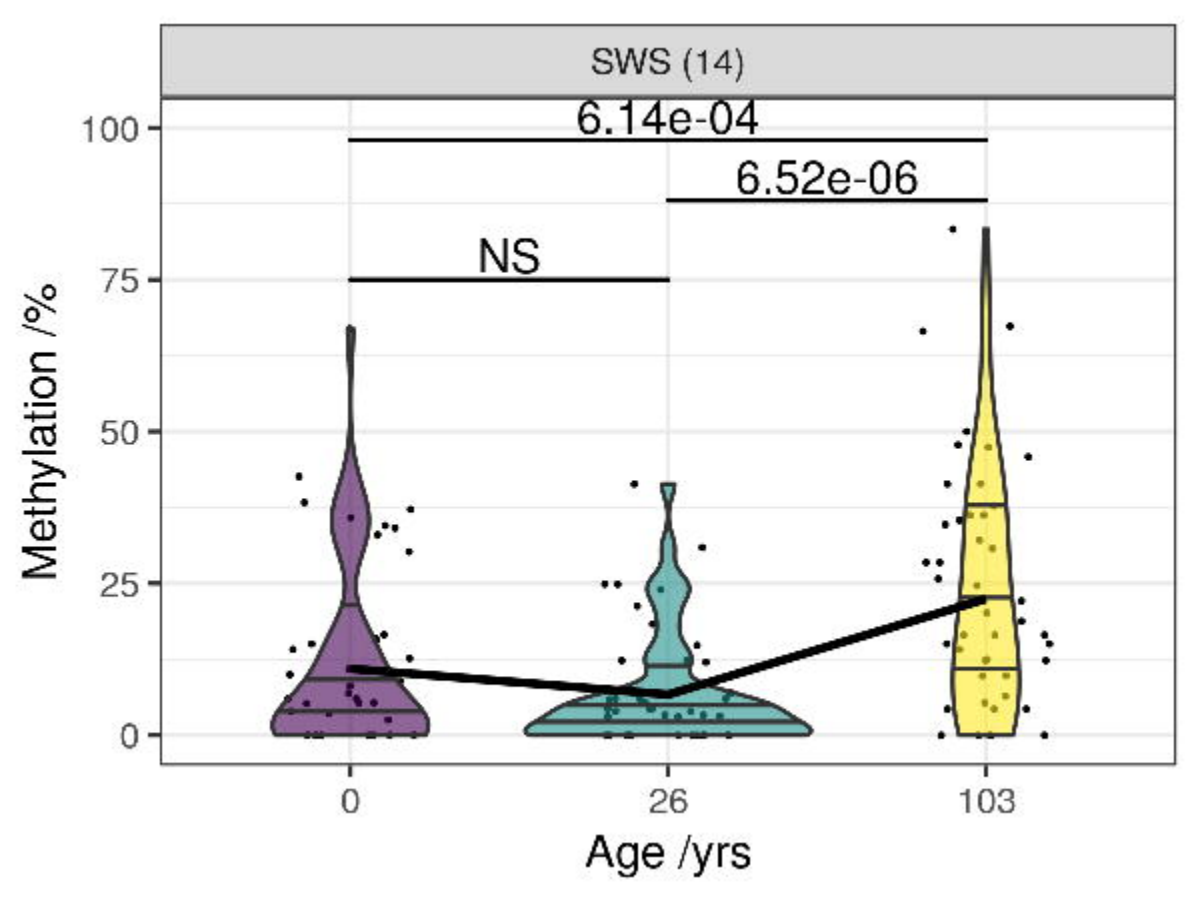
SWS (14)
6.14e-04
6.52e-06
NS
100
75
50
25
0
Methylation /%
0
26
103
Age /yrs

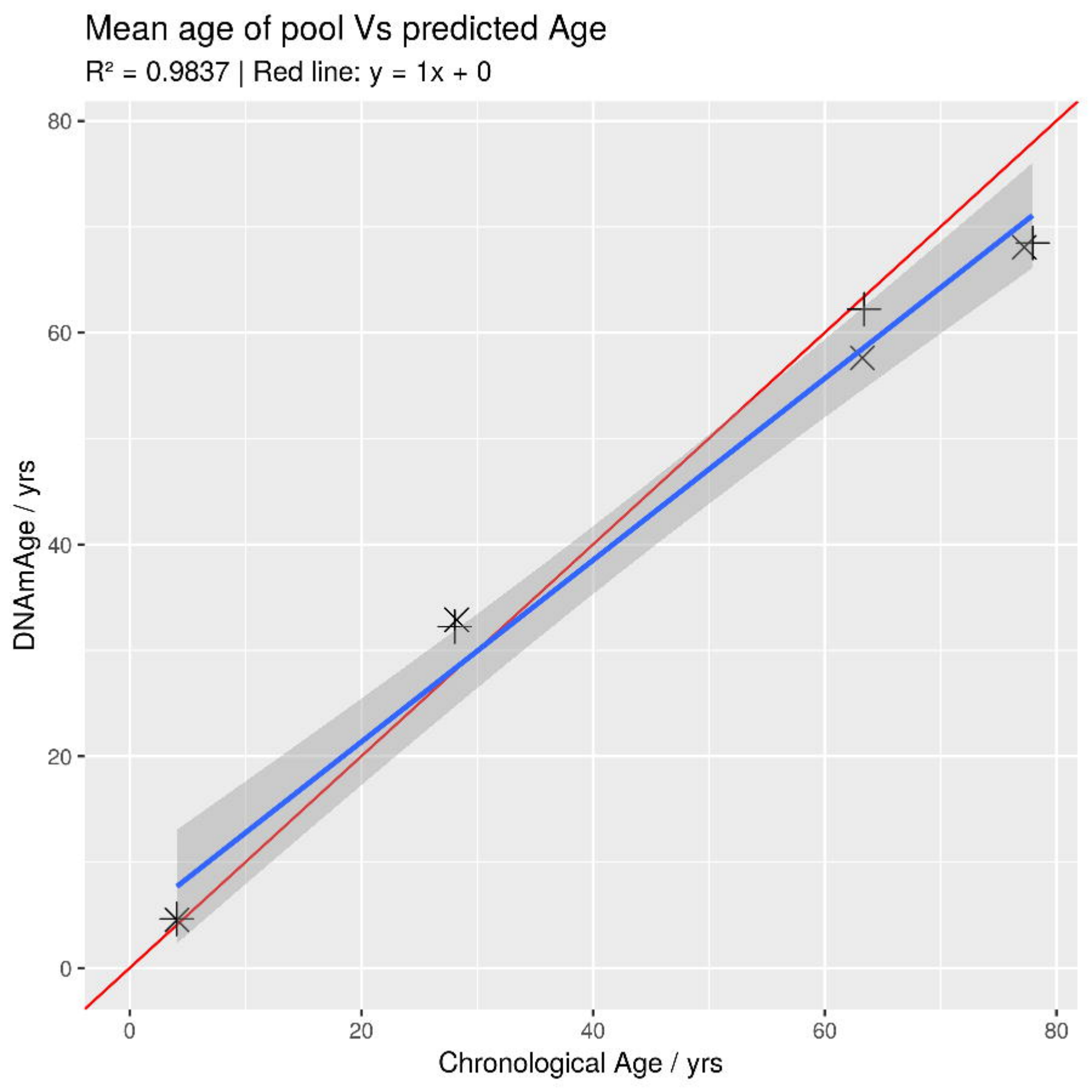
Mean age of pool Vs predicted Age
R² = 0.9837 | Red line: y = 1x + 0
DNAmAge / yrs
Chronological Age / yrs
0
20
40
60
80

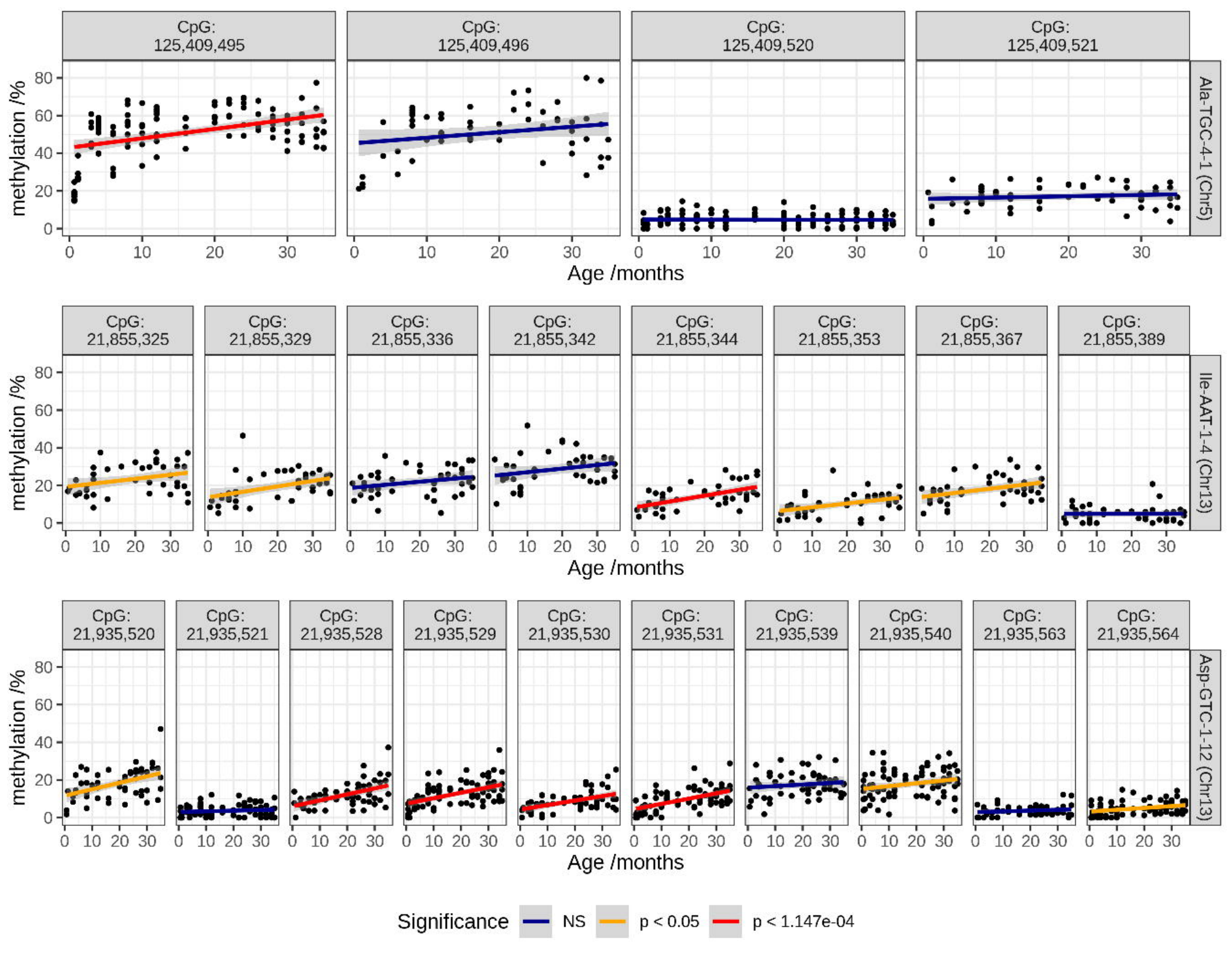
CpG:
125,409,495
CpG:
125,409,496
CpG:
125,409,520
CpG:
125,409,521
Ala-TGC-4-1 (Chr5)
methylation /%
Age /months
CpG:
21,855,325
CpG:
21,855,329
CpG:
21,855,336
CpG:
21,855,342
CpG:
21,855,344
CpG:
21,855,353
CpG:
21,855,367
CpG:
21,855,389
Ile-AAT-1-4 (Chr13)
methylation /%
Age /months
CpG:
21,935,520
CpG:
21,935,521
CpG:
21,935,528
CpG:
21,935,529
CpG:
21,935,530
CpG:
21,935,531
CpG:
21,935,539
CpG:
21,935,540
CpG:
21,935,563
CpG:
21,935,564
Asp-GTC-1-12 (Chr13)
methylation /%
Age /months
Significance
NS
p < 0.05
p < 1.147e-04

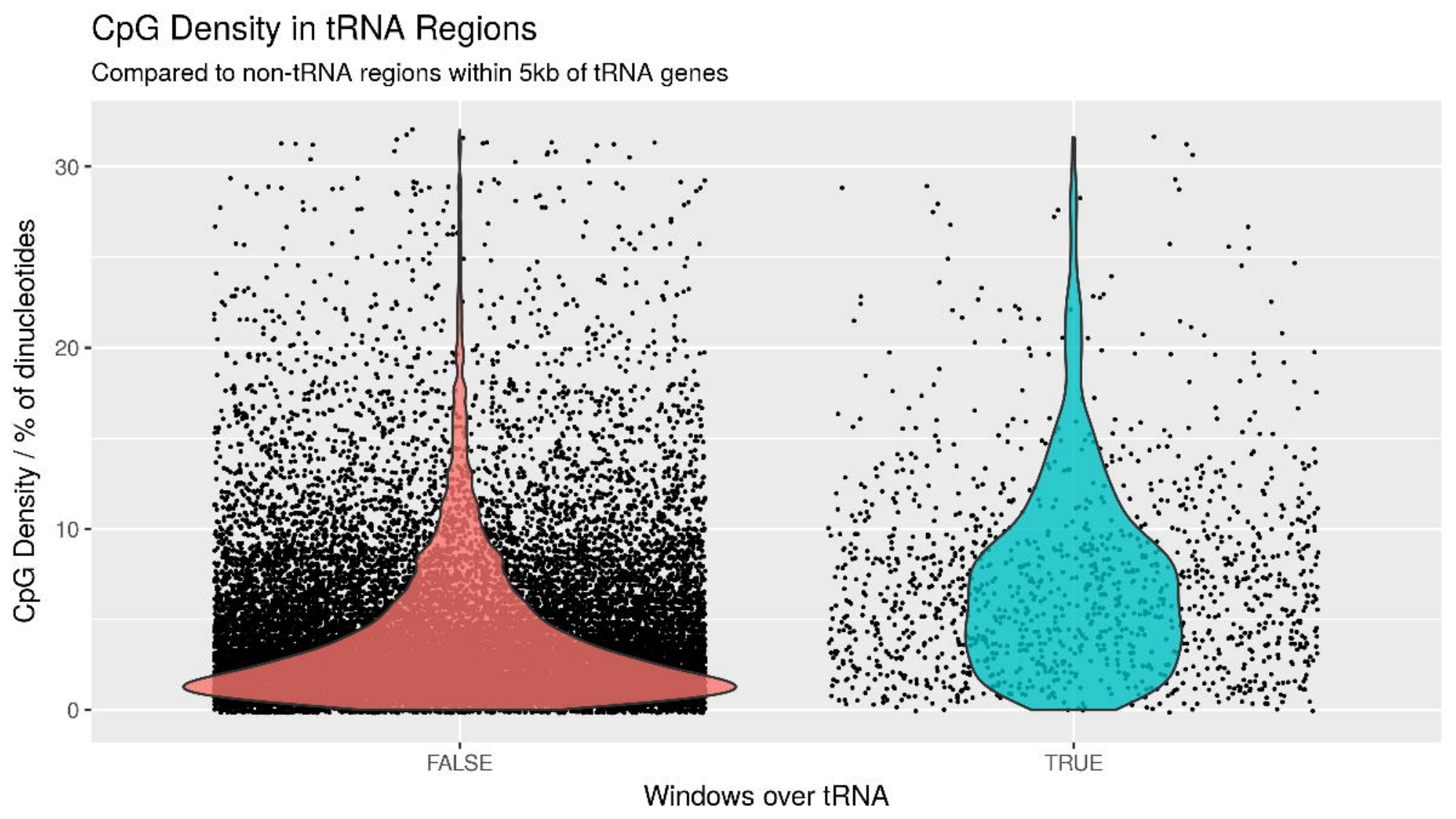
CpG Density in tRNA Regions
Compared to non-tRNA regions within 5kb of tRNA genes
CpG Density / % of dinucleotides
30
20
10
0
FALSE
TRUE
Windows over tRNA

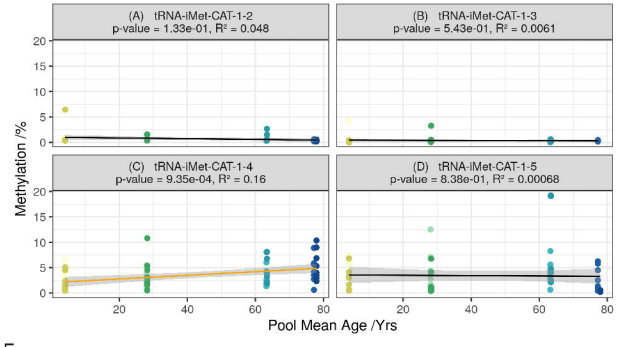
(A) tRNA-iMet-CAT-1-2
p-value = 1.33e-01, R² = 0.048
(B) tRNA-iMet-CAT-1-3
p-value = 5.43e-01, R² = 0.0061
(C) tRNA-iMet-CAT-1-4
p-value = 9.35e-04, R² = 0.16
(D) tRNA-iMet-CAT-1-5
p-value = 8.38e-01, R² = 0.00068
Methylation /%
Pool Mean Age /Yrs

E

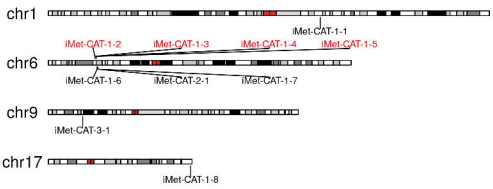
chr1
iMet-CAT-1-1
chr6
iMet-CAT-1-2
iMet-CAT-1-3
iMet-CAT-1-4
iMet-CAT-1-5
iMet-CAT-1-6
iMet-CAT-2-1
iMet-CAT-1-7
chr9
iMet-CAT-3-1
chr17
iMet-CAT-1-8

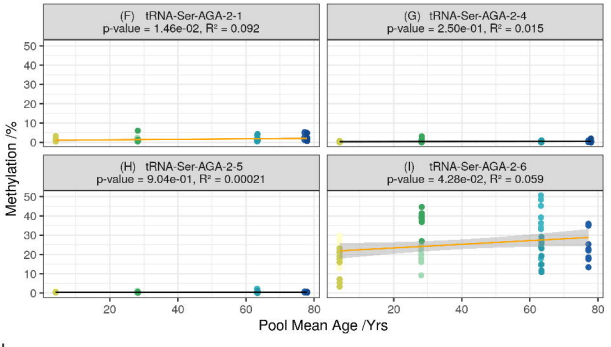
(F) tRNA-Ser-AGA-2-1
p-value = 1.46e-02, R² = 0.092
(G) tRNA-Ser-AGA-2-4
p-value = 2.50e-01, R² = 0.015
(H) tRNA-Ser-AGA-2-5
p-value = 9.04e-01, R² = 0.00021
(I) tRNA-Ser-AGA-2-6
p-value = 4.28e-02, R² = 0.059
Methylation /%
Pool Mean Age /Yrs

J

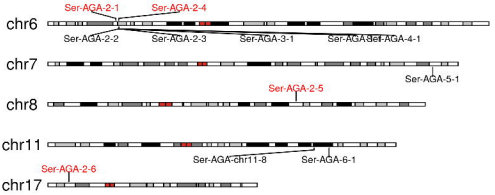
chr6
Ser-AGA-2-1
Ser-AGA-2-4
Ser-AGA-2-2
Ser-AGA-2-3
Ser-AGA-3-1
Ser-AGA-4-1
chr7
Ser-AGA-5-1
chr8
Ser-AGA-2-5
chr11
Ser-AGA-chr11-8
Ser-AGA-6-1
chr17
Ser-AGA-2-6

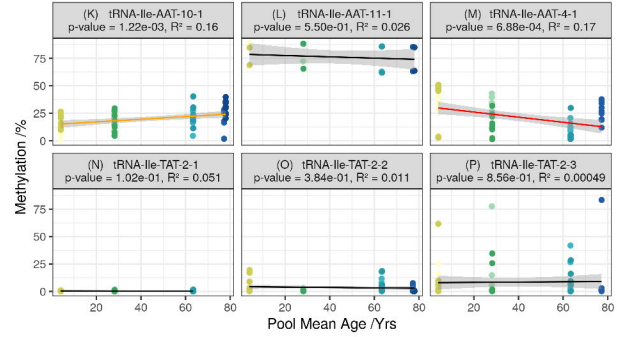
(K) tRNA-Ile-AAT-10-1
p-value = 1.22e-03, R² = 0.16
(L) tRNA-Ile-AAT-11-1
p-value = 5.50e-01, R² = 0.026
(M) tRNA-Ile-AAT-4-1
p-value = 6.88e-04, R² = 0.17
(N) tRNA-Ile-TAT-2-1
p-value = 1.02e-01, R² = 0.051
(O) tRNA-Ile-TAT-2-2
p-value = 3.84e-01, R² = 0.011
(P) tRNA-Ile-TAT-2-3
p-value = 8.56e-01, R² = 0.00049
Methylation /%
Pool Mean Age /Yrs

Q

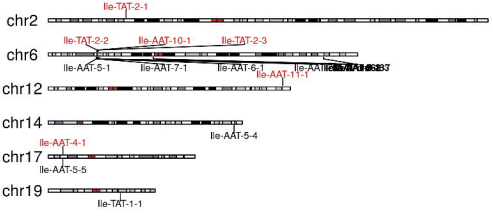
chr2
Ile-TAT-2-1
chr6
Ile-TAT-2-2
Ile-AAT-10-1
Ile-TAT-2-3
Ile-AAT-5-1
Ile-AAT-7-1
Ile-AAT-6-1
Ile-AAT-11-1
chr12
chr14
Ile-AAT-5-4
chr17
Ile-AAT-4-1
Ile-AAT-5-5
chr19
Ile-TAT-1-1

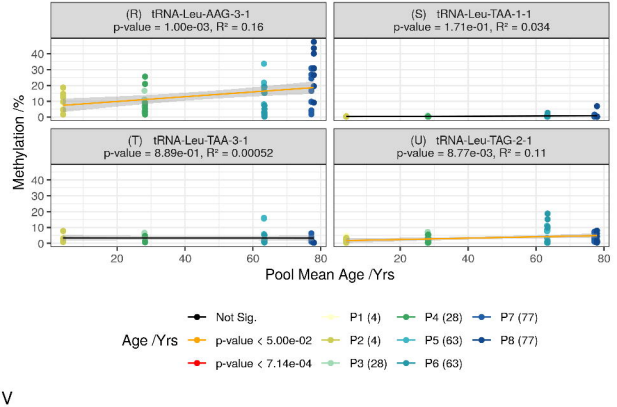
(R) tRNA-Leu-AAG-3-1
p-value = 1.00e-03, R² = 0.16
(S) tRNA-Leu-TAA-1-1
p-value = 1.71e-01, R² = 0.034
(T) tRNA-Leu-TAA-3-1
p-value = 8.89e-01, R² = 0.00052
(U) tRNA-Leu-TAG-2-1
p-value = 8.77e-03, R² = 0.11
Methylation /%
Pool Mean Age /Yrs
Age /Yrs
Not Sig.
p-value < 5.00e-02
p-value < 7.14e-04
P1 (4)
P2 (4)
P3 (28)
P4 (28)
P5 (63)
P6 (63)
P7 (77)
P8 (77)

V

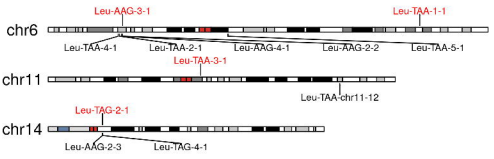
chr6
Leu-AAG-3-1
Leu-TAA-1-1
Leu-TAA-4-1
Leu-TAA-2-1
Leu-AAG-4-1
Leu-AAG-2-2
Leu-TAA-5-1
chr11
Leu-TAA-3-1
Leu-TAA-chr11-12
chr14
Leu-TAG-2-1
Leu-AAG-2-3
Leu-TAG-4-1

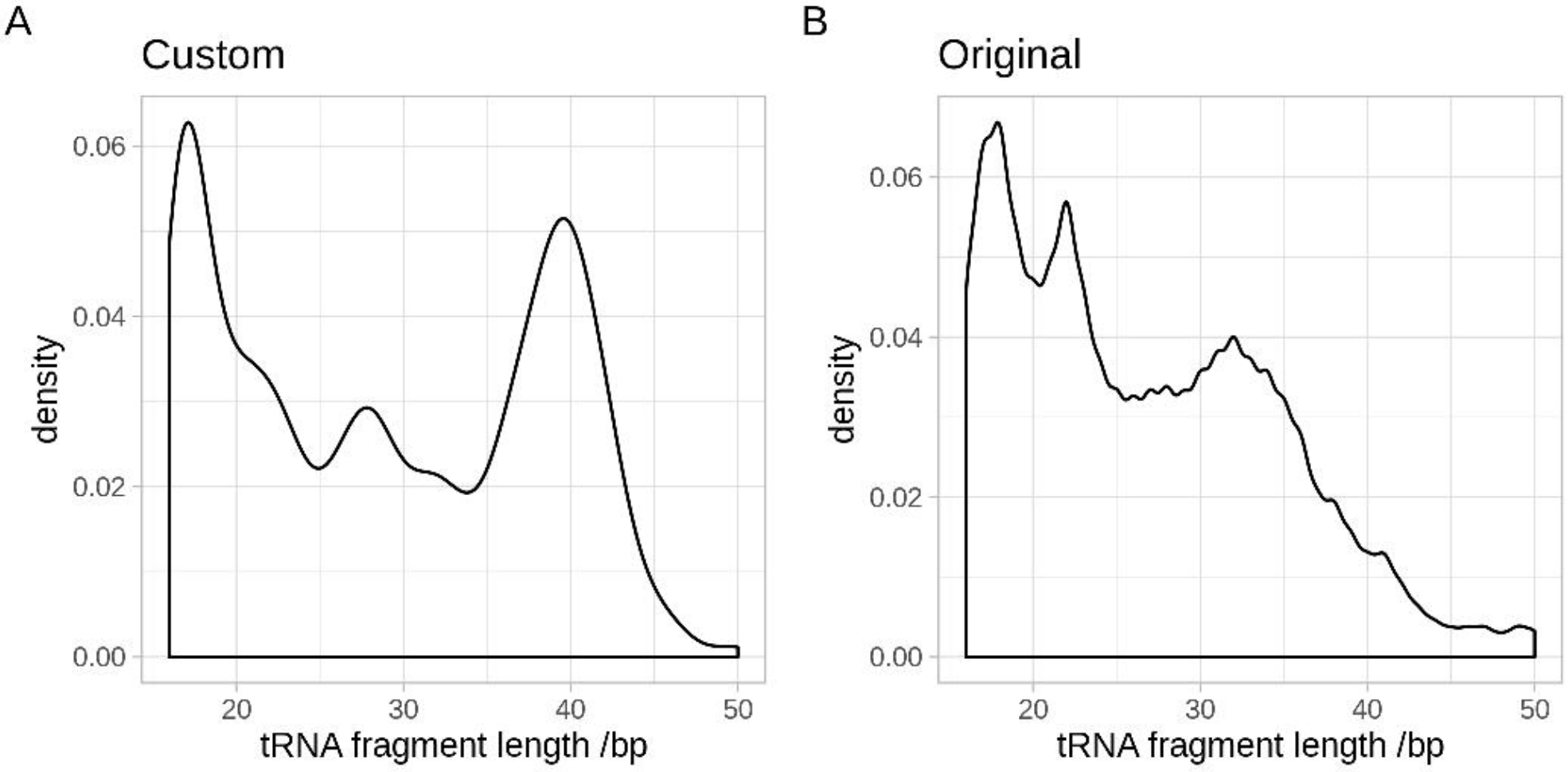
A
Custom
0.06
0.04
0.02
0.00
density
20
30
40
50
tRNA fragment length /bp
B
Original
0.06
0.04
0.02
0.00
density
20
30
40
50
tRNA fragment length /bp

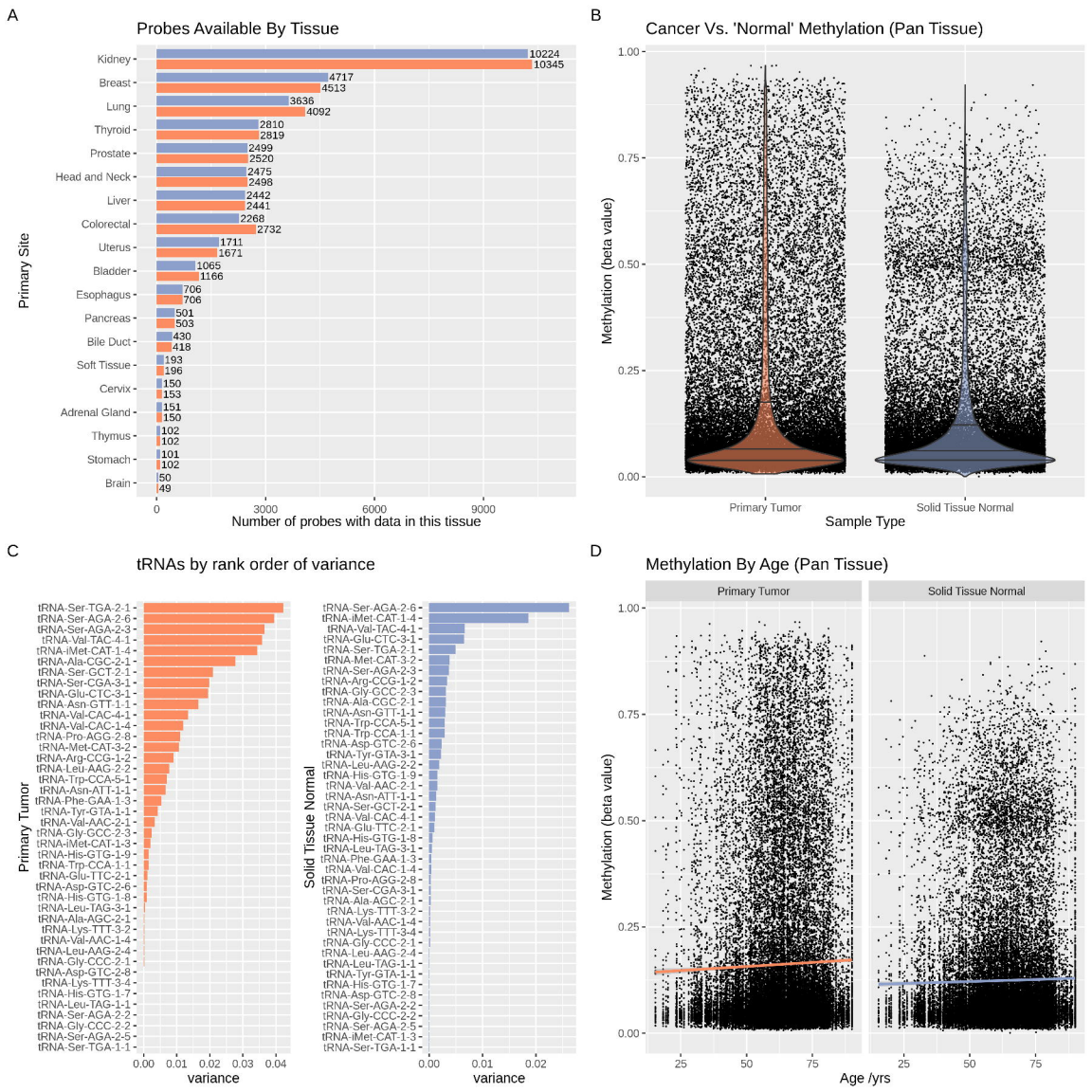
A
Probes Available By Tissue
Primary Site
Kidney
Breast
Lung
Thyroid
Prostate
Head and Neck
Liver
Colorectal
Uterus
Bladder
Esophagus
Pancreas
Bile Duct
Soft Tissue
Cervix
Adrenal Gland
Thymus
Stomach
Brain
10224
10345
4717
4513
3636
4092
2810
2819
2499
2520
2475
2498
2442
2441
2268
2732
1711
1671
1065
1166
706
706
501
503
430
418
193
196
150
153
151
150
102
102
101
102
50
49
0
3000
6000
9000
Number of probes with data in this tissue
B
Cancer Vs. 'Normal' Methylation (Pan Tissue)
Methylation (beta value)
1.00
0.75
0.50
0.25
0.00
Primary Tumor
Solid Tissue Normal
Sample Type
C
tRNAs by rank order of variance
Primary Tumor
tRNA-Ser-TGA-2-1
tRNA-Ser-AGA-2-6
tRNA-Ser-AGA-2-3
tRNA-Val-TAC-4-1
tRNA-iMet-CAT-1-4
tRNA-Ala-CGC-2-1
tRNA-Ser-GCT-2-1
tRNA-Ser-CGA-3-1
tRNA-Glu-CTC-3-1
tRNA-Asn-GTT-1-1
tRNA-Val-CAC-4-1
tRNA-Val-CAC-1-4
tRNA-Pro-AGG-2-8
tRNA-Met-CAT-3-2
tRNA-Arg-CCG-1-2
tRNA-Leu-AAC-2-2
tRNA-Trp-CCA-5-1
tRNA-Asn-ATT-1-1
tRNA-Phe-GAA-1-3
tRNA-Tyr-GTA-1-1
tRNA-Val-AAC-2-1
tRNA-Gly-GCC-2-3
tRNA-iMet-CAT-1-3
tRNA-His-GTG-1-9
tRNA-Trp-CCA-1-1
tRNA-Glu-TTC-2-1
tRNA-Asp-GTC-2-6
tRNA-His-GTG-1-8
tRNA-Leu-TAG-3-1
tRNA-Ala-AGC-2-1
tRNA-Lys-TTT-3-2
tRNA-Val-AAC-1-4
tRNA-Gly-CCC-2-1
tRNA-Leu-AAG-2-4
tRNA-Gly-CCC-2-1
tRNA-Asp-GTC-2-8
tRNA-Lys-TTT-3-4
tRNA-His-GTG-1-7
tRNA-Leu-TAG-1-1
tRNA-Ser-AGA-2-2
tRNA-Gly-CCC-2-2
tRNA-Ser-AGA-2-5
tRNA-Ser-TGA-1-1
0.00
0.01
0.02
0.03
0.04
variance
Solid Tissue Normal
tRNA-Ser-AGA-2-6
tRNA-iMet-CAT-1-4
tRNA-Val-TAC-4-1
tRNA-Glu-CTC-3-1
tRNA-Ser-TGA-2-1
tRNA-Met-CAT-3-2
tRNA-Ser-AGA-2-3
tRNA-Arg-CCG-1-2
tRNA-Gly-GCC-2-3
tRNA-Ala-CGC-2-1
tRNA-Asn-GTT-1-1
tRNA-Trp-CCA-5-1
tRNA-Trp-CCA-1-1
tRNA-Asp-GTC-2-6
tRNA-Tyr-GTA-3-1
tRNA-Leu-AAG-2-2
tRNA-His-GTG-1-9
tRNA-Val-AAC-2-1
tRNA-Asn-ATT-1-1
tRNA-Ser-GCT-2-1
tRNA-Val-CAC-4-1
tRNA-Glu-TTC-2-1
tRNA-His-GTG-1-8
tRNA-Leu-TAG-3-1
tRNA-Phe-GAA-1-3
tRNA-Val-CAC-1-4
tRNA-Pro-AGG-2-8
tRNA-Ser-CGA-3-1
tRNA-Ala-AGC-2-1
tRNA-Lys-TTT-3-2
tRNA-Val-AAC-1-4
tRNA-Lys-TTT-3-4
tRNA-Gly-CCC-2-1
tRNA-Leu-AAG-2-4
tRNA-Leu-TAG-1-1
tRNA-Tyr-GTA-1-1
tRNA-His-GTG-1-7
tRNA-Asp-GTC-2-8
tRNA-Ser-AGA-2-2
tRNA-Gly-CCC-2-2
tRNA-Ser-AGA-2-5
tRNA-iMet-CAT-1-3
tRNA-Ser-TGA-1-1
0.00
0.01
0.02
variance
D
Methylation By Age (Pan Tissue)
Primary Tumor
Solid Tissue Normal
Methylation (beta value)
1.00
0.75
0.50
0.25
0.00
25
50
75
Age /yrs

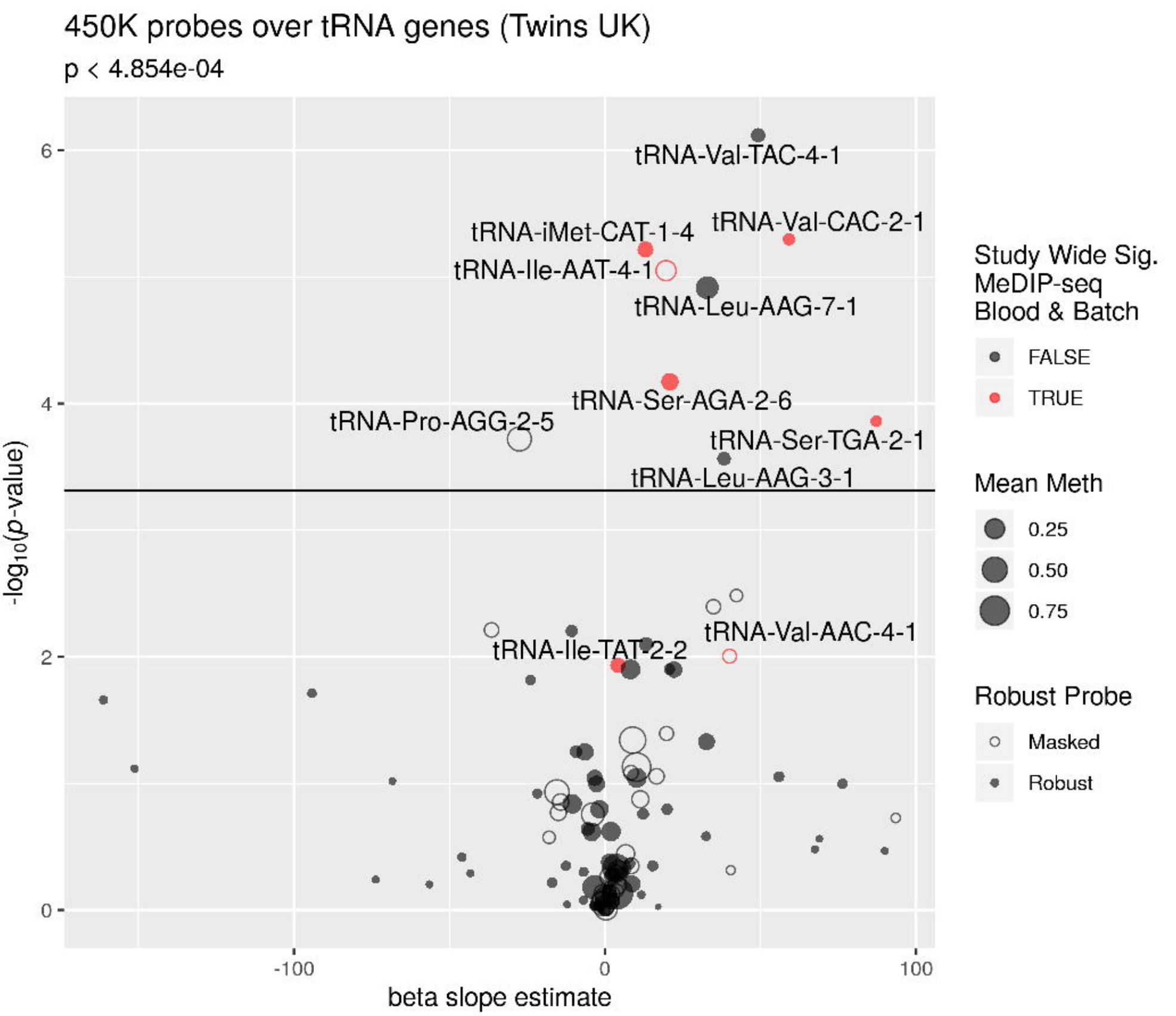
450K probes over tRNA genes (Twins UK)
p < 4.854e-04
tRNA-Val-TAC-4-1
tRNA-iMet-CAT-1-4
tRNA-Val-CAC-2-1
tRNA-Ile-AAT-4-1
tRNA-Leu-AAG-7-1
tRNA-Ser-AGA-2-6
tRNA-Pro-AGG-2-5
tRNA-Ser-TGA-2-1
tRNA-Leu-AAG-3-1
tRNA-Val-AAC-4-1
tRNA-Ile-TAT-2-2
6
4
2
0
-log10(p-value)
-100
0
100
beta slope estimate
Study Wide Sig.
MeDIP-seq
Blood & Batch
FALSE
TRUE
Mean Meth
0.25
0.50
0.75
Robust Probe
Masked
Robust